

<b>OCRWM</b>	<b>DESIGN CALCULATION OR ANALYSIS COVER SHEET</b>	1. QA: QA 2. Page 1						
3. System <div style="text-align: center;">Drip Shield</div>		4. Document Identifier <div style="text-align: center;">000-00C-PEC0-00100-000-00A</div>						
5. Title Structural Calculations of Drip Shield Exposed to Vibratory Ground Motion								
6. Group Analyses and Component Design								
7. Document Status Designation <div style="text-align: center;"> <input checked="" type="checkbox"/> Preliminary               <input type="checkbox"/> Final               <input type="checkbox"/> Cancelled         </div>								
8. Notes/Comments								
Attachments		Total Number of Pages						
List of attachments is presented in Section 8								
<b>RECORD OF REVISIONS</b>								
9. No.	10. Reason For Revision	11. Total # of Pgs.	12. Last Pg. #	13. Originator (Print/Sign/Date)	14. Checker (Print/Sign/Date)	15. QER (Print/Sign/Date)	16. Approved/Accepted (Print/Sign)	17. Date
00A	Initial Issue	79	IV-12	Sreten Mastilovic SIGNATURE ON FILE 16 JUNE 2003	Zekai Ceylan SIGNATURE ON FILE 6/16/03	Daniel J. Tunney SIGNATURE ON FILE 6/16/2003	Michael J. Anderson SIGNATURE ON FILE	6/16/03

## CONTENTS

1. PURPOSE .....	4
2. METHOD .....	5
3. ASSUMPTIONS .....	5
4. USE OF COMPUTER SOFTWARE .....	8
5. CALCULATION .....	9
5.1 MATERIAL PROPERTIES .....	9
5.2 FINITE ELEMENT REPRESENTATION .....	10
5.2.1 Ground-Motion Time History Cutoff .....	15
5.2.2 System Damping .....	17
6. RESULTS .....	18
6.1 EVENT WITH ANNUAL FREQUENCY OF OCCURRENCE $5 \cdot 10^{-4}$ 1/yr .....	18
6.2 EVENTS WITH ANNUAL FREQUENCY OF OCCURRENCE $1 \cdot 10^{-6}$ 1/yr .....	19
6.3 EVENTS WITH ANNUAL FREQUENCY OF OCCURRENCE $1 \cdot 10^{-7}$ 1/yr .....	20
6.4 SOME COMMENTS ON THE VIBRATORY SIMULATIONS .....	21
6.4.1 Some Complexities Inherent in the Nature of the Problem .....	21
6.4.2 Use of Shell Elements in FE Representation .....	22
6.4.3 Representation of WP and Pallet by WPP Assembly .....	23
6.4.4 Effect of Time-History Cutoff .....	24
6.4.5 Mesh Sensitivity .....	24
7. REFERENCES .....	25
8. ATTACHMENTS .....	28

## FIGURES

	<b>Page</b>
Figure 1. Setup for DS Vibratory Simulations .....	11
Figure 2. Cut-Away View of Setup for DS Vibratory Simulations.....	11
Figure 3. Contours of WPP Assembly and WP Mounted on Pallet.....	12
Figure 4. Maximum 1 <sup>st</sup> Principal Stress Time History for DS Plates.....	18
Figure 5. Energy Plots for Realization Number 11 at Annual Frequency of Occurrence 1·10 <sup>-6</sup> 1/yr .....	24

## TABLES

Table 1. Simulation Parameters .....	13
Table 2. Duration and Characteristic Times Corresponding to Ground Motions at.....	15
Annual Frequency of Occurrence 1·10 <sup>-6</sup> 1/yr .....	16
Table 3. Duration and Characteristic Times Corresponding to Ground Motions at.....	16
Annual Frequency of Occurrence 1·10 <sup>-7</sup> 1/yr .....	16
Table 4. Damaged Area at Annual Frequency of Occurrence of 1·10 <sup>-6</sup> 1/yr .....	20
Table 5. List of Electronic Files in Attachment V .....	28

## 1. PURPOSE

The objective of this calculation is twofold. First, to determine whether or not separation of interlocking drip shield (DS) segments occurs during vibratory ground motion. Second, if DS separation does not occur, to estimate the area of the DS for which the residual 1<sup>st</sup> principal stress exceeds a certain limit. (The area of DS plate-1 and DS plate-2 [see Attachment I] where the residual 1<sup>st</sup> principal stress exceeds a certain limit will be, for brevity, referred to as “the damaged area” throughout this document. Also, DS plate-1 and DS plate-2 will be referred to, for brevity, as “DS plates” henceforth.) The stress limit used throughout this document is defined as 50 percent of yield strength of the DS plate material, Titanium Grade 7 (Ti-7) (SB-265 R52400), at temperature of 150 °C (see Assumptions 3.9 and 3.11).

A set of 15 calculations is performed at two different annual frequencies of occurrence (annual exceedance frequency):  $10^{-6}$  per year (1/yr) and  $10^{-7}$  1/yr. (Note: Due to computational problems only five realizations at  $10^{-7}$  1/yr are presented in this document.) Additionally, one calculation is performed at the annual frequency of occurrence of  $5 \cdot 10^{-4}$  1/yr.

The scope of this document is limited to reporting whether or not the DS separation occurs. If the DS separation does not occur the scope is limited to reporting the calculation results in terms of the damaged area. All these results are evaluated for the DS plates.

This calculation is intended for use in support of the Total System Performance Assessment–License Application seismicity modeling. This calculation is associated with the DS design and was performed by the Waste Package Design group. AP-3.12Q, *Design Calculations and Analyses* (Ref. 1) is used to perform the calculation and develop the document. The DS is classified as Quality Level 1 (Ref. 5, p. 7). Therefore, this calculation is subject to the Quality Assurance Requirements and Description (Ref. 4).

The information provided by Attachment I is that of the potential design of the type of DS considered in this calculation, and provides the potential dimensions and materials for the DS design. Designs of the 21-PWR (Pressurized Water Reactor) waste package (WP) and emplacement pallet (pallet, for brevity, throughout the document) used in this calculation are those defined in References 24 and 22, respectively. All obtained results are valid for these designs only.

## 2. METHOD

The finite element (FE) mesh was created by using the commercially available ANSYS V5.6.2 FE code (Software Tracking Number [STN] 10364-5.6.2-01, Ref. 6). The FE calculations were then performed by using the commercially available LS-DYNA V960.1106 (STN 10300-960.1106-00, Ref. 7) FE code.

After the FE calculations were completed, the visual examinations of the simulated events were performed to determine whether or not the DSs were separated. If there was no indication of the DS separation, the results were provided in terms of the damaged area of the DS plates. The damaged area was estimated based on the residual 1<sup>st</sup> principal stress plot for the DS plates. It is important to acknowledge the conservatism of the criterion used to define the damaged area (conservatism independent of the choice of the residual stress threshold). Namely, the failure criterion (see Section 1 and Assumption 3.11) does not account for the possibility of crack arrest once the crack is nucleated (i.e., the area “fails” regardless of the residual stress distribution across the thickness of the DS plates).

## 3. ASSUMPTIONS

In the course of developing this document, the following assumptions are made regarding the structural calculation.

- 3.1 The density and Poisson’s ratio are not available for Ti-7, Ti-24 (Titanium Grade 24 [SB-265 R56405]), and Alloy 22 (SB-575 N06022), except at room temperature (RT) (20 °C). (Note: In regard to UNS designation for Ti-24, note that Ti-24 has the same mechanical properties as Ti-5 since the compositions are almost identical; see Ref. 12, Section II, Part B, SB-265, Table 2.) The RT density and RT Poisson’s ratio are assumed for these materials. The impact of using RT density and RT Poisson’s ratio is anticipated to be small. The rationale for this assumption is that the material properties in question do not have dominant impact on the calculation results. This assumption is used in Section 5.1 and corresponds to paragraph 5.2.8.4 of Reference 8.
- 3.2 The temperature-dependent material properties are not available for TSw2 (Topopah Spring Welded-Lithophysal Poor) rock except at RT. The TSw2 is used to represent the essentially unyielding drift walls (see Section 5.2) and the material properties are necessary only for the contact definitions. The corresponding RT material properties are assumed for this material. The impact of using RT material properties is anticipated to be small. The rationale for this assumption is that the material properties of the rock do not have an impact on the calculation results. This assumption is used in Section 5.1.
- 3.3 Some of the rate-dependent material properties are not available for Ti-7, Ti-24, and Alloy 22, at any strain rate. The material properties obtained under the static loading conditions are assumed for these materials. The impact of using material properties obtained under static loading conditions is anticipated to be small. The rationale for this assumption is that the change of mechanical properties of subject materials (Ref. 32, Fig. 28) at the peak strain rates that typically occur during the earthquake simulation does not have significant

effect on the results presented in this calculation. The maximum plastic-strain rate in the DS plates observed in this calculation is  $185 \text{ s}^{-1}$  (as indicated by maximum slopes of the effective-plastic-strain time histories presented in Fig. IV-9). It is important to recognize that this strain rate is the maximum among all  $10^{-6} \text{ 1/yr}$  realizations among all DS-plate elements; the typical strain rate is significantly lower. As an example, see the strain rates for the elements in the immediate neighborhood of the element characterized by this singular strain rate (Fig. IV-10a); the average strain rate is approximately  $85 \text{ s}^{-1}$  (Fig. IV-10b). It should be noted that realization number 9 is conspicuous among the  $10^{-6} \text{ 1/yr}$  realizations for large number of high-intensity WP-pallet impacts (Ref. 13, Table 6.1.3-3) resulting in exceptionally large damaged area of the DS (see Table 4). More typically, the next two largest strain rates among  $10^{-6} \text{ 1/yr}$  realizations appear to be the ones in realizations 6 and 11, and they do not exceed  $15 \text{ s}^{-1}$  (see Figs. IV-11 and IV-12). This assumption is used in Section 5.1 and corresponds to paragraph 5.2.5 in Reference 8.

- 3.4 The Poisson's ratio of Alloy 22 is not available in literature. The Poisson's ratio of Alloy 625 (SB-443 N06625) is assumed for Alloy 22. The impact of this assumption is anticipated to be negligible. The rationale for this assumption is that the chemical compositions of Alloy 22 and Alloy 625 are similar (see Ref. 9 [Table "Chemical Composition in Weight %"] and Ref. 10 [p. 143], respectively). This assumption is used in Section 5.1 and corresponds to paragraph 5.2.8.2 of Reference 8.
- 3.5 The modulus of elasticity and Poisson's ratio of the TSw2 are characterized by significant scatter of data (see Ref. 28, Tables 3 and 4, respectively). For the purpose of the present calculation modulus of elasticity is assumed to be  $33 \text{ GPa}$ , and Poisson's ratio 0.21. The rationale for this assumption is that these values agree well with typical values of said properties for most rocks of interest (see Ref. 28, Tables 3 and 4). This assumption is used in Section 5.1.
- 3.6 The density of the TSw2 is assumed to be  $2370 \text{ kg/m}^3$ . The rationale for this assumption is that this value agrees well with all Topopah Spring Welded rocks and is not exceeded by any of other rocks presented in Reference 23 (Table 2). It should be noted that this assumption has no effect on the calculation results since density of the rock affects only masses of the essentially rigid invert and the rigid drift walls. This assumption is used in Section 5.1.
- 3.7 The friction coefficients for metal-to-metal contact and metal-to-rock contact are considered random parameters in this calculation. The range of values for both of these friction coefficients is 0.2 to 0.8. The rationale for this assumption follows:

Reference 26 (Table 3.2.1, p. 3-26) provides coefficients of static and sliding friction for various metals and other materials. However, coefficients of friction for the materials used in this calculation are not specifically mentioned in this handbook. The potential for long-term corrosion to modify the sliding friction must also be considered in defining the friction coefficient. In this situation, the appropriate coefficients of friction for the repository

components have high uncertainty. It is then appropriate to pick a distribution of values for the coefficients of friction that encompass a range of materials and a range of mechanical responses from little or no sliding between components to substantial sliding between components.

A distribution of values for the friction coefficient between 0.2 and 0.8 will achieve these goals (see Table 1 and Ref. 16, Table I-4). First, this distribution is broad enough to encompass typical values of the dry sliding friction coefficients for a wide variety of metals and other materials (see, Reference 26, Table 3.2.1, p. 3-26). Second, the appropriateness of this range is independently confirmed by seismic analyses for spent fuel storage racks (Ref. 27). This distribution is also broad enough to represent a range of mechanical response for the DS. A friction coefficient near 0.2 maximizes sliding of the DS on the invert. Similarly, a friction coefficient near 0.8 minimizes that sliding.

This assumption is used in Section 5.2.

- 3.8 The variation of functional friction coefficient between the static and dynamic value as a function of relative velocity of the surfaces in contact is not available in literature for the materials used in this calculation (see Section 5.2). Therefore, the effect of relative velocity of the surfaces in contact is neglected in these calculations by assuming that the functional friction coefficient and static friction coefficient are both equal to the dynamic friction coefficient. The impact of this assumption on results presented in this document is anticipated to be negligible. The rationale for this conservative assumption is that it maximizes the relative motion of unanchored repository components by minimizing the friction coefficient within the given FE-analysis framework. This assumption is used in Section 5.2.
- 3.9 The temperature of the DS is assumed to be 150 °C for temperature-dependent material properties. The rationale for this assumption is that this temperature is conservative for most of the regulatory period for high-temperature operating modes (97 percent of the regulatory period [see Reference 21, Figure 6-3]) and strictly conservative for low-temperature operating modes. This assumption is used in Sections 1 and 5.1.
- 3.10 The thickness of the DS plates is reduced by 2 mm. The rationale for this assumption is that the DS plates will degrade due to corrosion, during the 10,000-year regulatory period.  $1 \cdot 10^{-4}$  mm/yr corresponds to 73<sup>rd</sup> percentile of corrosion rate for Ti-7 (Ref. 20 [Fig. 2] and Ref. 3 [file WDgTi7Sand]). A thinning of this size is expected to account for the corrosion on both sides of the DS plates ( $2 \cdot 10,000 \text{ years} \cdot 1 \times 10^{-4} \text{ mm/yr} = 2 \text{ mm}$ ). This assumption is used in Section 5.2.
- 3.11 The residual stress threshold is assumed to be a constant value, equal to 50 percent of the yield strength of Ti-7. The basis for this assumption is the data provided in Reference 14. This calculation will determine areas over the DS plates where the residual stress values exceed 50 percent of Ti-7 yield strength. This assumption is used in Sections 1 and 2.

#### 4. USE OF COMPUTER SOFTWARE

One of the FE analysis computer codes used for this calculation is ANSYS V5.6.2, which is obtained from Software Configuration Management in accordance with the appropriate procedure (Ref. 2), and is identified by STN 10364-5.6.2-01 (Ref. 6). ANSYS V5.6.2 is a qualified commercially available FE code. The calculations using ANSYS V5.6.2 software are executed on four Hewlett-Packard (HP) 9000 series UNIX workstations (Operating System HP-UX 11.00) identified with the YMP (Yucca Mountain Project) property tag numbers 151324, 151325, 151664, and 151665, located in Las Vegas, Nevada. The development of FE mesh by ANSYS is appropriate and fully within the range of the validation performed for ANSYS V5.6.2 code. Access to the code is granted by the Software Configuration Management in accordance with the appropriate procedures.

The input files (identified by .inp file extension) and output files (identified by .out file extension) for ANSYS V5.6.2 are listed in Section 8, and provided in Attachment V.

The qualified FE analysis computer code used for this calculation is Livermore Software Technology Corporation (LSTC) LS-DYNA V960.1106 (Ref. 7). LS-DYNA V960.1106 is obtained from Software Configuration Management in accordance with the appropriate procedure (Ref. 2) and is identified by STN 10300-960.1106-00. Double-precision version of LS-DYNA V960.1106 is appropriate for its intended use. The LS-DYNA V960.1106 evaluation performed for this calculation is fully within the range of the validation performed for the LS-DYNA V960.1106 code. The calculations are executed on eight HP 9000 series UNIX workstations (Operating System HP-UX 11.00) identified with the YMP property tag numbers 151324, 151325, 150688, 150689, 150690, 151691, 151664, and 151665 located in Las Vegas, Nevada.

The input files (identified by .k, .dat, and .inc file extensions) and output files (d3hsp, d3plot, and messag) for LS-DYNA V960.1106 are listed in Section 8, and provided in Attachment V. (LS-DYNA V960.1106 energy-output file glstat is provided for realization number 11 at annual frequency of occurrence  $1 \cdot 10^{-6} \text{ 1/yr}$ )

As identified in Section 6, LSPOST V2 (LSTC) is a postprocessor used for visual display and graphical representation of data that is exempt of the requirements defined in Reference 2 (Section 2.1.2).



## 5. CALCULATION

### 5.1 MATERIAL PROPERTIES

Material properties used in these calculations are listed in this section. The material properties are evaluated for 150 °C (Assumption 3.9). Some of the temperature-dependent and rate-dependent material properties are not available for Ti-7, Ti-24, Alloy 22, and TSw2 rock. Therefore, RT density and RT Poisson's ratio are used for Ti-7, Ti-24, and Alloy 22 (see Assumption 3.1). The RT material properties are used for TSw2 rock (Assumption 3.2). Finally, the material properties obtained under the static loading conditions are used for all materials in this calculation (Assumption 3.3).

SB-265 R52400 (Titanium Grade 7 [Ti-7]) (Note: All properties of Ti-7, with exception of Poisson's ratio, are obtained from Reference 11.):

Density = 4520  $kg/m^3$  (at RT)

Yield strength = 209 MPa (at 150 °C)

Poisson's ratio = 0.32 (at RT) (Ref. 19, Section "Mechanical Properties")

Modulus of elasticity = 101  $GPa$  (at 150 °C)

Hardening (tangent) modulus = 0.448  $GPa$  (at 150 °C)

SB-265 R56405 (Titanium Grade 24 [Ti-24]; in regard to this UNS designation, note that Ti-24 has the same mechanical properties with Ti-5 since the compositions are almost identical, see Ref. 12, Section II, Part B, SB-265, Table 2) (Note: All properties of Ti-24, with exception of density and Poisson's ratio, are obtained from Reference 11.):

Density = 4430  $kg/m^3$  (at RT) (Ref. 15, page 620)

Yield strength = 750 MPa (at 150 °C)

Poisson's ratio = 0.34 (at RT) (Ref. 15, page 621)

Modulus of elasticity = 108  $GPa$  (at 150 °C)

Hardening (tangent) modulus = 1.52  $GPa$  (at 150 °C)

SB-575 N06022 (Alloy 22) (Note: All properties of Alloy 22, with exception of density and Poisson's ratio, are obtained from Reference 13.):

Density = 8690  $kg/m^3$  (at RT) (Ref. 9, Section "Properties of Alloy 22")

Yield strength = 310 MPa (at 150 °C)

Poisson's ratio = 0.278 (at RT) (Ref. 9, Section “Mechanical Properties”) (see Assumption 3.4)

Modulus of elasticity = 199 GPa (at 150 °C)

Hardening (tangent) modulus = 1.77 GPa (at 150 °C)

TSw2 Rock:

Density = 2370 kg/m<sup>3</sup> (at RT) (Assumption 3.6)

Poisson's ratio = 0.21 (at RT) (Assumption 3.5)

Modulus of elasticity = 33.0 GPa (at RT) (Assumption 3.5)

## 5.2 FINITE ELEMENT REPRESENTATION

Three-dimensional FE representation, used for the vibratory ground-motion simulations, is developed in ANSYS V5.6.2, by using the dimensions provided in Attachment I and References 22 and 24. The FE representation is presented in Figure 1. A corresponding cutaway view (portions of various parts are removed to offer a more revealing outlook) is presented in Figure 2. As seen in these figures, the FE representation consists of three interlocking DSs, the WPP (waste package-pallet) assembly, the invert surface, and the lateral and longitudinal boundaries.

Three interlocking DSs have identical geometry (see Attachment I). It is important to recognize that their purpose is different. The middle DS is represented as bilinear elastoplastic (with kinematic hardening) and finely meshed. All results presented in this document are evaluated exclusively for the DS plates of the middle DS. The other two DSs (called “peripheral DSs” henceforth) are represented as rigid (with exception of their DSC plates) and more coarsely meshed. The purpose of the peripheral DSs is to ensure realistic boundary conditions for the middle DS.

The longitudinal boundary provides constraints for the unanchored repository components in the longitudinal direction. It represents both the neighboring WPP assembly and the neighboring DS. The lateral boundary represents the repository emplacement drift. The lateral and longitudinal boundaries are both rigid and fixed to the invert by tied-interface contacts (for the tied-interface contacts, see Ref. 18, page 6.29). Thus, the motion of the boundaries and the invert is completely synchronous.

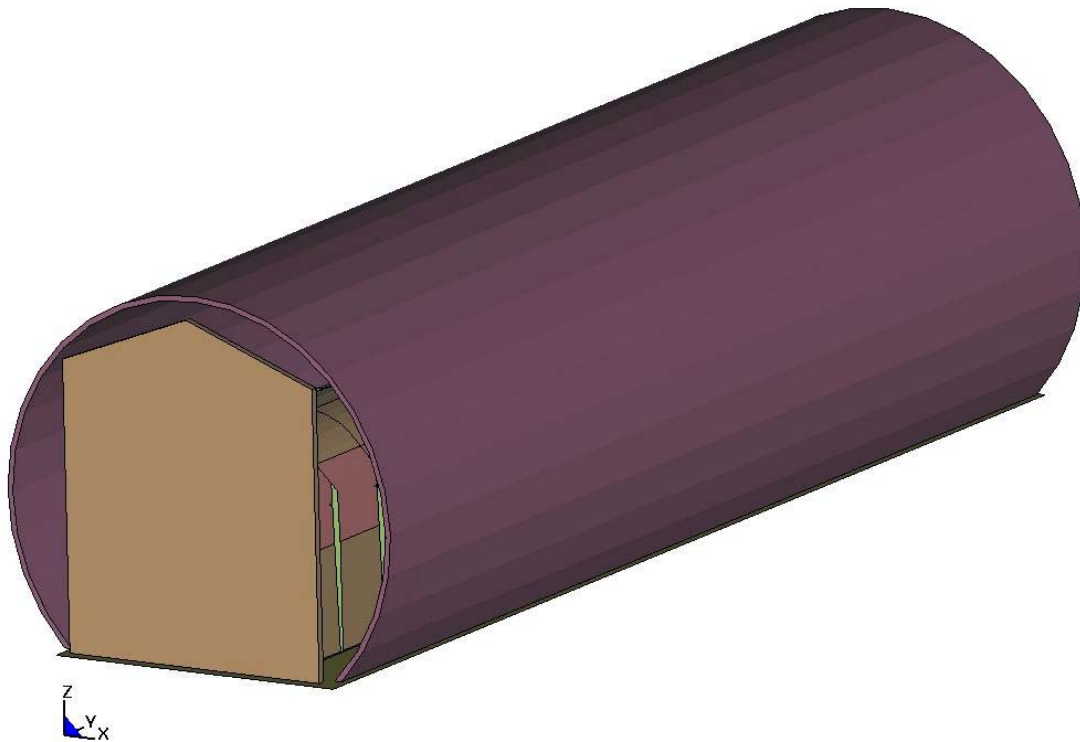


Figure 1. Setup for DS Vibratory Simulations

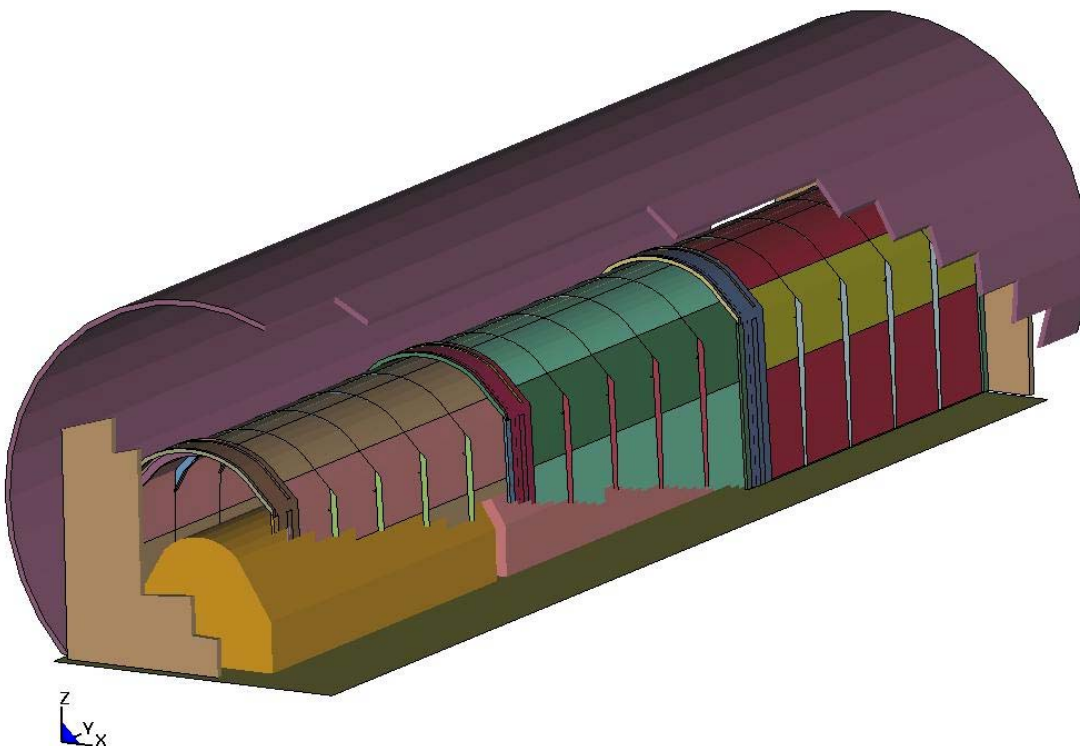


Figure 2. Cutaway View of Setup for DS Vibratory Simulations

The WPP assembly is a structure developed for computational convenience. The main purpose of WPP assemblies is to impose proper boundary conditions on the DSs (most importantly the middle DS) in both conservative (from the standpoint of the DS damaged area) and time-efficient manner. Thus, the structure of the 21-PWR WP and pallet is simplified by reducing their FE representation to a rigid thick-wall structure of uniform density (WPP assembly). The geometry of the WPP assembly is defined based on the contour of the WP mounted on the pallet (see Fig. 3). The most relevant outside dimensions of the WP mounted on the pallet are matched by FE representation and kept unchanged during the vibratory simulation (since the WP in this FE representation cannot move relative to the pallet [see Section 6.4.3 for detailed discussion]). The thickness of the WPP assembly is determined by using the material properties (including density) of Alloy 22, and matching the total masses of the WP and pallet as presented in References 24 and 22. The initial longitudinal distance between the neighboring WPP assemblies,  $0.1\text{ m}$ , is based on the initial longitudinal distance between the neighboring WP (Ref. 25, Table 2). The benefit of using this approach is to reduce the computer execution time while preserving the features of the problem most relevant to the structural response of the middle DS. (For further discussion of the WPP assembly see Section 6.4.2.)

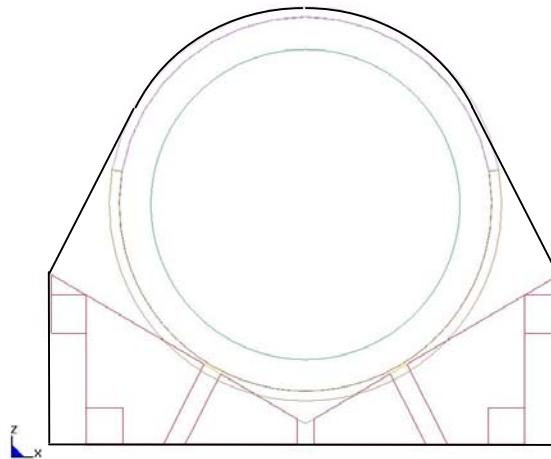


Figure 3. Contours of WPP Assembly and WP Mounted on Pallet

Three components of the ground-motion acceleration time history are simultaneously applied on the platform representing the invert surface. The invert surface is essentially unyielding (elastic). (This is just a formal LS-DYNA requirement; the same acceleration time history applied to all platform nodes result in zero deformation by definition). Externally applied momentum is transferred to all freestanding (unanchored) objects solely by the way of friction and impact.

The DSC (DS connector) support beams, the DSC connector guides, the DS connector guides, the support beam-connectors, the peripheral bulkheads, and the boundary walls are represented by 8-node solid (brick) elements. All other parts are represented by 4-node shell elements. In general, the shell elements are adequate for representation of structural components as long as their dominant mode of deformation is bending. (It is important to note that this analysis is focused on the DS plates; the stress state in other DS parts is of interest only to the extent it affects the DS-plates results.) The shell elements used for representation of the DS plates have five integration points

through the shell thickness. The use of shell elements in the FE representation of DS is further discussed in Section 6.4.2.

For the simulation of the DSs exposed to vibratory ground motion, the thickness of the DS plates is reduced by 2 mm (from 15 mm to 13 mm; see Assumption 3.10). It must be emphasized, though, that the objective of this calculation is not to rigorously evaluate the thickness reduction of the DS plates due to corrosion or the corrosion-acceleration effects. A depth of corroded layer of 2 mm is, therefore, a conservatism within the stated objective of this calculation (see Section 1). It should also be noted that the overall thickness of the parts of the DS plates covered by the internal and external support plates is conservatively reduced by 4 mm, implying the thickness reduction of 2 mm per plate at each location.

Contacts are specified between all parts that can interact. In absence of more specific data, the dynamic friction coefficients for all contacts are randomly sampled from a uniform distribution between 0.2 and 0.8 (see Assumption 3.7). One metal-to-metal friction coefficient and one metal-to-rock friction coefficient are sampled for each realization (see Table 1), and applied to all metal-to-metal and metal-to-rock contacts. In other words, the friction coefficients vary from realization to realization (random sampling) but all metal-to-metal contacts have the same friction coefficient in a specific realization regardless of the contact pair; the same applies to metal-to-rock contacts. Moreover, the functional friction coefficient used by LS-DYNA V960.1106 FE code is defined in terms of static and dynamic friction coefficients, and relative velocity of the surfaces in contact (Ref. 18, p. 6.9). The effect of the relative velocity of the surfaces in contact is introduced by the way of a fitting parameter - exponential decay coefficient. The variation of friction coefficient between the static and dynamic value as a function of relative velocity of the surfaces in contact is not available in literature for the materials used in this calculation. Therefore, it is not possible to objectively evaluate the exponential decay coefficient. Hence, the effect of the relative velocity of the surfaces in contact is neglected in these calculations by assuming that the functional friction coefficient and the static friction coefficient are equal to the dynamic friction coefficient. This approach provides the bounding set of results by minimizing the friction coefficient within the given FE-analysis framework (Assumption 3.8).

The stochastic (uncertain) input parameters for 15 realizations are listed in Table 1 (see Ref. 16, Table I-4). The values of the friction coefficients presented in Table 1 are, for the purpose of this calculation, presented (and used) with two significant digits. The ground motion (acceleration, velocity, and displacement) time histories are available in References 29, 30, and 31. (The time histories presented in these references are for the purpose of this study reduced. The time history cutoff and the simulation duration are discussed in detail in Section 5.2.1 [see Tables 2 and 3] and Attachment II.)

The FE representation is then used in LS-DYNA V960.1106 to perform a transient dynamic analysis of the interlocking DSs exposed to vibratory ground motion.

Table 1. Simulation Parameters

Realization Number	Ground Motion Number	Friction Coefficient (-)	
		Metal to metal	Metal to rock
1	7	0.80	0.34
2	16	0.33	0.49
3	4	0.50	0.62
4	8	0.60	0.22
5	11	0.20	0.24
6	1	0.27	0.69
7	2	0.71	0.60
8	13	0.56	0.54
9	10	0.55	0.36
10	9	0.36	0.41
11	5	0.42	0.67
12	6	0.65	0.73
13	12	0.75	0.31
14	14	0.29	0.45
15	3	0.46	0.78

The simulation is performed in two steps. First step is the vibratory part. During this computational phase the three components of ground-motion acceleration time history are simultaneously applied to all invert nodes. The stochastic (uncertain) input parameters for 15 simulations of events corresponding to annual frequencies of occurrence  $1 \cdot 10^{-6}$  1/yr and  $1 \cdot 10^{-7}$  1/yr are listed in Table 1 (Ref. 16, Table I-4). In the course of this vibratory simulation neither system damping nor contact damping (between the unanchored objects) are applied. This, admittedly conservative, approach is used in order to prevent unwanted interference of the damping with the rigid-body motion of unanchored structures that could contaminate results. The second step of the simulation is the post-vibratory relaxation. During this computational phase the motion of the invert nodes is constrained in all three directions, and the only load applied to freestanding objects is the acceleration of gravity. In the course of this phase the system damping is applied globally (to all objects). The goal of this step is to obtain steady-state results (i.e., residual stresses) in a reasonable time, and the purpose of the global system damping is to reduce this time as much as possible (see Section 5.2.2 for details). The specified duration (0.5 s) of this post-vibratory relaxation part of simulation is such to allow for the steady-state stresses to establish, which can be verified by visual inspection of the residual stress distributions by LS-POST V2.

The mesh of the FE representation is appropriately generated and refined in appropriate regions according to standard engineering practice. Thus, the accuracy and representativeness of the results of this calculation are deemed acceptable (see Section 6.4 and Attachments II and III for discussion of results). The uncertainties are taken into account by random sampling (from appropriate probability distributions) of the calculation inputs that are inherently stochastic (uncertain) and characterized by a large scatter of data (namely, ground-motion time histories and friction coefficients). The results are reasonable compared to the inputs and suitable for the intended use.

### 5.2.1 Ground-Motion Time History Cutoff

Structural calculations of DS exposed to vibratory ground motion are extremely computationally intense. This is not surprising having in mind:

- the complex FE representation (Section 5.2),
- the highly nonlinear nature of the problem (large deformation plasticity, friction, impacts, etc.),
- the small computational time step necessary to ensure convergence ( $\approx 1 \mu s$  or less, see d3hsp files in Attachment V), and
- the long durations of the ground-motion time histories ( $\approx 30 - 40 s$ , see Refs. 29, 30, and 31).

In order to obtain credible results in a reasonable time, it is necessary to reduce the duration of seismic excitation used in the simulation.

Therefore, most realizations at the annual frequency of occurrence  $1 \cdot 10^{-6} \text{ 1/yr}$  are terminated at time corresponding to 95 percent of the externally applied energy. (For brevity, the maximum time corresponding to 95 percent of energy of ground motion is, in the remainder of this document, called “95%-time”. Similarly the maximum time corresponding to 90 percent of energy of ground motion is called “90%-time”, and the minimum time corresponding to 5 percent of energy of ground motion is called “5%-time”. Note that all three time instances are determined by taking into account all three components of ground motion.) In two  $1 \cdot 10^{-6} \text{ 1/yr}$  realizations (number 11 and 15, see Attachment II) the termination time is extended beyond this 95%-energy cutoff to examine the effect of the cutoff (i.e., the ending time is larger than the 95%-time).

Table 2 presents the duration of each simulation, and characteristic times used to define the duration. The time in the fifth column is the starting time of the simulation. (In other words, the starting point of simulation [ $t = 0$ ] corresponds to this time in Reference 29.) If the starting time of the simulation is not zero, the three components of initial velocity, specified in LS-DYNA input file (see as an example Attachment V: 1E-6\RN1\seisDSiv.k, lines 460 through 462), correspond to this time in Reference 29. The starting time, for most realizations, corresponds to the beginning of the ground motion. The ending time is typically the 95%-time (see again Ref. 29). The calculated duration of the simulation is obtained by subtracting the starting time from the ending time.

As previously mentioned, the duration that is actually run during simulation is, in a couple of cases, different from the duration presented in Table 2. Specifically, the realizations 11 and 15 are extended beyond the 95%-time for the purpose of examining the damage-evolution trend as a function of time-history cutoff (see Attachment II).

Finally, Table 3 presents the duration and characteristic times for five  $1 \cdot 10^{-7} \text{ 1/yr}$  realizations performed in this study (see Reference 30). The most pronounced difference between  $1 \cdot 10^{-6} \text{ 1/yr}$  realizations and  $1 \cdot 10^{-7} \text{ 1/yr}$  realizations is that the latter are run only up to the time indicating unambiguously the DS separation.

Table 2. Duration and Characteristic Times Corresponding to Ground Motions at  
Annual Frequency of Occurrence  $1 \cdot 10^{-6} \text{ 1/yr}$

Ground Motion Number	5%-Time (s)	90%-Time (s)	95%-Time (s)	Starting Time (s)	Ending Time (s)	Duration of Simulation (s)	Realization Number
1	0.85	5.21	7.05	0	7.1	7.1	6
2	0.58	6.05	8.13	0	8.2	8.2	7
3	1.7	3.64	5.04	0	7.0	7.0	15
4	1.3	10.2	15.0	0	15.0	15.0	3
5	2.0	7.46	10.3	0	20.0	20.0	11
6	2.3	9.20	9.96	0	10.0	10.0	12
7	4.0	11.1	11.6	4.0	11.6	7.6	1
8	1.1	5.12	5.99	0	6.0	6.0	4
9	0.79	6.98	8.18	0	8.2	8.2	10
10	1.6	7.66	10.8	0	10.8	10.8	9
11	2.1	8.30	10.3	0	10.3	10.3	5
12	1.4	12.2	13.6	0	13.6	13.6	13
13	1.9	12.7	17.0	1.9	12.7	10.8	8
14	7.2	19.8	21.5	7.2	21.5	14.3	14
16	3.8	9.57	11.8	3.8	11.8	8.0	2

The duration of simulation presented in seventh column of Table 3 represent termination time without prior numerical instability. Continuation of the simulation beyond this time (i.e., extension of the duration of simulation) results in the numerical instability for all realizations presented in Table 3, with exception of realization number 5. All other  $1 \cdot 10^{-7} \text{ 1/yr}$  realizations, not presented in Table 3, also failed due to the numerical instability but without the DS separation prior to failure (see Section 6.3). Therefore, no conclusion can be based on these runs and they are not presented in this document.

Table 3. Duration and Characteristic Times Corresponding to Ground Motions at  
Annual Frequency of Occurrence  $1 \cdot 10^{-7} \text{ 1/yr}$

Ground Motion Number	5%-Time (s)	90%-Time (s)	95%-Time (s)	Starting Time (s)	Ending Time (s)	Duration of Simulation (s)	Realization Number
1	1.3	6.5	7.5	0	3.9	3.9	6
2	0.80	5.8	7.4	0	3.1	3.1	7
9	0.70	6.7	8.0	0	3.6	3.6	10
11	2.1	8.5	10.3	2.1	10.3	8.2	5
13	1.9	15.2	19.5	1.9	5.0	3.1	8



### 5.2.2 System Damping

In order to obtain steady-state results (i.e., residual stresses) in a reasonable time, it is necessary to apply damping in the course of the post-vibratory relaxation. The system damping is applied globally.

As discussed in Reference 17 (Section 28.2), the most appropriate damping constant for the system is usually the critical damping constant. Therefore,

$$DC = 2 \cdot \omega_{\min} = 2 \cdot 58 = 116 \text{ rad/s}$$

Where  $\omega_{\min} = 2 \cdot \pi \cdot 9.3 \approx 58 \text{ rad/s}$  is the minimum circular non-zero frequency of the DS (see Attachment V [Modal Analysis\drip2MOD.out, line #7792] for the minimum non-zero frequency of 9.3 Hz). Keeping in mind that the objects we are dealing with in this study are unanchored, the damping constant is conservatively reduced to  $DC = 50 \text{ rad/s}$ , to avoid over-damping of the system.

## 6. RESULTS

Attachment V includes the input files and results files that show execution of the programs occurred correctly. The damaged areas have been obtained by interactively using the postprocessor LSPOST V2. LS-POST V2 is also used for visual inspection of the DS configuration during the simulation in order to determine whether or not there is DS separation.

Recall that the area of the DS plates where the residual 1<sup>st</sup> principal stress exceeds certain limit is, for brevity, called “damaged area” throughout this document (see Section 1).

### 6.1 EVENT WITH ANNUAL FREQUENCY OF OCCURRENCE $5 \cdot 10^{-4}$ 1/yr □

The event with annual frequency of occurrence  $5 \cdot 10^{-4}$  1/yr is evaluated at temperature of 150 °C. The simulation started at 3.0 s of the ground motion time history (corresponding to 5 percent of energy of ground motion), and the ending time was 15 s (corresponding to 65 percent of energy of ground motion) (see Ref. 31). This duration covered the most intense period of the ground motion time history. Further extension of the simulation is considered unnecessary based on the results presented in this section.

The ground motion with annual frequency of occurrence  $5 \cdot 10^{-4}$  1/yr is much less intense than its  $1 \cdot 10^{-6}$  1/yr counterparts (not to mention  $1 \cdot 10^{-7}$  1/yr). Consequently, the extent of rigid-body motion during the  $5 \cdot 10^{-4}$  1/yr vibratory simulation is very limited and the maximum residual 1<sup>st</sup> principal stress is less than 3 MPa (see Fig. 4).

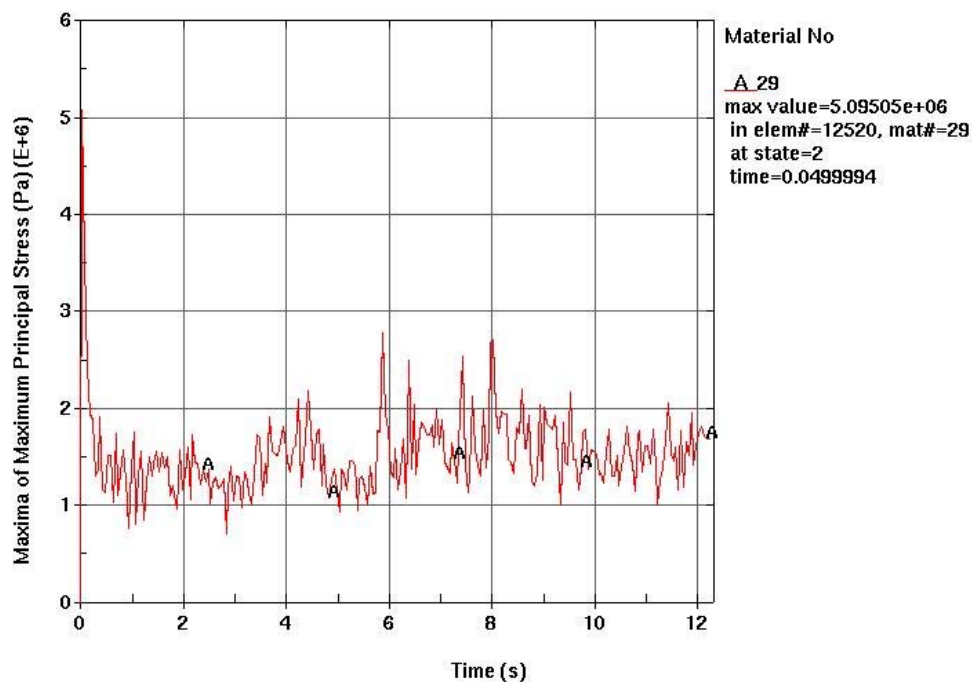


Figure 4. Maximum 1<sup>st</sup> Principal Stress Time History for DS Plates

The singular behavior at the onset of simulation is nonphysical (unrelated to the nature of the problem). It is a consequence of a small initial gap between the DS and the invert in the FE representation. Thus, the stress peak at the beginning of the simulation results from the settling of the DS on the invert and should be disregarded (see detailed discussion of the similar effect in Ref. 13, Section 6.3.1).

In summary, it can be concluded that the DS plates remain undamaged throughout the  $5 \cdot 10^{-4}$  1/yr event (i.e., the DS-plate area exceeding the established stress threshold is zero).

## 6.2 EVENTS WITH ANNUAL FREQUENCY OF OCCURRENCE $1 \cdot 10^{-6}$ 1/yr □

The events at annual frequency of occurrence  $1 \cdot 10^{-6}$  1/yr are evaluated at temperature of 150 °C.

There is no DS separation during the simulation of vibratory ground motion in any  $1 \cdot 10^{-6}$  1/yr realization. It must be stressed, though, that realization number 6 could be a subject of debate when it comes to DS separation and is therefore discussed herein. According to the final configuration of DSs presented in Figure IV-8, one of the peripheral DSs is skewed with respect to the middle DS to the extent that there is an overlap on one side (of that end) that exceeds the ordinary overlap in the connector region. Keeping in mind that: 1) the overlap is extremely small and, thus, inconsequential from the standpoint of WP protection (it would not expose the WP to rockfall); 2) the longitudinal wall does not give full credit to the DS connector assembly when it comes to the prevention of DS separation; and 3) the DS-separation effect is significantly amplified by the representation of the peripheral DS as rigid, it seems reasonable to neglect this small DS overlap.

The damaged area is evaluated only in the DS plates of the middle DS. Throughout this document the damaged area is also presented as a fraction of the total area of the DS plates. This area is  $38.2667 \text{ m}^2$ , as calculated in Reference 11 (Section 5.6).

Table 4 presents the damaged area resulting from 14 realizations at the annual frequency of occurrence of  $1 \cdot 10^{-6}$  1/yr that were completed without any numerical problems. Realization number 13 failed due to numerical instability. The damaged area is evaluated based on the residual 1<sup>st</sup> principal stress plot (see Section 1) by using postprocessor LSPOST V2.

According to results presented in Table 4, the damaged area for  $1 \cdot 10^{-6}$  1/yr realizations vary within a wide range. The maximum and minimum damaged area correspond to 2.13 percent (realization number 9) and 0.12 percent (realization number 14) of the total area of the DS plates, respectively. The average damaged area is 0.70 percent of the total area of the DS plates. Note that realization number 9, characterized by the largest damaged area, is conspicuous not only for the large number of WP-DS impacts but also for their intensity (see Ref. 13, Section 6.1.3).

Table 4. Damaged Area at Annual Frequency of Occurrence of  $1 \cdot 10^{-6}$  1/yr

Realization Number	Ground Motion Number	Damaged Area ( $m^2$ ; % of total area)
1	7	0.113; 0.30%
2	16	0.055; 0.14%
3	4	0.248; 0.65%
4	8	0.105; 0.27%
5	11	0.257; 0.67%
6	1	0.427; 1.12%
7	2	0.479; 1.25%
8	13	0.100; 0.26%
9	10	0.814; 2.13%
10	9	0.192; 0.50%
11	5	0.456; 1.19%
12	6	0.376; 0.98%
14	14	0.0456; 0.12%
15	3	0.0989; 0.26%

### 6.3 EVENTS WITH ANNUAL FREQUENCY OF OCCURRENCE $1 \cdot 10^{-7}$ 1/yr □

The ground motions at annual frequency of occurrence of  $1 \cdot 10^{-7}$  1/yr are much more intense than their counterparts at  $1 \cdot 10^{-6}$  1/yr. As an example the maximum peak ground acceleration reached in ground motion 9 is approximately  $34 \cdot g$  ( $g = 9.81 \text{ m/s}^2$  being acceleration of gravity), while the maximum peak ground velocity in ground motion 3 is approximately  $16 \text{ m/s}$  (see Ref. 30). Hence, the kinematics of the unanchored repository components is characterized by plethora of rigid-body motion and high-speed impacts (see Figs. IV-1 through IV-7). As a consequence of this high-intensity loading only one  $1 \cdot 10^{-7}$  1/yr realization (number 5) terminated without numerical instability. The objective of  $1 \cdot 10^{-7}$  1/yr realizations is limited, therefore, only to reporting the separation of DS segments in the course of simulation before the numerical instability occurs.

All five  $1 \cdot 10^{-7}$  1/yr realizations presented in Table 3 indicate the DS separation. The extent of the overlap of the DSs is illustrated by Figures IV-3 through IV-7. It is extremely important to recognize, though, that none of these simulations, with exception of realization number 5, reached 95%-time. Thus, although it is acceptable to claim that the DS separation occurred in all these realizations, it is not possible to determine a meaningful upper bound for the extent of this separation. The previously mentioned exception is realization number 5 that is terminated at 95%-time without numerical instability. According to Figure IV-3 the maximum extent of the DS overlap for this realization is less than 12 percent of the total DS length. This is the only overlap extent that can be determined with reasonable certainty.

## 6.4 SOME COMMENTS ON THE VIBRATORY SIMULATIONS

The purpose of this section is to emphasize some complexities of the simulation of the unanchored structures exposed to the vibratory ground motion, and to discuss their effects on the calculation results presented in this document.

The complexities inherent to the nature of the problem (enumerated at the beginning of Section 6.4.1) render a detailed FE representation prohibitively time-consuming. Consequently, it is necessary to simplify the FE representation without adversely affecting the results. All simplifications introduced in the course of development of the FE representation are generally conservative from the standpoint of the estimate of the damaged area. This conservatism is necessitated by the reasons of the computational economy.

It is also important to recognize the conservatism of the criterion used to define the damaged area (independently of the conservatism related to the choice of the residual stress threshold, which is beyond the scope of this work). Specifically, the method used to evaluate the damaged area conservatively neglects the residual stress distribution across the thickness of the DS plates (i.e., it does not account for the possibility of crack arrest once the crack is nucleated).

### 6.4.1 Some Complexities Inherent in the Nature of the Problem

The structural calculations of the interlocking DSs exposed to the vibratory ground motion are beset with complexities inherent in the nature of the problem.

First, the externally applied loads (i.e., the ground motion time histories) are extremely intense. This causes a variety of problems even at  $1 \cdot 10^{-6}$  1/yr level but is especially troublesome at  $1 \cdot 10^{-7}$  1/yr.

Second, the phenomena are highly nonlinear. Momentum is transferred among the repository emplacement drift and unanchored repository components (DS and WPP assembly) solely by the way of friction and impact. Geometrical nonlinearity (large deformations) is coupled with nonlinear constitutive behavior of materials (elastoplastic behavior with kinematic hardening).

Third, capturing both the large-scale kinematics and the occasional small-scale deformations (i.e., localized impacts) imposes extremely difficult meshing requirements.

Fourth, the extraordinary meshing requirements are, together with the intensity of ground motion, mainly responsible for the very small time step (approximately a microsecond, depending on annual frequency of occurrence and particular ground-motion time history). The very small time step is, in turn, necessary for simulation of a long-duration event ( $\approx 30 - 40$  s).

All discussed complexities impose extreme computational requirements. Consequently, it is requisite to sacrifice some details while retaining all pertinent features of the problem. The two most important simplifications were: 1) use of shell elements for representation of not only the DS plates but also some of the support structure, and 2) representation of the WP and pallet as a single entity (WPP assembly). These are discussed in the following sections.

### 6.4.2 Use of Shell Elements in FE Representation

As discussed in Section 5.2, the time-efficient shell elements are used in the FE representation of the DS not only to represent the DS plates but also some of their support structure (most notably the bulkheads and support beams, see Attachment I). It is necessary to discuss a few aspects of the representation of the DS-plate support structure by shell elements.

First, this representation underestimates bending stiffness of the support structure, which may result in somewhat exaggerated deformation of the DS plates and, consequently, in a conservative estimate of the DS damaged area.

Second, the connections between the DS parts represented by shell elements (for example, bulkheads and DS plates) are established by sharing the nodes on the intersection lines (or planes). These common nodes between the connected DS parts somewhat exaggerate the role of the shell reference (middle) surface compared to the actual physical situation when the connection is established by the way of the surfaces of the connected parts. In other words, the middle shell surface close to the connections may take over, in some degree, the role of the actual physical surface of the connected parts. But the effect of this aspect of the use of the shell elements is conservatively bounded as long as the shell reference (middle) surface is taken into account in the evaluation of the damaged area.

Third, the connections between the DS-plate support structure and the DS plates are discontinuities that serve as preferential sites for development of the damaged area (see Ref. 11, Figures II-6 and II-7 as an example). The underestimated bending stiffness of the DS support structure is not, in this case, necessarily conservative. It must be recognized, though, that this effect is not pronounced when the loading of the DS is more uniform. (Figures II-6 and II-7 in Reference 11, referring to the rockfall on DS, are examples of extremely localized type of deformation.) For the moderate intensities of ground motion, such as those characterizing  $1 \cdot 10^{-6}$  1/yr realizations, the DS kinematics is such that the distribution of the impact load from the DS-invert interaction is relatively uniform. In the cases when DS impacts the invert with some angle of inclination, the effect of more localized loading is captured by the DSC support beams and the support beam-connectors that are represented by solid elements. Similarly, in the case of the interaction between DS and WPP assembly, if their kinematics is such to cause the inclined (i.e., localized) impact, the impact location is necessarily close to the DS end, and the effect of discontinuity is again captured by the DSC support beams and the support beam-connectors.

Finally, it is important to recognize that this discussion applies to simulations at annual frequencies of occurrence of  $5 \cdot 10^{-4}$  1/yr and  $1 \cdot 10^{-6}$  1/yr; as previously mentioned, for  $1 \cdot 10^{-7}$  1/yr realizations only the kinematics of the DSs is of interest.

### 6.4.3 Representation of WP and Pallet by WPP Assembly

As discussed in Section 5.2, the structures of the 21-PWR WP and pallet are, for the purpose of these calculations, simplified by reducing their FE representation to a rigid thick-wall structure of uniform density (WPP assembly). The main purpose of WPP assemblies is to ensure boundary conditions for the DSs (most importantly the middle DS) that are conservative (from the standpoint of the DS damaged area) and time-efficient.

In adopting this approach it is important to acknowledge the results presented in Reference 13. These results indicate that there is no WP-DS interaction at the annual frequency of occurrence of  $5 \cdot 10^{-4}$  1/yr (Ref. 13, Section 6.3), and that this interaction at the annual frequency of occurrence of  $1 \cdot 10^{-6}$  1/yr occurs rarely and is characterized by relatively modest impact speeds (mostly between 1 m/s and 2 m/s) (Ref. 13, Section 6.1.3). On the other hand, the interaction between the pallet and the DS takes place more frequently than the interaction between the WP and the DS due to the much smaller clearance between the former two repository components compared to the one between the latter two components. Thus, the representation of the WP and the pallet as a single entity – with mass equal the cumulative mass of both repository components – is conservative from the standpoint of the damaged area resulting from the WP-DS and pallet-DS interactions for simulations at annual frequencies of occurrence of  $5 \cdot 10^{-4}$  1/yr and  $1 \cdot 10^{-6}$  1/yr.

In the case of realizations at annual frequency of occurrence of  $1 \cdot 10^{-7}$  1/yr, the kinematics of unanchored repository components is more complex (see, for example, Attachment IV and Ref. 13, Section 6.2.3) due to the much more intense ground motion. Thus, the representation of the WP and the pallet as a single structural entity (WPP assembly) may not capture with sufficient accuracy the damaged area of the DS plates. Nonetheless, the FE representation is still adequate since all  $1 \cdot 10^{-7}$  1/yr realizations whose results are presented in this document end with the DS separation and the damaged area is not evaluated (since it is not of primary importance).

Finally, it must be noted that the WPP assembly is likely cause of the contact instabilities that halt the  $1 \cdot 10^{-7}$  1/yr realizations. As discussed previously, this assembly is represented as a thick-walled structure with total mass of the WP and the pallet being uniformly distributed over all WPP-assembly nodes. Since WPP assembly is relatively coarsely meshed and it does not have any interior structure, each WPP-assembly node has extremely large nodal mass. Consequently, in the case of a high-speed impact between the WPP assembly and the DS, instability may occur as a result of enormous momentum being transferred from the WPP assembly to a very small portion of the DS. (The localized nature of the transfer is promoted by the fact that the WPP assembly is represented as rigid.) This problem can be addressed by appropriate modifications of the FE representation (for example, by adding some interior structure into the WPP assembly and by refining its FE mesh). These modifications are not deemed necessary in this study since the numerical instability does not affect the conservatively bounding results reported for the  $1 \cdot 10^{-7}$  1/yr calculations in this document.

#### 6.4.4 Effect of Time-History Cutoff

The cutoff of ground-motion time history is discussed in detail in Section 5.2 and Attachment II. The effect of the cutoff on the calculation results is negligible according to the detailed study presented in Attachment II. Energy plots in Figure 5 support this claim.

Figure 5 presents energies (total, kinetic, internal, and hourglass) for realization number 11 at  $1 \cdot 10^{-6}$  1/yr annual frequency of occurrence. The kinetic energy plot indicates that practically there is no motion by the end of simulation. Also, the total energy does not increase substantially anymore. Both of these observations support the claim that the further ground motion cannot substantially change the results presented in this document. (Note also that the hourglass energy is negligible compared to the total energy of the system [for the hourglass control, see Ref. 17, page 3.4].)

#### 6.4.5 Mesh Sensitivity

Finally, the mesh-sensitivity study presented in Attachment III indicates that the DS mesh size does not have notable effect on the calculation results from the viewpoint of the results presented in this document.

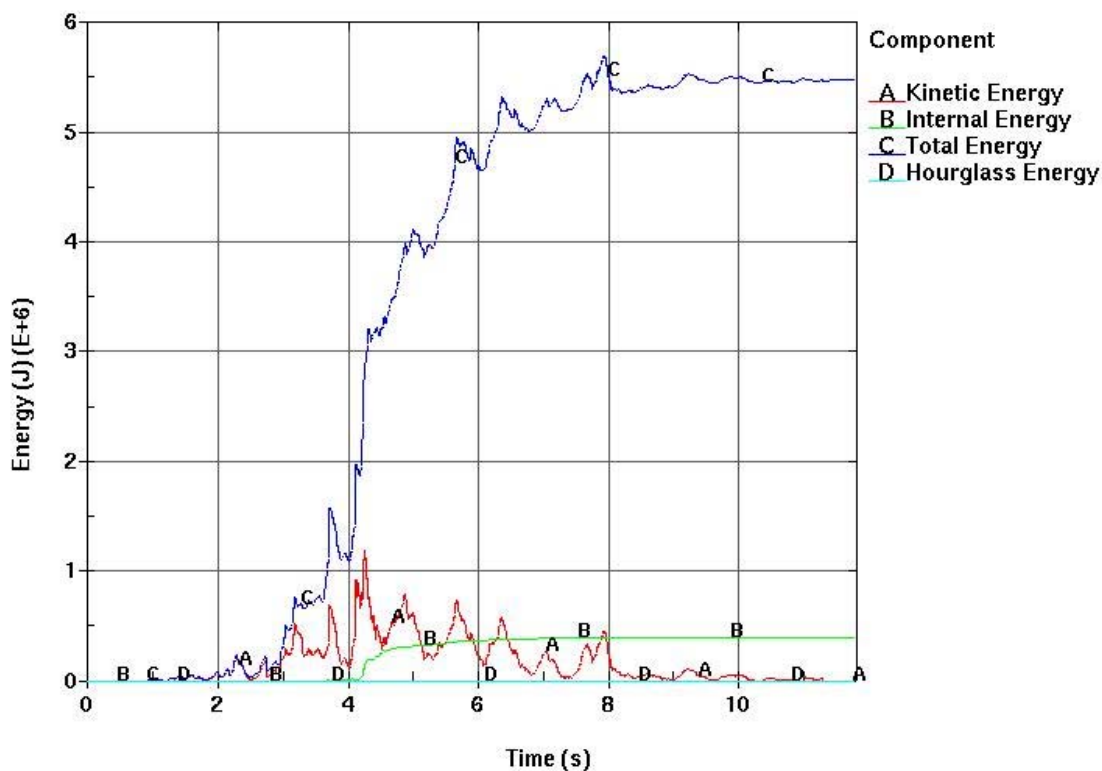


Figure 5. Energy Plots for Realization Number 11 at Annual Frequency of Occurrence  $1 \cdot 10^{-6}$  1/yr



## 7. REFERENCES

1. AP-3.12Q, Rev. 2, ICN 0. *Design Calculations and Analyses*. Washington, D.C.: U.S. Department of Energy, Office of Civilian Radioactive Waste Management. ACC: DOC.20030403.0003.
2. AP-SI.1Q, Rev. 5. *Software Management*. Washington, D.C.: U.S. Department of Energy, Office of Civilian Radioactive Waste Management. ACC: DOC.20030422.0012.
3. MO0010SPASIL02.002. Silica Adjusted General Corrosion Rates of Alloy 22 and Titanium Grade 7. Submittal date: 10/10/2000.
4. DOE (U.S. DOE (U.S. Department of Energy) 2003. *Quality Assurance Requirements and Description*. DOE/RW-0333P, Rev. 13. Washington, D.C.: U.S. Department of Energy, Office of Civilian Radioactive Waste Management. ACC: DOC.20030422.0003.
5. CRWMS M&O 2001. *Classification of the MGR Emplacement Drift System*. ANL-EDS-SE-000001 REV 01. Las Vegas, Nevada: CRWMS M&O. ACC: MOL.20010227.0043.
6. BSC (Bechtel SAIC Company) 2002. *Software Code: ANSYS*. V5.6.2. HP-UX 11.00. 10364-5.6.2-01.
7. BSC (Bechtel SAIC Company) 2002. *Software Code: LS-DYNA*. V960.1106. HP9000. 10300-960.1106-00.
8. McKenzie, D.G., IV. 2002. *Waste Package Design Methodology Report*. TDR-MGR-MD-000006 REV 02. Las Vegas, Nevada: Bechtel SAIC Company. ACC: MOL.20020404.0085.
9. MO0003RIB00071.000. Physical and Chemical Characteristics of Alloy 22. Submittal date: 03/13/2000.
10. ASM (American Society for Metals) 1980. *Properties and Selection: Stainless Steels, Tool Materials and Special-Purpose Metals*. Volume 3 of *Metals Handbook*. 9th Edition. Benjamin, D., ed. Metals Park, Ohio: American Society for Metals. TIC: 209801.
11. BSC (Bechtel SAIC Company) 2003. *Drip Shield Structural Response to Rock Fall*. 000-00C-TED0-00500-000-00A. Las Vegas, Nevada: Bechtel SAIC Company. ACC: ENG.20030327.0001.
12. ASME (American Society of Mechanical Engineers) 2001. *2001 ASME Boiler and Pressure Vessel Code (includes 2002 addenda)*. New York, New York: American Society of Mechanical Engineers. TIC: 251425.
13. BSC (Bechtel SAIC Company) 2003. *Structural Calculations of Waste Package Exposed to Vibratory Ground Motion*. 000-00C-EBS0-00300-000-00B. Las Vegas, Nevada:

- Bechtel SAIC Company. ACC: ENG.20030520.0003.
14. MO0303SPARESST.000. Residual Stress Failure Criteria for Seismic Damage Models of the Drip Shield and Waste Package. Submittal date: 03/04/2003.
  15. ASM International 1990. *Properties and Selection: Nonferrous Alloys and Special-Purpose Materials*. Volume 2 of *ASM Handbook*. Formerly 10th Edition, Metals Handbook. 5th Printing 1998. [Materials Park, Ohio]: ASM International. TIC: 241059.
  16. MO0301SPASIP27.004. Sampling of Stochastic Input Parameters for Rockfall Calculations and for Structural Response Calculations Under Vibratory Ground Motions. Submittal date: 01/15/2003.
  17. Hallquist, J.O. 1998. *LS-DYNA, Theoretical Manual*. Livermore, California: Livermore Software Technology Corporation. TIC: 238997.
  18. Livermore Software Technology Corporation. 2001. *LS-DYNA Keyword User's Manual*. Version 960. Two volumes. Livermore, California: Livermore Software Technology Corporation. TIC: 252119.
  19. MO0003RIB00073.000. Physical and Chemical Characteristics of TI Grades 7 and 16. Submittal date: 03/13/2000.
  20. CRWMS M&O 2000. *Calculation of General Corrosion Rate of Drip Shield and Waste Package Outer Barrier to Support WAPDEG Analysis*. CAL-EBS-PA-000002 REV 01. Las Vegas, Nevada: CRWMS M&O. ACC: MOL.20001024.0075.
  21. BSC (Bechtel SAIC Company) 2001. *Repository Multiple Waste Package Thermal Calculation*. CAL-WIS-TH-000010 REV 00. Las Vegas, Nevada: Bechtel SAIC Company. ACC: MOL.20010814.0330.
  22. BSC (Bechtel SAIC Company) 2003. *Emplacement Pallet*. 000-MW0-TEP0-00101-000-00A, and -00102-000-00A. 2 Sheets. Las Vegas, Nevada: Bechtel SAIC Company. ACC: ENG.20030205.0007; ENG.20030205.0008.
  23. MO9808RIB00041.000. Reference Information Base Data Item: Rock Geomechanical Properties. Submittal date: 08/05/1998.
  24. BSC (Bechtel SAIC Company) 2001. *Repository Design, Waste Package, Project 21-PWR Waste Package with Absorber Plates, Sheet 1 of 3, Sheet 2 of 3, and Sheet 3 of 3*. DWG-UDC-ME-000001 REV A. Las Vegas, Nevada: Bechtel SAIC Company. ACC: MOL.20020102.0174.
  25. Williams, N.H. 2002. "Thermal Inputs for Evaluations Supporting TSPA-LA." Interoffice memorandum from N.H. Williams (BSC) to Distribution, September 16, 2002, 0911024159, with enclosures. ACC: MOL.20021008.0141.

26. Avallone, E.A. and Baumeister, T., III, eds. 1987. *Marks' Standard Handbook for Mechanical Engineers*. 9th Edition. New York, New York: McGraw-Hill. TIC: 206891.
27. DeGrassi, G. 1992. *Review of the Technical Basis and Verification of Current Analysis Methods Used to Predict Seismic Response of Spent Nuclear Fuel Racks*. NUREG/CR-5912. Washington, DC: U.S. Nuclear Regulatory Commission. TIC: 253724.
28. MO0003RIB00079.000. Rock Mechanical Properties. Submittal date: 03/30/2000.
29. MO0301TMHIS106.001. Acceleration, Velocity, and Displacement Time Histories for the Repository Level at 10-6 Annual Exceedance Frequency.. Submittal date: 01/28/2003.
30. MO0211AVTMH107.001. Acceleration, Velocity, and Displacement Spectrally Conditioned Time Histories for the Repository Level at 10-7 Annual Exceedance Frequency. Submittal date: 11/12/2002.
31. MO0211TMHIS104.002. Acceleration, Velocity, and Displacement Time Histories for the Repository Level at 5X10-4 Annual Exceedance Frequency. Submittal date: 11/14/2002.
32. Nicholas, T. 1980. *Dynamic Tensile Testing of Structural Materials Using A Split Hopkinson Bar Apparatus*. AFWAL-TR-80-4053. Wright-Patterson Air Force Base, Ohio: Air Force Wright Aeronautical Laboratories. TIC: 249469.

## 8. ATTACHMENTS

Attachment I (24 pages): Design sketch (*Interlocking Drip Shield* [SK-0230 REV 00, 24 sheets])

Attachment II (2 pages): Effect of Acceleration Time History Cutoff on Results

Attachment III (1 page): Mesh Objectivity

Attachment IV (12 pages): Plots

Attachment V (2 Compact Discs): ANSYS V5.6.2 and LS-DYNA V960.1106 electronic files

Table 5 provides a list of files submitted on compact discs as Attachment V.

Table 5. List of Electronic Files in Attachment V

### CONTENT OF CD1

Directory			
File name	Size (kB)	Date of Creation	Time
<b>1E-6\FER</b>			
drip2.inp	41	04/16/2003	01:55 pm
drip2.out	292	04/16/2003	01:55 pm
drip2A.inp	38	04/16/2003	01:55 pm
drip2A.out	261	04/16/2003	01:55 pm
drip2B.inp	38	04/16/2003	01:55 pm
drip2B.out	260	04/16/2003	01:55 pm
<b>1E-6\Refined Mesh\FER</b>			
drip2A.inp	38	04/16/2003	01:54 pm
drip2A.out	261	04/16/2003	01:54 pm
drip2B.inp	38	04/16/2003	01:54 pm
drip2B.out	260	04/16/2003	01:54 pm
drip2rm2.inp	41	04/16/2003	01:54 pm
drip2rm2.out	303	04/16/2003	01:54 pm
<b>1E-6\Refined Mesh\RN10</b>			
a9h1.dat	26	04/16/2003	01:12 pm
a9h2.dat	26	04/16/2003	01:12 pm
a9v.dat	28	04/16/2003	01:12 pm
constraint.dat	18	04/16/2003	01:12 pm
d3hsp	11066	04/16/2003	01:12 pm
d3hsp1	154	04/16/2003	01:12 pm
d3plot	14500	04/16/2003	01:12 pm
d3plot175	11289	04/16/2003	01:12 pm
element1.inc	1650	04/16/2003	02:02 pm
element2.inc	138	04/16/2003	02:02 pm
element3.inc	138	04/16/2003	02:02 pm
element4.inc	115	04/16/2003	02:02 pm
messag	12	04/16/2003	01:12 pm
messag0	91	04/16/2003	01:12 pm
nodes1.inc	1799	04/16/2003	02:02 pm
nodes2.inc	157	04/16/2003	02:02 pm
nodes3.inc	157	04/16/2003	02:02 pm
nodes4.inc	134	04/16/2003	02:02 pm
nodese15.inc	6	04/16/2003	02:02 pm
nodese16.inc	1	04/16/2003	02:02 pm
nodese17.inc	1	04/16/2003	02:02 pm

Title: Structural Calculations of Drip Shield Exposed to Vibratory Ground Motion

Document Identifier: 000-00C-PEC0-00100-000-00A

Page 29 of 40

nodese18.inc	1	04/16/2003	02:02 pm
nodese19.inc	1	04/16/2003	02:02 pm
nodeset.inc	21	04/16/2003	02:02 pm
nodeset1.inc	4	04/16/2003	02:02 pm
nodeset2.inc	1	04/16/2003	02:02 pm
nodeset3.inc	1	04/16/2003	02:02 pm
relaxDSs.k	1	04/16/2003	01:12 pm
segmen18.inc	3	04/16/2003	02:02 pm
segmen19.inc	9	04/16/2003	02:02 pm
seisDS.k	18	04/16/2003	01:12 pm
<b>1E-6\RN1</b>			
acc7h1.dat	26	04/16/2003	01:30 pm
acc7h2.dat	26	04/16/2003	01:30 pm
acc7v.dat	25	04/16/2003	01:30 pm
constraint.dat	18	04/16/2003	01:30 pm
d3hsp	9887	04/16/2003	01:30 pm
d3hsp1	155	04/16/2003	01:30 pm
d3plot	14086	04/16/2003	01:30 pm
d3plot82	6164	04/16/2003	01:30 pm
element1.inc	717	04/16/2003	02:06 pm
element2.inc	138	04/16/2003	02:06 pm
element3.inc	138	04/16/2003	02:06 pm
element4.inc	115	04/16/2003	02:06 pm
messag	13	04/16/2003	01:30 pm
messag0	72	04/16/2003	01:30 pm
nodes1.inc	798	04/16/2003	02:06 pm
nodes2.inc	157	04/16/2003	02:06 pm
nodes3.inc	157	04/16/2003	02:06 pm
nodes4.inc	134	04/16/2003	02:06 pm
nodese15.inc	2	04/16/2003	02:06 pm
nodese16.inc	1	04/16/2003	02:06 pm
nodese17.inc	1	04/16/2003	02:06 pm
nodese18.inc	1	04/16/2003	02:06 pm
nodese19.inc	1	04/16/2003	02:06 pm
nodeset.inc	21	04/16/2003	02:06 pm
nodeset1.inc	3	04/16/2003	02:06 pm
nodeset2.inc	1	04/16/2003	02:06 pm
nodeset3.inc	1	04/16/2003	02:06 pm
relaxDSs.k	1	04/16/2003	01:30 pm
segmen18.inc	3	04/16/2003	02:06 pm
segmen19.inc	9	04/16/2003	02:06 pm
seisDSiv.k	18	04/16/2003	01:30 pm
<b>1E-6\RN10</b>			
a9h1.dat	26	04/16/2003	01:11 pm
a9h2.dat	26	04/16/2003	01:11 pm
a9v.dat	28	04/16/2003	01:11 pm
constraint.dat	18	04/16/2003	01:11 pm
d3hsp	7709	04/16/2003	01:11 pm
d3hsp1	152	04/16/2003	01:11 pm
d3plot	14086	04/16/2003	01:10 pm
d3plot88	6164	04/16/2003	01:10 pm
element1.inc	717	04/16/2003	01:56 pm
element2.inc	138	04/16/2003	01:56 pm
element3.inc	138	04/16/2003	01:56 pm
element4.inc	115	04/16/2003	01:56 pm
messag	10	04/16/2003	01:11 pm
messag0	67	04/16/2003	01:11 pm
nodes1.inc	798	04/16/2003	01:56 pm
nodes2.inc	157	04/16/2003	01:56 pm

Title: Structural Calculations of Drip Shield Exposed to Vibratory Ground Motion

Document Identifier: 000-00C-PEC0-00100-000-00A

Page 30 of 40

nodes3.inc	157	04/16/2003	01:56 pm
nodes4.inc	134	04/16/2003	01:56 pm
nodeset1.inc	21	04/16/2003	01:56 pm
nodeset1.inc	3	04/16/2003	01:56 pm
nodeset2.inc	184	04/16/2003	01:56 pm
nodeset3.inc	4	04/16/2003	01:56 pm
nodeset4.inc	2	04/16/2003	01:56 pm
nodeset5.inc	1	04/16/2003	01:56 pm
relaxDSs.k	1	04/16/2003	01:11 pm
segmen18.inc	3	04/16/2003	01:56 pm
segmen19.inc	9	04/16/2003	01:56 pm
seisOXO.k	11	04/16/2003	01:11 pm
<b>1E-6\RN11</b>			
element1.inc	717	04/16/2003	01:58 pm
element2.inc	138	04/16/2003	01:58 pm
element3.inc	138	04/16/2003	01:58 pm
element4.inc	115	04/16/2003	01:58 pm
nodes1.inc	798	04/16/2003	01:58 pm
nodes2.inc	157	04/16/2003	01:58 pm
nodes3.inc	157	04/16/2003	01:58 pm
nodes4.inc	134	04/16/2003	01:58 pm
nodes15.inc	2	04/16/2003	01:58 pm
nodes16.inc	1	04/16/2003	01:58 pm
nodes17.inc	1	04/16/2003	01:58 pm
nodes18.inc	1	04/16/2003	01:58 pm
nodes19.inc	1	04/16/2003	01:58 pm
nodeset.inc	21	04/16/2003	01:58 pm
nodeset1.inc	3	04/16/2003	01:58 pm
nodeset2.inc	1	04/16/2003	01:58 pm
nodeset3.inc	1	04/16/2003	01:58 pm
segmen18.inc	3	04/16/2003	01:58 pm
segmen19.inc	9	04/16/2003	01:58 pm
<b>1E-6\RN11\LongRun</b>			
ac5h1.dat	54	04/16/2003	01:20 pm
ac5h2.dat	54	04/16/2003	01:20 pm
ac5v.dat	49	04/16/2003	01:20 pm
constraint.dat	18	04/16/2003	01:20 pm
d3hsp	7944	04/16/2003	01:20 pm
d3hsp1	154	04/16/2003	01:20 pm
d3hsp2	46	5/12/2003	03:54 pm
d3hsp3	40	5/12/2003	03:54 pm
d3hsp4	40	5/12/2003	03:54 pm
d3hsp5	62	5/12/2003	03:54 pm
d3hsp6	154	5/12/2003	03:54 pm
d3plot	14086	04/16/2003	01:20 pm
d3plot206	6164	5/12/2003	03:55 pm
glstat	1106	04/16/2003	01:20 pm
messag	12	5/12/2003	03:53 pm
messag0	89	5/12/2003	03:53 pm
messag1	18	5/12/2003	03:53 pm
messag2	21	5/12/2003	03:53 pm
messag3	15	5/12/2003	03:53 pm
messag4	15	5/12/2003	03:53 pm
messag5	37	5/12/2003	03:53 pm
relaxDSs.k	1	5/12/2003	03:53 pm
seisDS.k	18	5/12/2003	03:53 pm
<b>1E-6\RN11\ShortRun</b>			
a5h1.dat	17	04/16/2003	01:19 pm
a5h2.dat	17	04/16/2003	01:19 pm

Title: Structural Calculations of Drip Shield Exposed to Vibratory Ground Motion

Document Identifier: 000-00C-PEC0-00100-000-00A

Page 31 of 40

a5v.dat	16	04/16/2003	01:19 pm
constraint.dat	18	04/16/2003	01:19 pm
d3hsp	7752	04/16/2003	01:19 pm
d3hsp1	154	04/16/2003	01:19 pm
d3plot	14086	04/16/2003	01:18 pm
d3plot109	6164	04/16/2003	01:18 pm
messag	12	04/16/2003	01:19 pm
messag0	82	04/16/2003	01:19 pm
relaxDSs.k	1	04/16/2003	01:19 pm
seisDS.k	18	04/16/2003	01:19 pm
<b>1E-6\RN12</b>			
a6h1.dat	17	04/16/2003	01:21 pm
a6h2.dat	16	04/16/2003	01:21 pm
a6v.dat	15	04/16/2003	01:21 pm
constraint.dat	18	04/16/2003	01:21 pm
d3hsp	2	04/16/2003	01:21 pm
d3hsp1	25	04/16/2003	01:21 pm
d3hsp2	151	04/16/2003	01:21 pm
d3plot	14086	04/16/2003	01:21 pm
d3plot106	6164	04/16/2003	01:21 pm
element1.inc	717	04/16/2003	01:59 pm
element2.inc	138	04/16/2003	01:59 pm
element3.inc	138	04/16/2003	01:59 pm
element4.inc	115	04/16/2003	01:59 pm
messag	9	04/16/2003	01:21 pm
messag0	60	04/16/2003	01:21 pm
nodes1.inc	798	04/16/2003	01:59 pm
nodes2.inc	157	04/16/2003	01:59 pm
nodes3.inc	157	04/16/2003	01:59 pm
nodes4.inc	134	04/16/2003	01:59 pm
nodeset.inc	21	04/16/2003	01:59 pm
nodeset1.inc	3	04/16/2003	01:59 pm
nodeset2.inc	184	04/16/2003	01:59 pm
nodeset3.inc	4	04/16/2003	01:59 pm
nodeset4.inc	2	04/16/2003	01:59 pm
nodeset5.inc	1	04/16/2003	01:59 pm
relaxDSs.k	1	04/16/2003	01:21 pm
segmen18.inc	3	04/16/2003	01:59 pm
segmen19.inc	9	04/16/2003	01:59 pm
seisOXO.k	11	04/16/2003	01:21 pm
<b>1E-6\RN14</b>			
acc14h1.dat	49	04/16/2003	01:31 pm
acc14h2.dat	48	04/16/2003	01:31 pm
acc14v.dat	49	04/16/2003	01:31 pm
constraint.dat	18	04/16/2003	01:31 pm
d3hsp	10045	04/16/2003	01:31 pm
d3hsp1	154	04/16/2003	01:31 pm
d3plot	14086	04/16/2003	01:31 pm
d3plot149	6164	04/16/2003	01:31 pm
element1.inc	717	04/16/2003	02:07 pm
element2.inc	138	04/16/2003	02:07 pm
element3.inc	138	04/16/2003	02:07 pm
element4.inc	115	04/16/2003	02:07 pm
messag	12	04/16/2003	01:31 pm
messag0	106	04/16/2003	01:31 pm
nodes1.inc	798	04/16/2003	02:07 pm
nodes2.inc	157	04/16/2003	02:07 pm
nodes3.inc	157	04/16/2003	02:07 pm
nodes4.inc	134	04/16/2003	02:07 pm

Title: Structural Calculations of Drip Shield Exposed to Vibratory Ground Motion

Document Identifier: 000-00C-PEC0-00100-000-00A

Page 32 of 40

nodese15.inc	2	04/16/2003	02:07 pm
nodese16.inc	1	04/16/2003	02:07 pm
nodese17.inc	1	04/16/2003	02:07 pm
nodese18.inc	1	04/16/2003	02:07 pm
nodese19.inc	1	04/16/2003	02:07 pm
nodeset.inc	21	04/16/2003	02:07 pm
nodeset1.inc	3	04/16/2003	02:07 pm
nodeset2.inc	1	04/16/2003	02:07 pm
nodeset3.inc	1	04/16/2003	02:07 pm
relaxDSs.k	1	04/16/2003	01:31 pm
segmen18.inc	3	04/16/2003	02:07 pm
segmen19.inc	9	04/16/2003	02:07 pm
seisDSiv.k	18	04/16/2003	01:31 pm
<b>1E-6\RN15</b>			
element1.inc	717	04/16/2003	02:07 pm
element2.inc	138	04/16/2003	02:07 pm
element3.inc	138	04/16/2003	02:07 pm
element4.inc	115	04/16/2003	02:07 pm
nodes1.inc	798	04/16/2003	02:07 pm
nodes2.inc	157	04/16/2003	02:07 pm
nodes3.inc	157	04/16/2003	02:07 pm
nodes4.inc	134	04/16/2003	02:07 pm
nodese15.inc	2	04/16/2003	02:07 pm
nodese16.inc	1	04/16/2003	02:07 pm
nodese17.inc	1	04/16/2003	02:07 pm
nodese18.inc	1	04/16/2003	02:07 pm
nodese19.inc	1	04/16/2003	02:07 pm
nodeset.inc	21	04/16/2003	02:07 pm
nodeset1.inc	3	04/16/2003	02:07 pm
nodeset2.inc	1	04/16/2003	02:07 pm
nodeset3.inc	1	04/16/2003	02:07 pm
segmen18.inc	3	04/16/2003	02:07 pm
segmen19.inc	9	04/16/2003	02:07 pm
<b>1E-6\RN15\LongRun</b>			
accc3h1.dat	12	04/16/2003	01:39 pm
accc3h2.dat	12	04/16/2003	01:39 pm
accc3v.dat	12	04/16/2003	01:39 pm
constraint.dat	18	04/16/2003	01:39 pm
d3hsp	7701	04/16/2003	01:39 pm
d3hsp1	154	04/16/2003	01:39 pm
d3plot	14086	04/16/2003	01:40 pm
d3plot76	6164	04/16/2003	01:40 pm
messag	12	04/16/2003	01:39 pm
messag0	62	04/16/2003	01:39 pm
relaxDSs.k	1	04/16/2003	01:39 pm
seisDS.k	18	04/16/2003	01:39 pm
<b>1E-6\RN15\ShortRun</b>			
a3h1.dat	8	04/16/2003	01:32 pm
a3h2.dat	8	04/16/2003	01:32 pm
a3v.dat	8	04/16/2003	01:32 pm
constraint.dat	18	04/16/2003	01:32 pm
d3hsp	7670	04/16/2003	01:32 pm
d3hsp1	154	04/16/2003	01:32 pm
d3plot	14086	04/16/2003	01:32 pm
d3plot56	6164	04/16/2003	01:32 pm
messag	12	04/16/2003	01:32 pm
messag0	50	04/16/2003	01:32 pm
relaxDSs.k	1	04/16/2003	01:32 pm
seisDS.k	18	04/16/2003	01:32 pm



Title: Structural Calculations of Drip Shield Exposed to Vibratory Ground Motion

Document Identifier: 000-00C-PEC0-00100-000-00A

Page 33 of 40

1E-6IRN2			
acc16h1.dat	13	05/19/2003	06:42 am
acc16h2.dat	13	05/19/2003	06:42 am
acc16v.dat	13	05/19/2003	06:42 am
constraint.dat	18	05/19/2003	06:42 am
d3hsp	9816	05/19/2003	06:42 am
d3hsp1	154	05/19/2003	06:42 am
d3plot	14086	05/19/2003	06:43 am
d3plot87	6164	05/19/2003	06:43 am
element1.inc	717	05/19/2003	06:42 am
element2.inc	138	05/19/2003	06:42 am
element3.inc	138	05/19/2003	06:42 am
element4.inc	115	05/19/2003	06:42 am
messag	12	05/19/2003	06:42 am
messag0	68	05/19/2003	06:42 am
nodes1.inc	798	05/19/2003	06:42 am
nodes2.inc	157	05/19/2003	06:42 am
nodes3.inc	157	05/19/2003	06:42 am
nodes4.inc	134	05/19/2003	06:42 am
nodese15.inc	2	05/19/2003	06:42 am
nodese16.inc	1	05/19/2003	06:42 am
nodese17.inc	1	05/19/2003	06:42 am
nodese18.inc	1	05/19/2003	06:42 am
nodese19.inc	1	05/19/2003	06:42 am
nodeset.inc	21	05/19/2003	06:42 am
nodeset1.inc	3	05/19/2003	06:42 am
nodeset2.inc	1	05/19/2003	06:42 am
nodeset3.inc	1	05/19/2003	06:42 am
relaxDSs.k	1	05/19/2003	06:42 am
segmen18.inc	3	05/19/2003	06:42 am
segmen19.inc	9	05/19/2003	06:42 am
seisDSiv.k	18	05/19/2003	06:42 am
1E-6IRN3			
a4h1.dat	24	05/29/2003	04:26 pm
a4h2.dat	24	05/29/2003	04:26 pm
a4v.dat	24	05/29/2003	04:26 pm
constraint.dat	18	05/29/2003	04:26 pm
d3hsp	7656	05/29/2003	04:26 pm
d3hsp1	91	05/29/2003	04:25 pm
d3hsp2	25	05/29/2003	04:25 pm
d3hsp3	153	05/29/2003	04:25 pm
d3plot	14086	05/29/2003	04:24 pm
d3plot159	6164	05/29/2003	04:24 pm
element1.inc	717	05/29/2003	04:25 pm
element2.inc	138	05/29/2003	04:25 pm
element3.inc	138	05/29/2003	04:25 pm
element4.inc	115	05/29/2003	04:25 pm
messag	11	05/29/2003	04:25 pm
messag0	28	05/29/2003	04:25 pm
messag1	86	05/29/2003	04:25 pm
messag2	21	05/29/2003	04:25 pm
nodes1.inc	798	05/29/2003	04:25 pm
nodes2.inc	157	05/29/2003	04:25 pm
nodes3.inc	157	05/29/2003	04:25 pm
nodes4.inc	134	05/29/2003	04:25 pm
nodeset.inc	21	05/29/2003	04:25 pm
nodeset1.inc	3	05/29/2003	04:25 pm
nodeset2.inc	184	05/29/2003	04:25 pm
nodeset3.inc	4	05/29/2003	04:25 pm

Title: Structural Calculations of Drip Shield Exposed to Vibratory Ground Motion

Document Identifier: 000-00C-PEC0-00100-000-00A

Page 34 of 40

nodeset4.inc	2	05/29/2003	04:25 pm
nodeset5.inc	1	05/29/2003	04:25 pm
relaxDSs.k	1	05/29/2003	04:25 pm
segmen18.inc	3	05/29/2003	04:25 pm
segmen19.inc	9	05/29/2003	04:25 pm
seisDSiv.k	11	05/29/2003	04:25 pm
<b>1E-6\RN4</b>			
a8h1.dat	20	04/16/2003	01:24 pm
a8h2.dat	21	04/16/2003	01:24 pm
a8v.dat	19	04/16/2003	01:24 pm
constraint.dat	18	04/16/2003	01:24 pm
d3hsp	7744	04/16/2003	01:24 pm
d3hsp1	154	04/16/2003	01:24 pm
d3plot	14086	04/16/2003	01:24 pm
d3plot66	6164	04/16/2003	01:23 pm
element1.inc	717	04/16/2003	02:03 pm
element2.inc	138	04/16/2003	02:03 pm
element3.inc	138	04/16/2003	02:03 pm
element4.inc	115	04/16/2003	02:03 pm
messag	12	04/16/2003	01:24 pm
messag0	58	04/16/2003	01:24 pm
nodes1.inc	798	04/16/2003	02:03 pm
nodes2.inc	157	04/16/2003	02:03 pm
nodes3.inc	157	04/16/2003	02:03 pm
nodes4.inc	134	04/16/2003	02:03 pm
nodese15.inc	2	04/16/2003	02:03 pm
nodese16.inc	1	04/16/2003	02:03 pm
nodese17.inc	1	04/16/2003	02:03 pm
nodese18.inc	1	04/16/2003	02:03 pm
nodese19.inc	1	04/16/2003	02:03 pm
nodeset.inc	21	04/16/2003	02:03 pm
nodeset1.inc	3	04/16/2003	02:03 pm
nodeset2.inc	1	04/16/2003	02:03 pm
nodeset3.inc	1	04/16/2003	02:03 pm
relaxDSs.k	1	04/16/2003	01:24 pm
segmen18.inc	3	04/16/2003	02:03 pm
segmen19.inc	9	04/16/2003	02:03 pm
seisDS.k	18	04/16/2003	01:24 pm
<b>1E-6\RN5</b>			
a11h1.dat	33	04/16/2003	01:24 pm
a11h2.dat	33	04/16/2003	01:24 pm
a11v.dat	33	04/16/2003	01:24 pm
constraint.dat	18	04/16/2003	01:24 pm
d3hsp	7851	04/16/2003	01:24 pm
d3hsp1	154	04/16/2003	01:24 pm
d3plot	14086	04/16/2003	01:25 pm
d3plot109	6164	04/16/2003	01:25 pm
element1.inc	717	04/16/2003	02:04 pm
element2.inc	138	04/16/2003	02:04 pm
element3.inc	138	04/16/2003	02:04 pm
element4.inc	115	04/16/2003	02:04 pm
messag	12	04/16/2003	01:24 pm
messag0	85	04/16/2003	02:04 pm
nodes1.inc	798	04/16/2003	02:04 pm
nodes2.inc	157	04/16/2003	02:04 pm
nodes3.inc	157	04/16/2003	02:04 pm
nodes4.inc	134	04/16/2003	02:04 pm
nodese15.inc	2	04/16/2003	02:04 pm
nodese16.inc	1	04/16/2003	02:04 pm

Title: Structural Calculations of Drip Shield Exposed to Vibratory Ground Motion

Document Identifier: 000-00C-PEC0-00100-000-00A

Page 35 of 40

nodese17.inc	1	04/16/2003	02:04 pm
nodese18.inc	1	04/16/2003	02:04 pm
nodese19.inc	1	04/16/2003	02:04 pm
nodeset.inc	21	04/16/2003	02:04 pm
nodeset1.inc	3	04/16/2003	02:04 pm
nodeset2.inc	1	04/16/2003	02:04 pm
nodeset3.inc	1	04/16/2003	02:04 pm
relaxDSs.k	1	04/16/2003	01:24 pm
segmen18.inc	3	04/16/2003	02:03 pm
segmen19.inc	9	04/16/2003	02:03 pm
seisDS.k	18	04/16/2003	01:24 pm
<b>1E-6IRN6</b>			
a1h1.dat	23	04/16/2003	01:33 pm
a1h2.dat	23	04/16/2003	01:33 pm
a1v.dat	23	04/16/2003	01:33 pm
constraint.dat	18	04/16/2003	01:33 pm
d3hsp	7797	04/16/2003	01:33 pm
d3hsp1	159	04/16/2003	01:33 pm
d3plot	14086	04/16/2003	01:33 pm
d3plot79	6164	04/16/2003	01:33 pm
element1.inc	717	04/16/2003	02:08 pm
element2.inc	138	04/16/2003	02:08 pm
element3.inc	138	04/16/2003	02:08 pm
element4.inc	115	04/16/2003	02:08 pm
messag	17	04/16/2003	01:33 pm
messag0	121	04/16/2003	01:33 pm
nodes1.inc	798	04/16/2003	02:08 pm
nodes2.inc	157	04/16/2003	02:08 pm
nodes3.inc	157	04/16/2003	02:08 pm
nodes4.inc	134	04/16/2003	02:08 pm
nodeset.inc	21	04/16/2003	02:08 pm
nodeset2.inc	184	04/16/2003	02:08 pm
nodeset3.inc	4	04/16/2003	02:08 pm
nodeset4.inc	24	04/16/2003	02:08 pm
relaxDSs.k	1	04/16/2003	01:33 pm
segmen18.inc	3	04/16/2003	02:08 pm
segmen19.inc	9	04/16/2003	02:08 pm
seisDSnd.k	11	04/16/2003	01:33 pm
<b>1E-6IRN7</b>			
a2h1.dat	26	04/16/2003	01:26 pm
a2h2.dat	28	04/16/2003	01:26 pm
a2v.dat	26	04/16/2003	01:26 pm
constraint.dat	18	04/16/2003	01:26 pm
d3hsp	7709	04/16/2003	01:26 pm
d3hsp1	152	04/16/2003	01:26 pm
d3plot	14086	04/16/2003	01:26 pm
d3plot88	6164	04/16/2003	01:26 pm
element1.inc	717	04/16/2003	02:04 pm
element2.inc	138	04/16/2003	02:04 pm
element3.inc	138	04/16/2003	02:04 pm
element4.inc	115	04/16/2003	02:04 pm
messag	10	04/16/2003	01:26 pm
messag0	67	04/16/2003	01:26 pm
nodes1.inc	798	04/16/2003	02:04 pm
nodes2.inc	157	04/16/2003	02:04 pm
nodes3.inc	157	04/16/2003	02:04 pm
nodes4.inc	134	04/16/2003	02:04 pm
nodeset.inc	21	04/16/2003	02:04 pm
nodeset1.inc	3	04/16/2003	02:04 pm

Title: Structural Calculations of Drip Shield Exposed to Vibratory Ground Motion

Document Identifier: 000-00C-PEC0-00100-000-00A

Page 36 of 40

nodeset2.inc	184	04/16/2003	02:04 pm
nodeset3.inc	4	04/16/2003	02:04 pm
nodeset4.inc	2	04/16/2003	02:04 pm
nodeset5.inc	1	04/16/2003	02:04 pm
relaxDSs.k	1	04/16/2003	01:26 pm
segmen18.inc	3	04/16/2003	02:04 pm
segmen19.inc	9	04/16/2003	02:04 pm
seisOXO.k	11	04/16/2003	01:26 pm
<b>1E-6\RN8</b>			
accc13h1.dat	37	04/16/2003	01:27 pm
accc13h2.dat	36	04/16/2003	01:27 pm
accc13v.dat	37	04/16/2003	01:27 pm
constraint.dat	18	04/16/2003	01:27 pm
d3hsp	9871	04/16/2003	01:27 pm
d3hsp1	151	04/16/2003	01:27 pm
d3plot	14086	04/16/2003	01:27 pm
d3plot114	6164	04/16/2003	01:27 pm
element1.inc	717	04/16/2003	02:05 pm
element2.inc	138	04/16/2003	02:05 pm
element3.inc	138	04/16/2003	02:05 pm
element4.inc	115	04/16/2003	02:05 pm
messag	9	04/16/2003	01:27 pm
messag0	74	04/16/2003	01:27 pm
nodes1.inc	798	04/16/2003	02:05 pm
nodes2.inc	157	04/16/2003	02:05 pm
nodes3.inc	157	04/16/2003	02:05 pm
nodes4.inc	134	04/16/2003	02:05 pm
nodeset.inc	21	04/16/2003	02:05 pm
nodeset2.inc	184	04/16/2003	02:05 pm
nodeset3.inc	4	04/16/2003	02:05 pm
nodeset4.inc	2	04/16/2003	02:05 pm
relaxDSs.k	1	04/16/2003	01:27 pm
segmen18.inc	3	04/16/2003	02:05 pm
segmen19.inc	9	04/16/2003	02:05 pm
seisDSndR.k	11	04/16/2003	01:27 pm
<b>1E-6\RN9</b>			
a10h1.dat	8	04/16/2003	01:28 pm
a10h2.dat	8	04/16/2003	01:28 pm
a10v.dat	9	04/16/2003	01:28 pm
constraint.dat	18	04/16/2003	01:28 pm
d3hsp	7655	04/16/2003	01:28 pm
d3hsp1	152	04/16/2003	01:28 pm
d3plot	14086	04/16/2003	01:28 pm
d3plot115	6164	04/16/2003	01:28 pm
element1.inc	717	04/16/2003	02:05 pm
element2.inc	138	04/16/2003	02:05 pm
element3.inc	138	04/16/2003	02:05 pm
element4.inc	115	04/16/2003	02:05 pm
messag	11	04/16/2003	01:28 pm
messag0	108	04/16/2003	01:28 pm
nodes1.inc	798	04/16/2003	02:05 pm
nodes2.inc	157	04/16/2003	02:05 pm
nodes3.inc	157	04/16/2003	02:05 pm
nodes4.inc	134	04/16/2003	02:05 pm
nodeset.inc	21	04/16/2003	02:05 pm
nodeset2.inc	184	04/16/2003	02:05 pm
nodeset3.inc	4	04/16/2003	02:05 pm
nodeset4.inc	2	04/16/2003	02:05 pm
relaxDSs.k	1	04/16/2003	01:28 pm

Title: Structural Calculations of Drip Shield Exposed to Vibratory Ground Motion

Document Identifier: 000-00C-PEC0-00100-000-00A

Page 37 of 40

segmen18.inc	3	04/16/2003	02:05 pm
segmen19.inc	9	04/16/2003	02:05 pm
seisDSndR.k	11	04/16/2003	01:28 pm
<b>1E-6\RN9\Freq Out</b>			
d3hsp	7584	05/19/2003	06:43 am
messag	36	05/19/2003	06:44 am
seisDSndR.k	11	05/19/2003	06:43 am
<b>5E-4</b>			
acc_h1.dat	44	04/16/2003	01:07 pm
acc_h2.dat	44	04/16/2003	01:07 pm
acc_v.dat	44	04/16/2003	01:07 pm
constraint.dat	18	04/16/2003	01:07 pm
d3hsp	9989	04/16/2003	01:07 pm
d3hsp1	152	04/16/2003	01:07 pm
d3plot	14086	04/16/2003	01:09 pm
d3plot124	6164	04/16/2003	01:09 pm
element1.inc	717	04/16/2003	01:08 pm
element2.inc	138	04/16/2003	01:08 pm
element3.inc	138	04/16/2003	01:08 pm
element4.inc	115	04/16/2003	01:08 pm
messag	11	04/16/2003	01:07 pm
messag0	92	04/16/2003	01:07 pm
nodes1.inc	798	04/16/2003	01:08 pm
nodes2.inc	157	04/16/2003	01:08 pm
nodes3.inc	157	04/16/2003	01:08 pm
nodes4.inc	134	04/16/2003	01:08 pm
nodese15.inc	2	04/16/2003	01:08 pm
nodese16.inc	1	04/16/2003	01:08 pm
nodese17.inc	1	04/16/2003	01:08 pm
nodese18.inc	1	04/16/2003	01:08 pm
nodese19.inc	1	04/16/2003	01:08 pm
nodeset.inc	21	04/16/2003	01:08 pm
nodeset1.inc	3	04/16/2003	01:08 pm
nodeset2.inc	1	04/16/2003	01:08 pm
nodeset3.inc	1	04/16/2003	01:08 pm
relaxDSs.k	1	04/16/2003	01:07 pm
segmen18.inc	3	04/16/2003	01:08 pm
segmen19.inc	9	04/16/2003	01:08 pm
seisDSiv.k	18	04/16/2003	01:07 pm
<b>ModalAnalysis</b>			
drip2MOD.inp	39	04/16/2003	01:47 pm
drip2MOD.out	282	04/16/2003	01:47 pm

## CONTENT OF CD2

<b>Directory</b>			
<b>File name</b>	<b>Size (kB)</b>	<b>Date of Creation</b>	<b>Time</b>
<b>1E-7\RN10</b>			
a9h1.dat	26	04/16/2003	01:42 pm
a9h2.dat	26	04/16/2003	01:42 pm
a9v.dat	26	04/16/2003	01:42 pm
d3hsp	7675	04/16/2003	01:42 pm
d3plot	14086	04/16/2003	01:41 pm
d3plot37	6164	04/16/2003	01:41 pm
element1.inc	717	04/16/2003	02:10 pm
element2.inc	138	04/16/2003	02:10 pm
element3.inc	138	04/16/2003	02:10 pm
element4.inc	115	04/16/2003	02:10 pm
messag	38	04/16/2003	01:42 pm

Title: Structural Calculations of Drip Shield Exposed to Vibratory Ground Motion

Document Identifier: 000-00C-PEC0-00100-000-00A

Page 38 of 40

nodes1.inc	798	04/16/2003	02:10 pm
nodes2.inc	157	04/16/2003	02:10 pm
nodes3.inc	157	04/16/2003	02:10 pm
nodeset.inc	21	04/16/2003	02:10 pm
nodeset1.inc	3	04/16/2003	02:10 pm
nodeset2.inc	184	04/16/2003	02:10 pm
nodeset3.inc	4	04/16/2003	02:10 pm
nodeset4.inc	2	04/16/2003	02:10 pm
nodeset5.inc	1	04/16/2003	02:10 pm
relaxDSs.k	1	04/16/2003	01:42 pm
segmen18.inc	3	04/16/2003	02:10 pm
segmen19.inc	9	04/16/2003	02:10 pm
seisOXO.k	11	04/16/2003	01:42 pm
<b>1E-7IRN5</b>			
acc11h1.dat	61	04/16/2003	01:37 pm
acc11h2.dat	61	04/16/2003	01:37 pm
acc11v.dat	61	04/16/2003	01:37 pm
constraint.dat	18	04/16/2003	01:37 pm
d3hsp	9977	04/16/2003	01:37 pm
d3hsp1	26	04/16/2003	01:37 pm
d3hsp2	48	04/16/2003	01:37 pm
d3hsp3	152	04/16/2003	01:37 pm
d3plot	14086	04/16/2003	01:37 pm
d3plot89	6164	04/16/2003	01:37 pm
element1.inc	717	04/16/2003	02:09 pm
element2.inc	138	04/16/2003	02:09 pm
element3.inc	138	04/16/2003	02:09 pm
element4.inc	115	04/16/2003	02:09 pm
messag	10	04/16/2003	01:37 pm
messag0	45	04/16/2003	01:37 pm
messag1	21	04/16/2003	01:37 pm
messag2	23	04/16/2003	01:37 pm
messag3	17	04/16/2003	01:37 pm
nodes1.inc	798	04/16/2003	02:09 pm
nodes2.inc	157	04/16/2003	02:09 pm
nodes3.inc	157	04/16/2003	02:09 pm
nodes4.inc	134	04/16/2003	02:09 pm
nodeset.inc	21	04/16/2003	02:09 pm
nodeset1.inc	3	04/16/2003	02:09 pm
nodeset2.inc	184	04/16/2003	02:09 pm
nodeset3.inc	4	04/16/2003	02:09 pm
nodeset4.inc	2	04/16/2003	02:09 pm
nodeset5.inc	1	04/16/2003	02:09 pm
relaxDSs.k	1	04/16/2003	01:37 pm
segmen18.inc	3	04/16/2003	02:09 pm
segmen19.inc	9	04/16/2003	02:09 pm
seisOXO.k	11	04/16/2003	01:37 pm
seisOXO1.k	1	04/16/2003	01:37 pm
<b>1E-7IRN6</b>			
a1h1.dat	25	04/16/2003	01:42 pm
a1h2.dat	25	04/16/2003	01:42 pm
a1v.dat	24	04/16/2003	01:42 pm
d3hsp	7674	04/16/2003	01:42 pm
d3hsp1	42	04/16/2003	01:42 pm
d3hsp2	17	05/29/2003	04:29 pm
d3plot	14086	04/16/2003	01:43 pm
d3plot37	12329	04/16/2003	01:43 pm
d3plot39	12329	05/29/2003	04:29 pm
element1.inc	717	04/16/2003	02:10 pm

Title: Structural Calculations of Drip Shield Exposed to Vibratory Ground Motion

Document Identifier: 000-00C-PEC0-00100-000-00A

Page 39 of 40

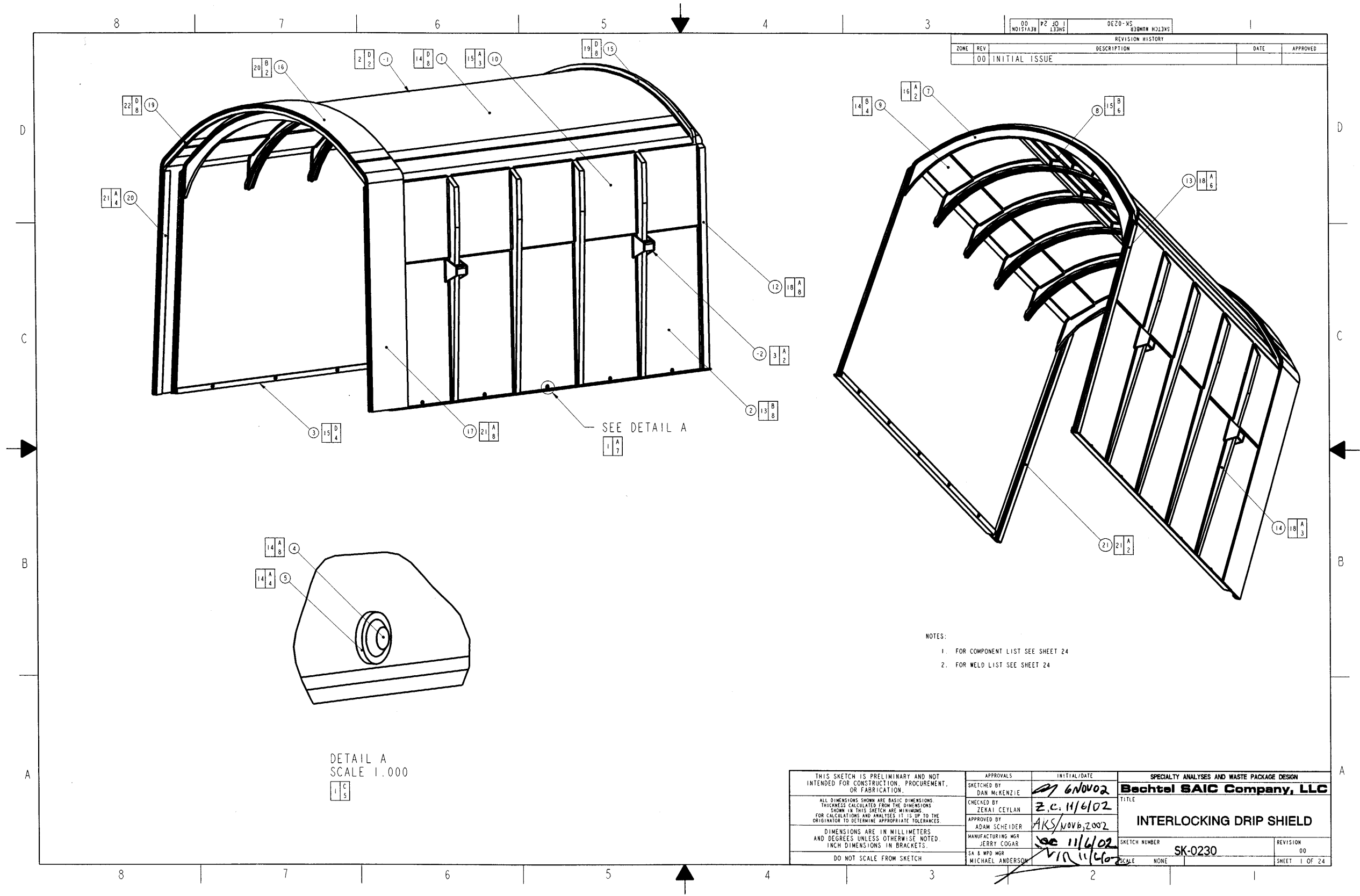
element2.inc	138	04/16/2003	02:10 pm
element3.inc	138	04/16/2003	02:10 pm
element4.inc	115	04/16/2003	02:10 pm
messag	20	04/16/2003	01:42 pm
messag0	45	04/16/2003	01:42 pm
nodes1.inc	798	04/16/2003	02:10 pm
nodes2.inc	157	04/16/2003	02:10 pm
nodes3.inc	157	04/16/2003	02:10 pm
nodes4.inc	134	04/16/2003	02:10 pm
nodeset.inc	21	04/16/2003	02:10 pm
nodeset1.inc	3	04/16/2003	02:10 pm
nodeset2.inc	184	04/16/2003	02:10 pm
nodeset3.inc	4	04/16/2003	02:10 pm
nodeset4.inc	2	04/16/2003	02:10 pm
nodeset5.inc	1	04/16/2003	02:10 pm
relaxDSs.k	1	04/16/2003	01:42 pm
segmen18.inc	3	04/16/2003	02:10 pm
segmen19.inc	9	04/16/2003	02:10 pm
seisOXO1.k	1	04/16/2003	01:42 pm
<b>1E-7\RN7</b>			
a2h1.dat	24	04/16/2003	01:35 pm
a2h2.dat	24	04/16/2003	01:35 pm
a2v.dat	24	04/16/2003	01:35 pm
d3hsp	7651	04/16/2003	01:35 pm
d3hsp1	40	04/16/2003	01:35 pm
d3plot	14086	04/16/2003	01:38 pm
d3plot32	6164	04/16/2003	01:37 pm
element1.inc	717	04/16/2003	02:09 pm
element2.inc	138	04/16/2003	02:09 pm
element3.inc	138	04/16/2003	02:09 pm
element4.inc	115	04/16/2003	02:09 pm
messag	35	04/16/2003	01:35 pm
messag0	9	04/16/2003	01:35 pm
nodes1.inc	798	04/16/2003	02:09 pm
nodes2.inc	157	04/16/2003	02:09 pm
nodes3.inc	157	04/16/2003	02:09 pm
nodes4.inc	134	04/16/2003	02:09 pm
nodeset.inc	21	04/16/2003	02:09 pm
nodeset1.inc	3	04/16/2003	02:09 pm
nodeset2.inc	184	04/16/2003	02:09 pm
nodeset3.inc	4	04/16/2003	02:09 pm
nodeset4.inc	2	04/16/2003	02:09 pm
nodeset5.inc	1	04/16/2003	02:09 pm
segmen18.inc	3	04/16/2003	02:09 pm
segmen19.inc	9	04/16/2003	02:09 pm
seisOXO.k	11	04/16/2003	01:35 pm
<b>1E-7\RN8</b>			
accc13h1.dat	135	04/16/2003	01:44 pm
accc13h2.dat	134	04/16/2003	01:44 pm
accc13v.dat	127	04/16/2003	01:44 pm
d3hsp	10328	04/16/2003	01:44 pm
d3plot	14086	04/16/2003	01:44 pm
d3plot32	6164	04/16/2003	01:44 pm
element1.inc	717	04/16/2003	02:11 pm
element2.inc	138	04/16/2003	02:11 pm
element3.inc	138	04/16/2003	02:11 pm
element4.inc	115	04/16/2003	02:11 pm
messag	33	04/16/2003	01:44 pm
nodes1.inc	798	04/16/2003	02:11 pm

nodes2.inc	157	04/16/2003	02:11 pm
nodes3.inc	157	04/16/2003	02:11 pm
nodes4.inc	134	04/16/2003	02:11 pm
nodeset.inc	21	04/16/2003	02:11 pm
nodeset1.inc	3	04/16/2003	02:11 pm
nodeset2.inc	184	04/16/2003	02:11 pm
nodeset3.inc	4	04/16/2003	02:11 pm
nodeset4.inc	2	04/16/2003	02:11 pm
nodeset5.inc	1	04/16/2003	02:11 pm
relaxDSs.k	1	04/16/2003	01:44 pm
segmen18.inc	3	04/16/2003	02:11 pm
segmen19.inc	9	04/16/2003	02:11 pm
seisOXO.k	11	04/16/2003	01:44 pm

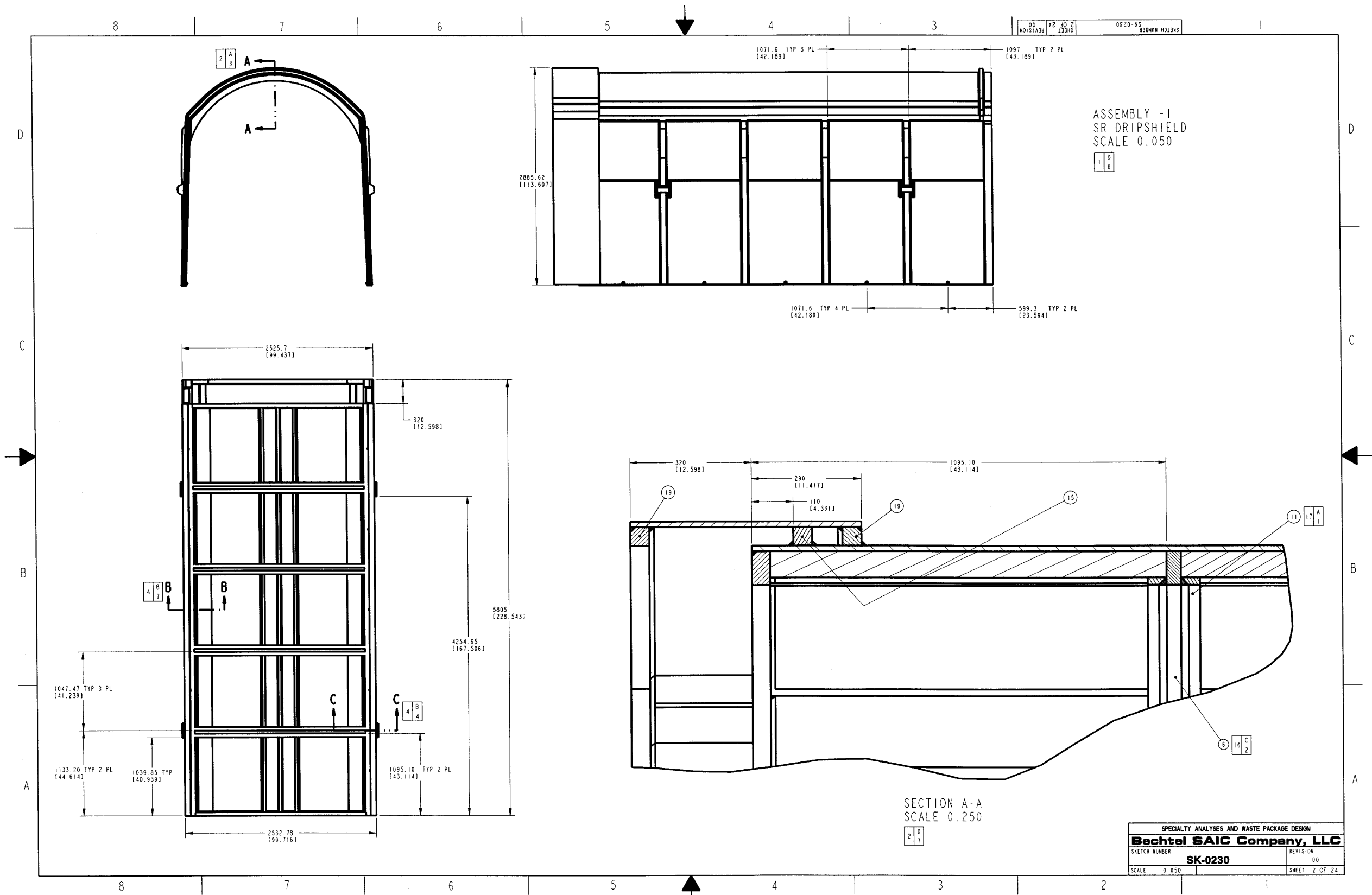
NOTE: The file sizes and times may vary with operating system.



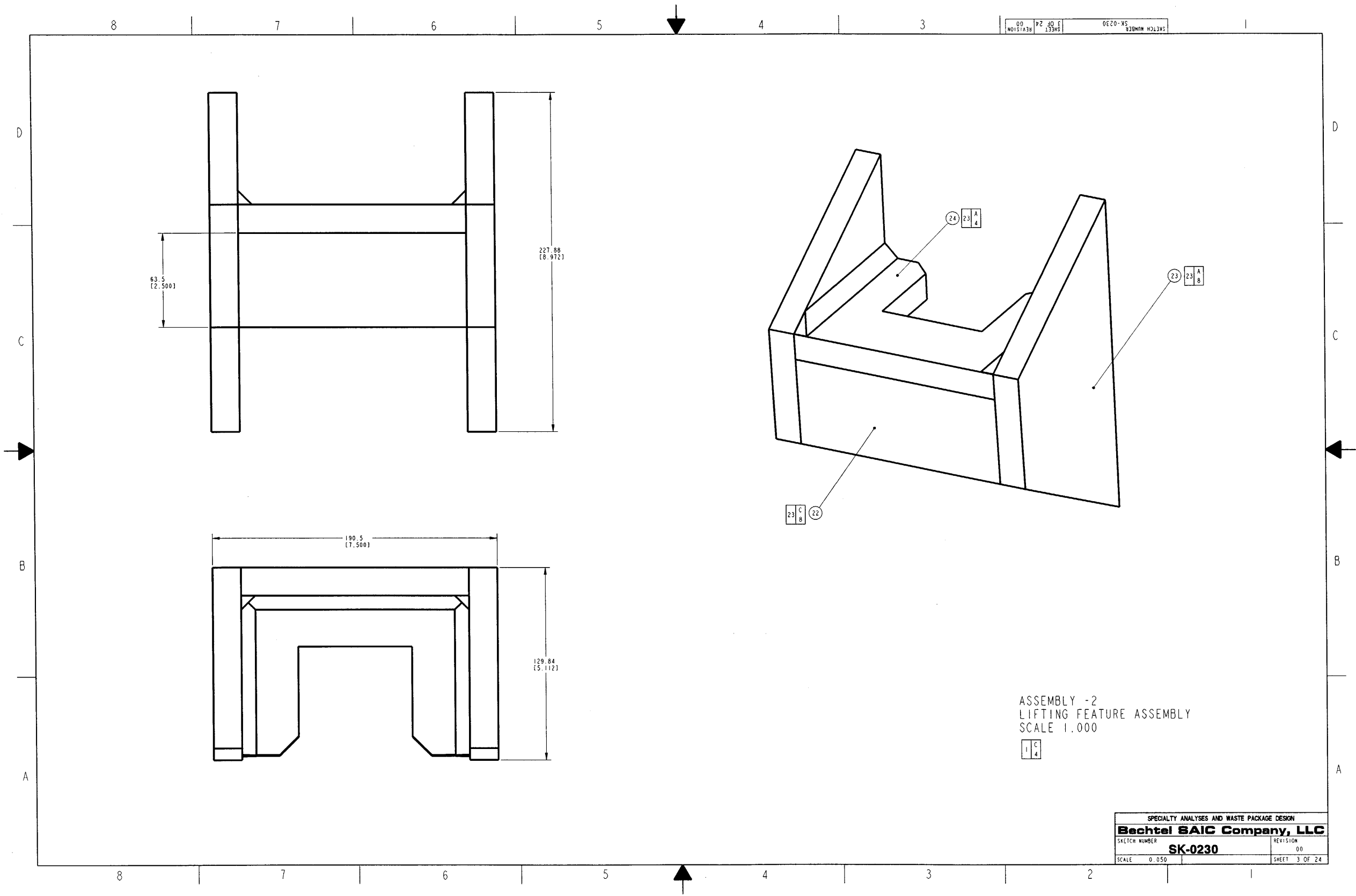
NAME: MCKENZIED2    OBJECT: SK-0230\_REV00\_1    DATE: 06-Nov-02 12:38:33



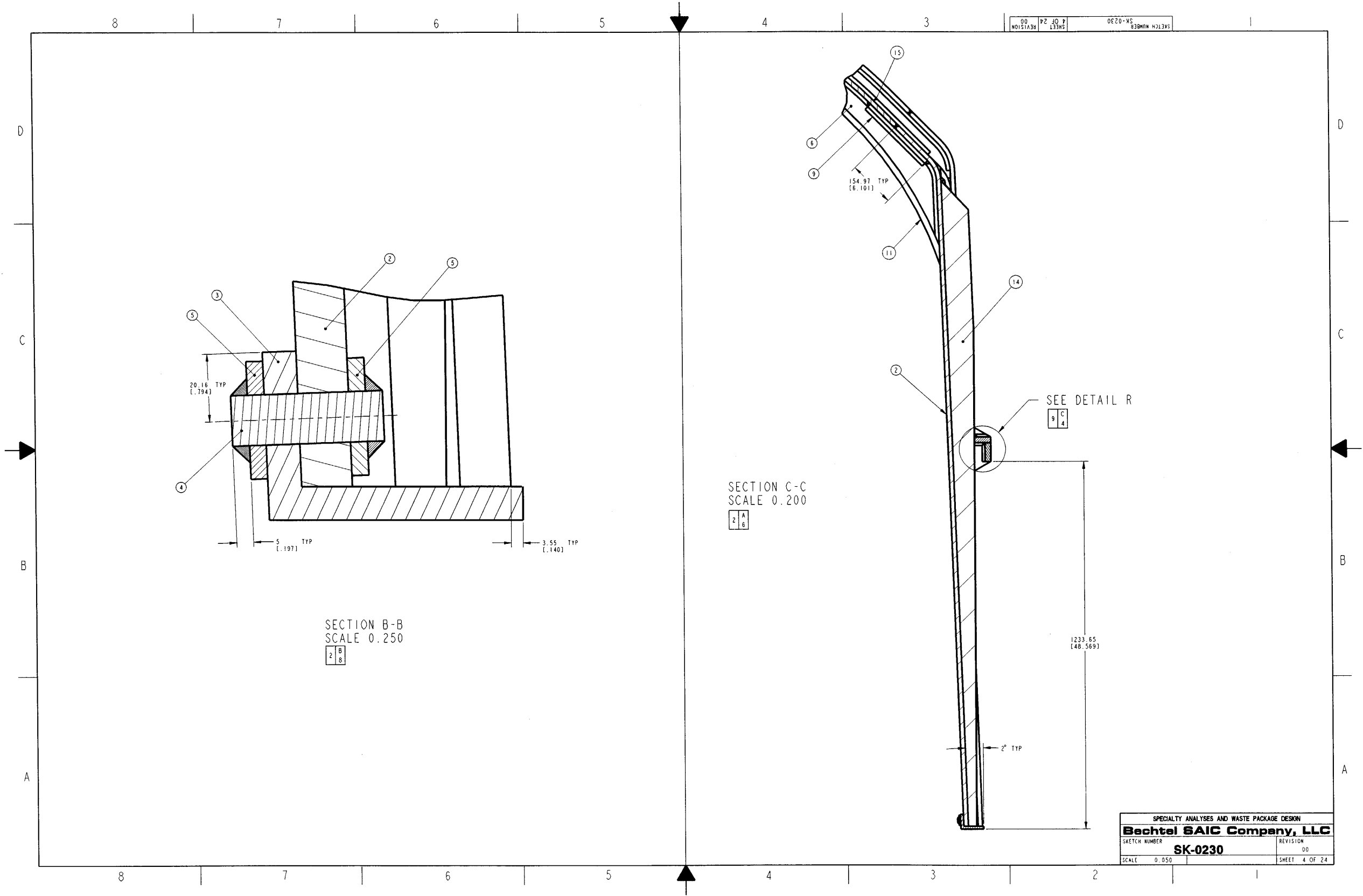
NAME: MCKENZIED2    OBJECT: SK-0230\_REV00\_2    DATE: 06-Nov-02 12:38:35



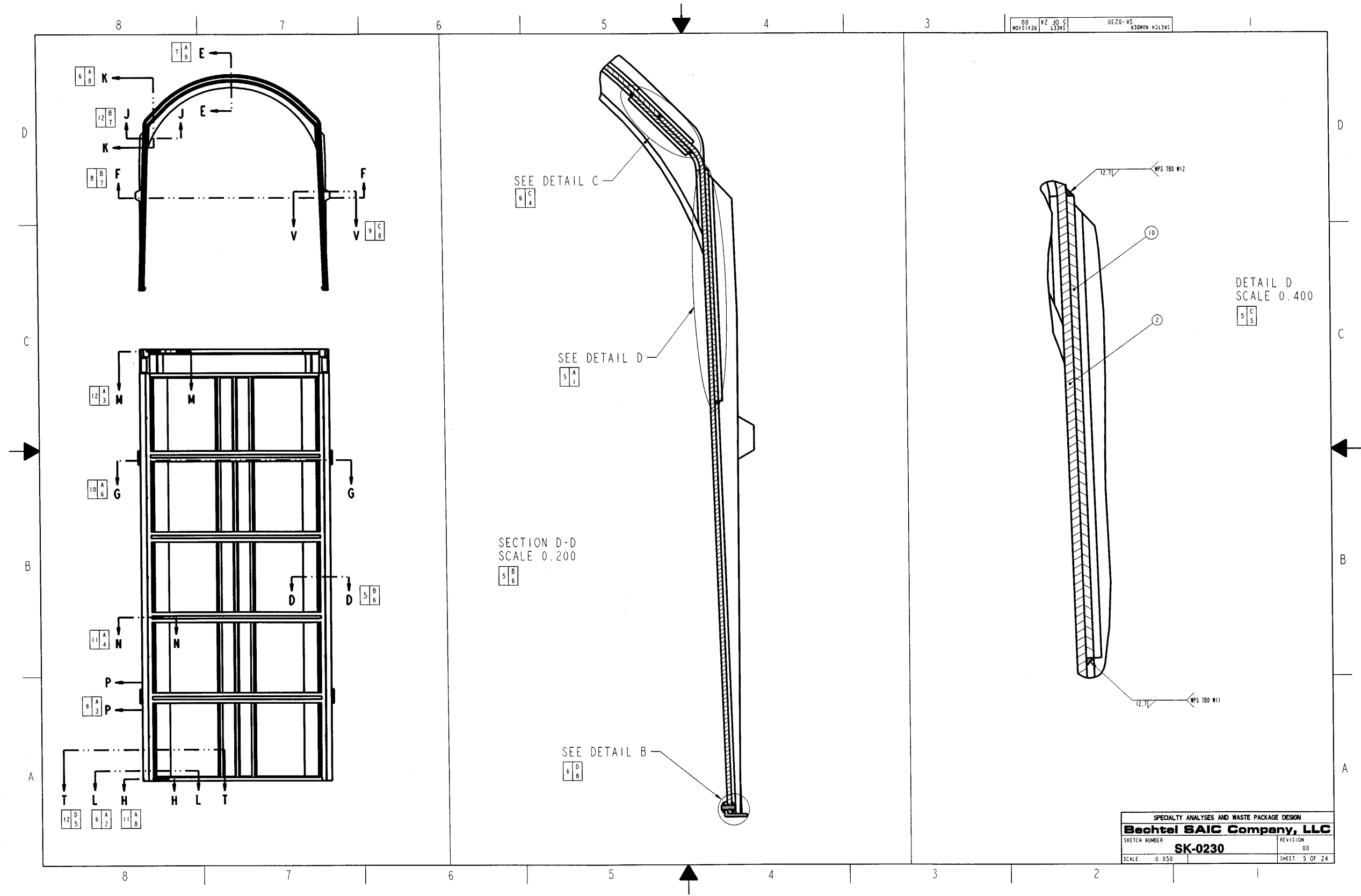
NAME: MCKENZIED2    OBJECT: SK-0230\_REV00\_3    DATE: 06-Nov-02 12:38:38



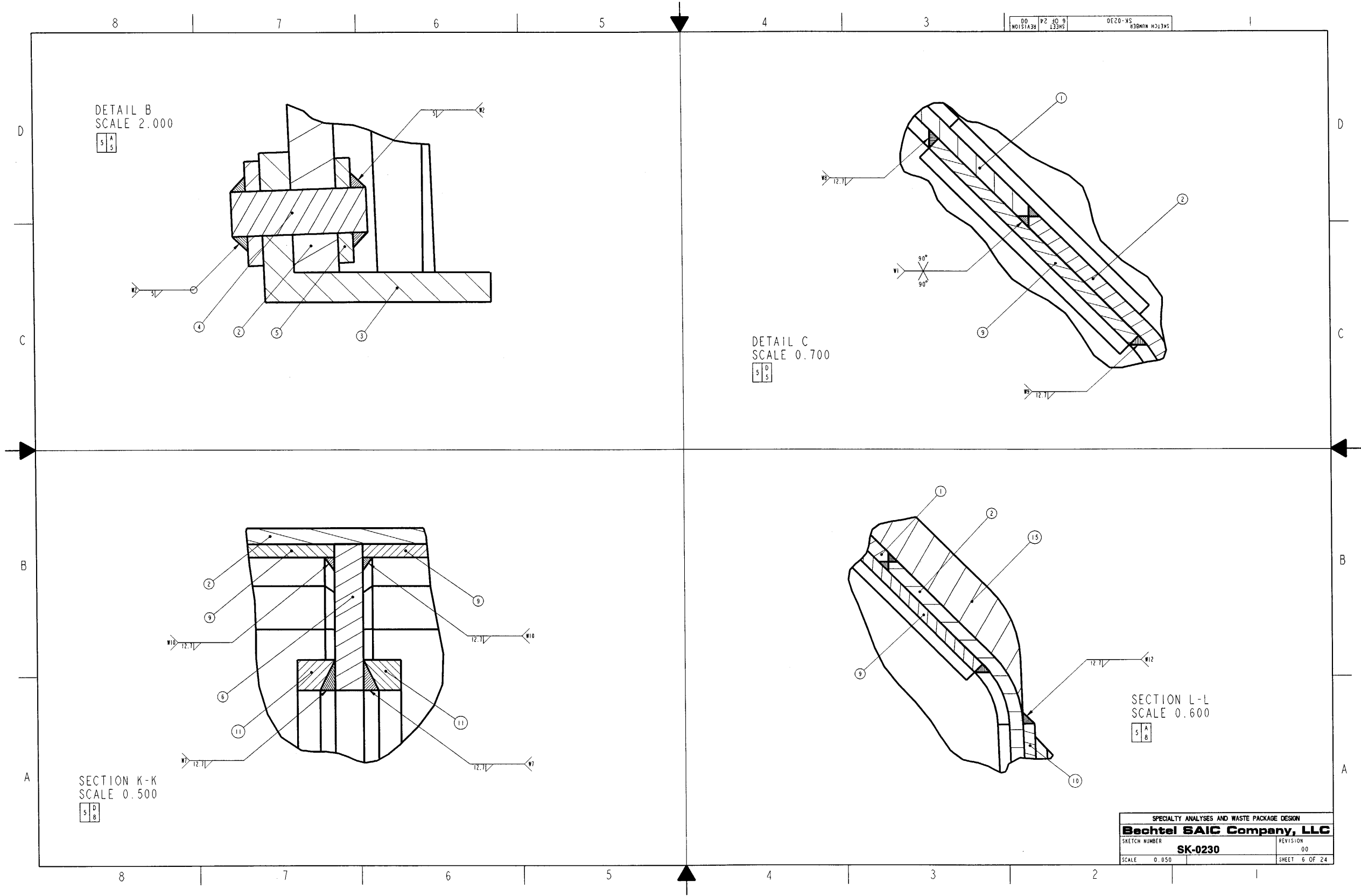
NAME: MCKENZIED2    OBJECT: SK-0230\_REV00\_4    DATE: 06-Nov-02 12:38:38



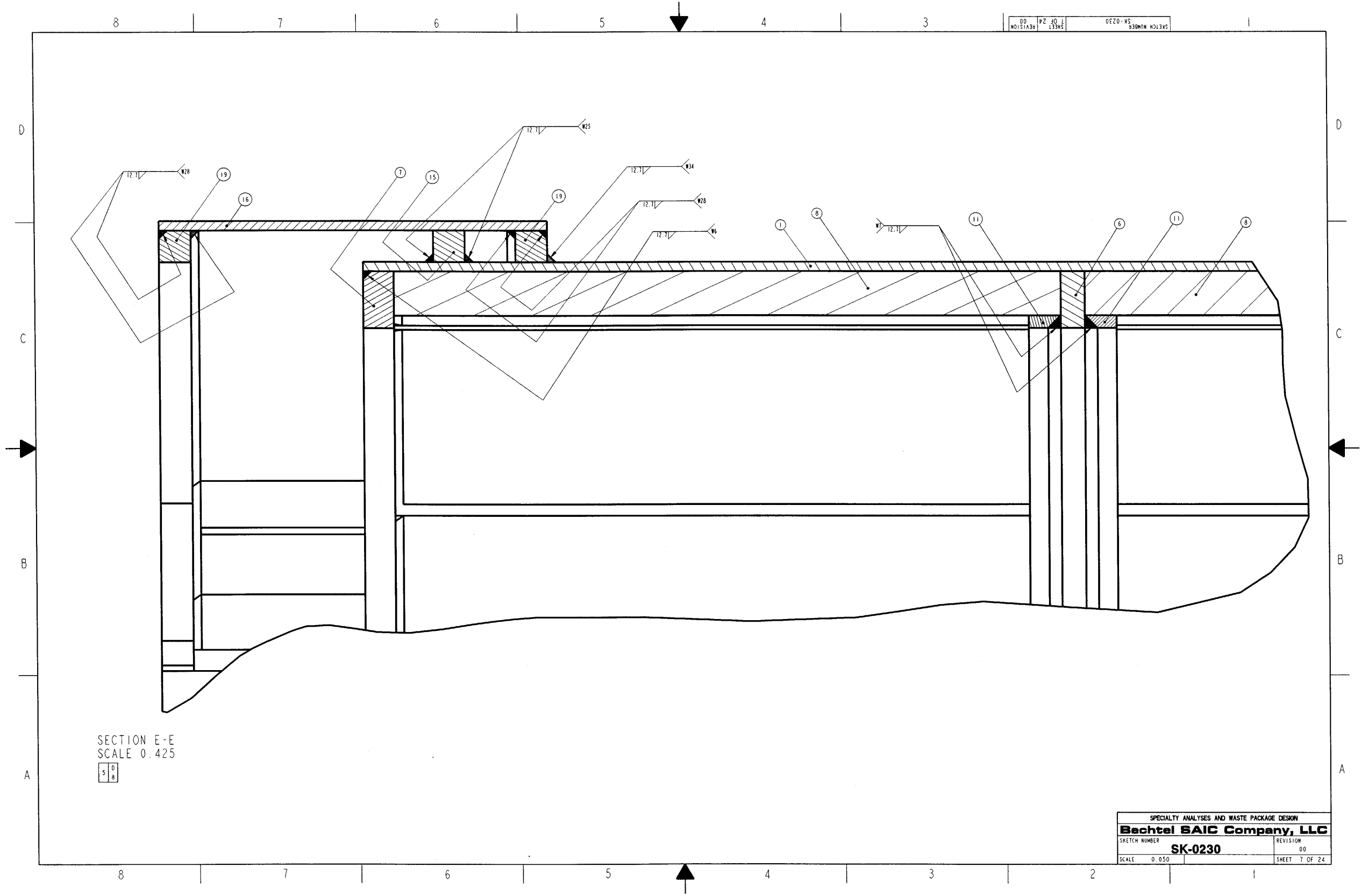
NAME: MCKENZIED2      OBJECT: SK-0230\_REV00\_5      DATE: 06-NOV-02 12:38:40



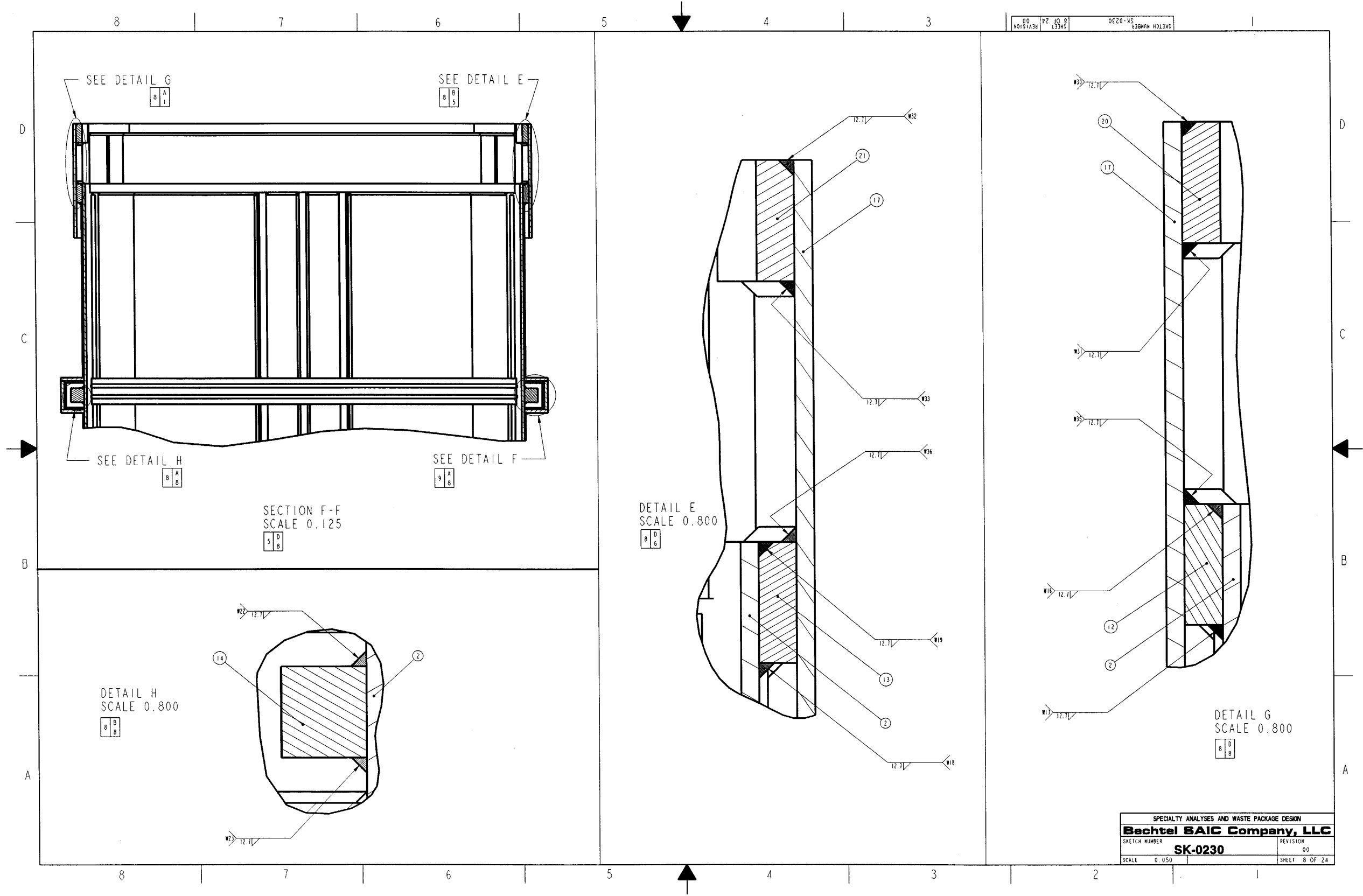
NAME: MCKENZIED2    OBJECT: SK-0230\_REV00\_6    DATE: 06-Nov-02 12:38:42



NAME : MCKENZIED2    OBJECT : SK-0230\_REV00\_7    DATE : 06-Nov-02 12:38:43



NAME: MCKENZIED2    OBJECT: SK-0230\_REV00\_8    DATE: 06-Nov-02 12:38:44

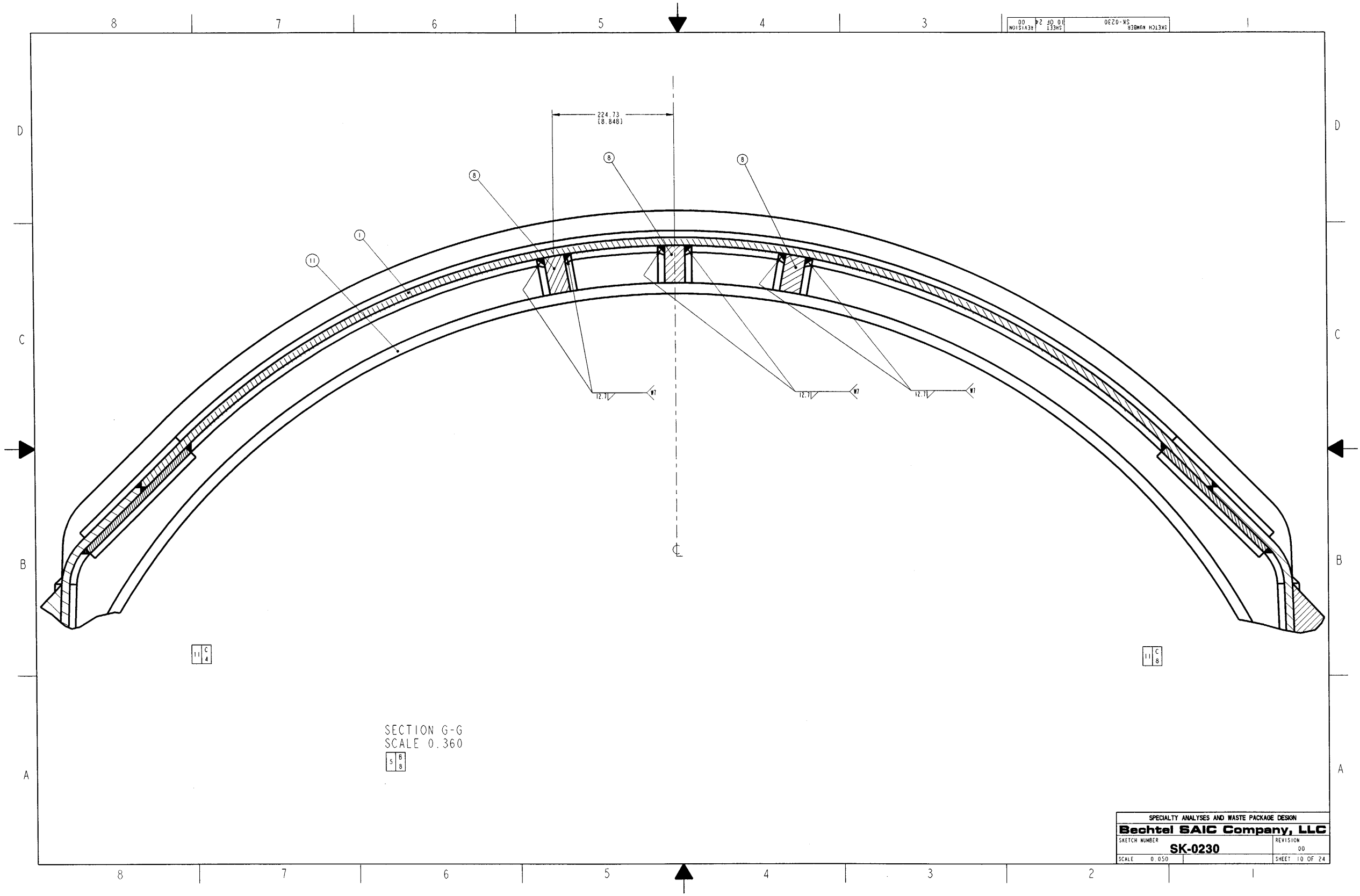




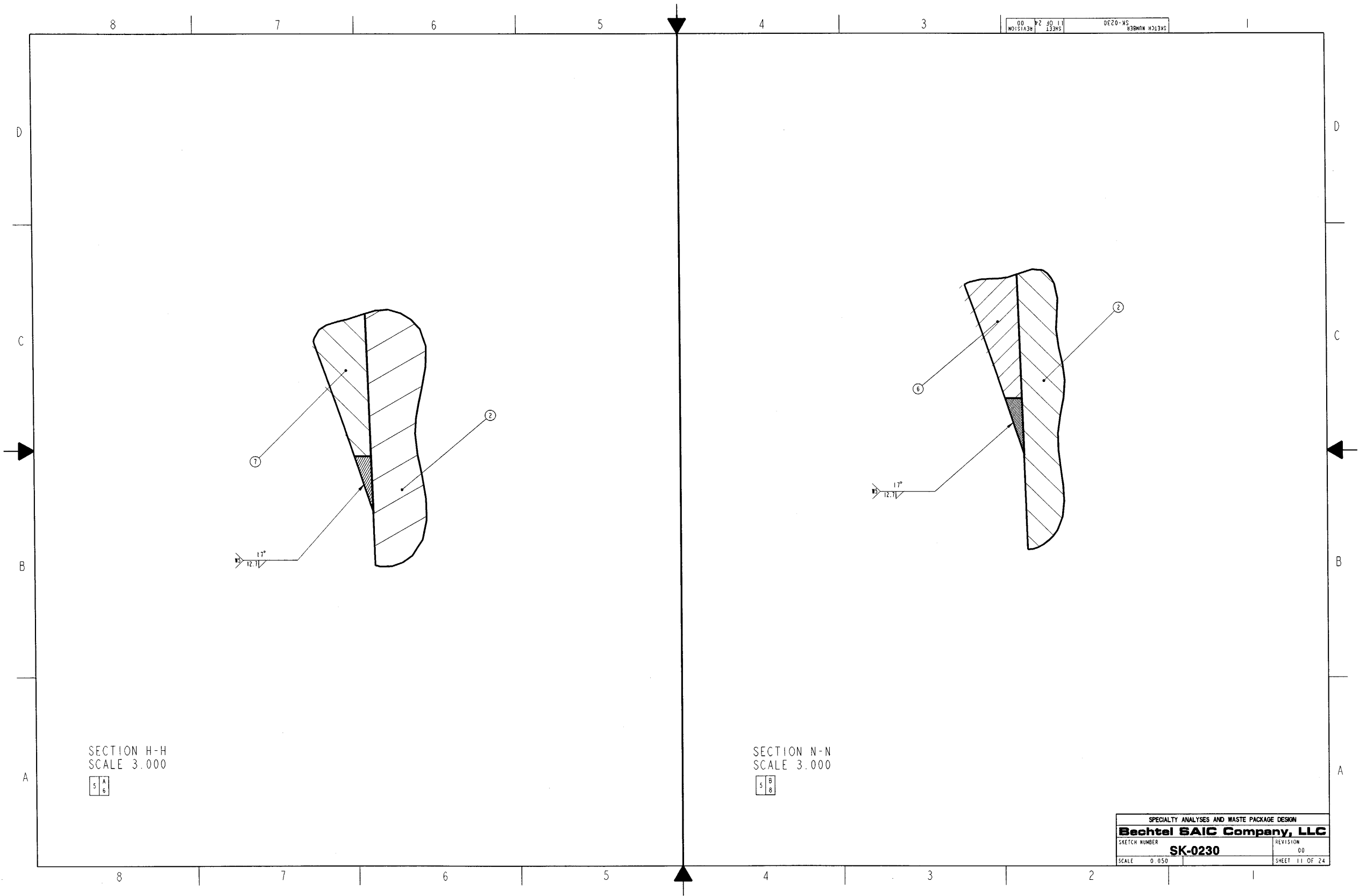
NAME: MCKENZIED2      OBJECT: SK-0230\_REV00\_9      DATE: 06-Nov-02      12:38:46



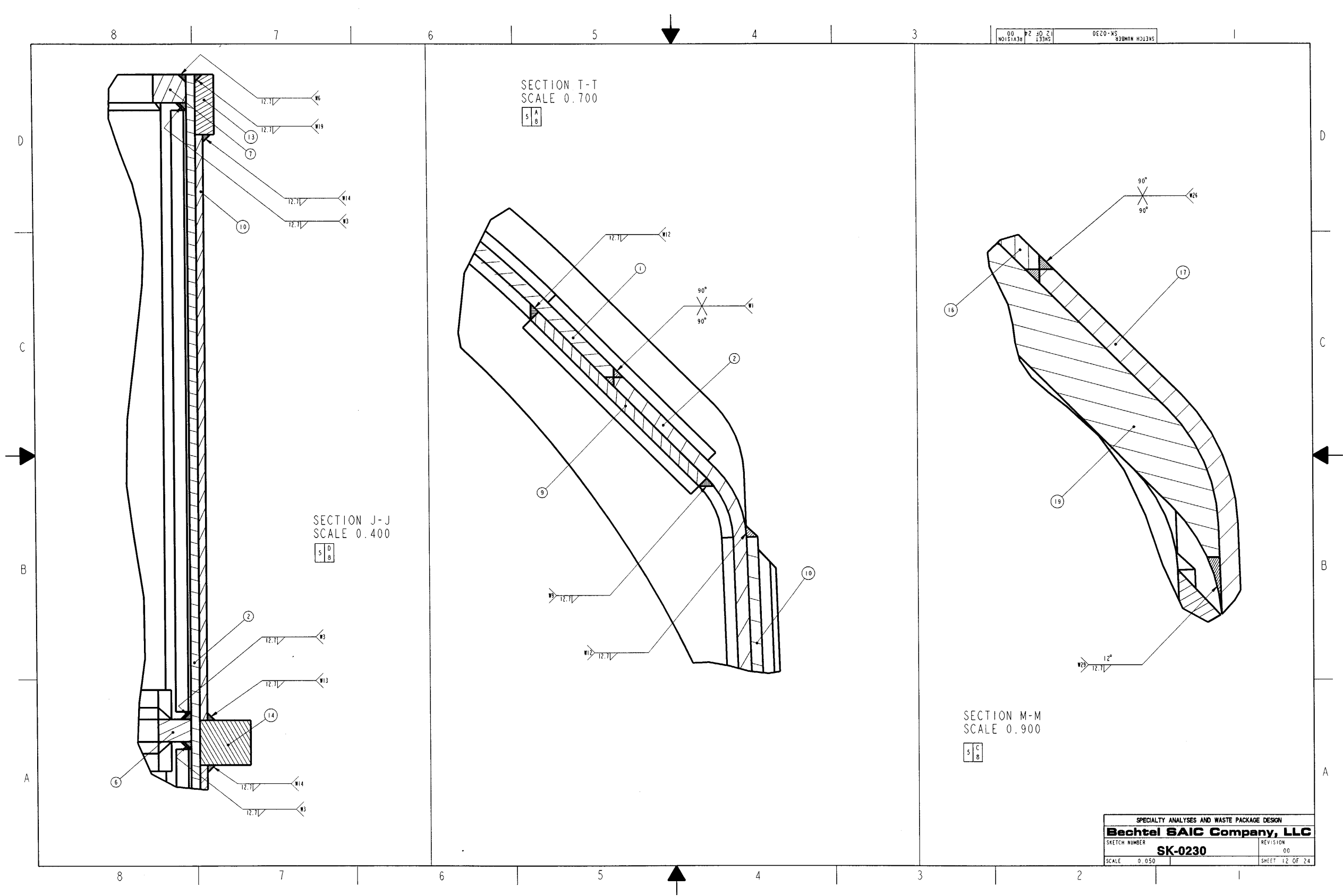
NAME: MCKENZIE D2    OBJECT: SK-0230\_REV00\_10    DATE: 06-Nov-02 12:38:48



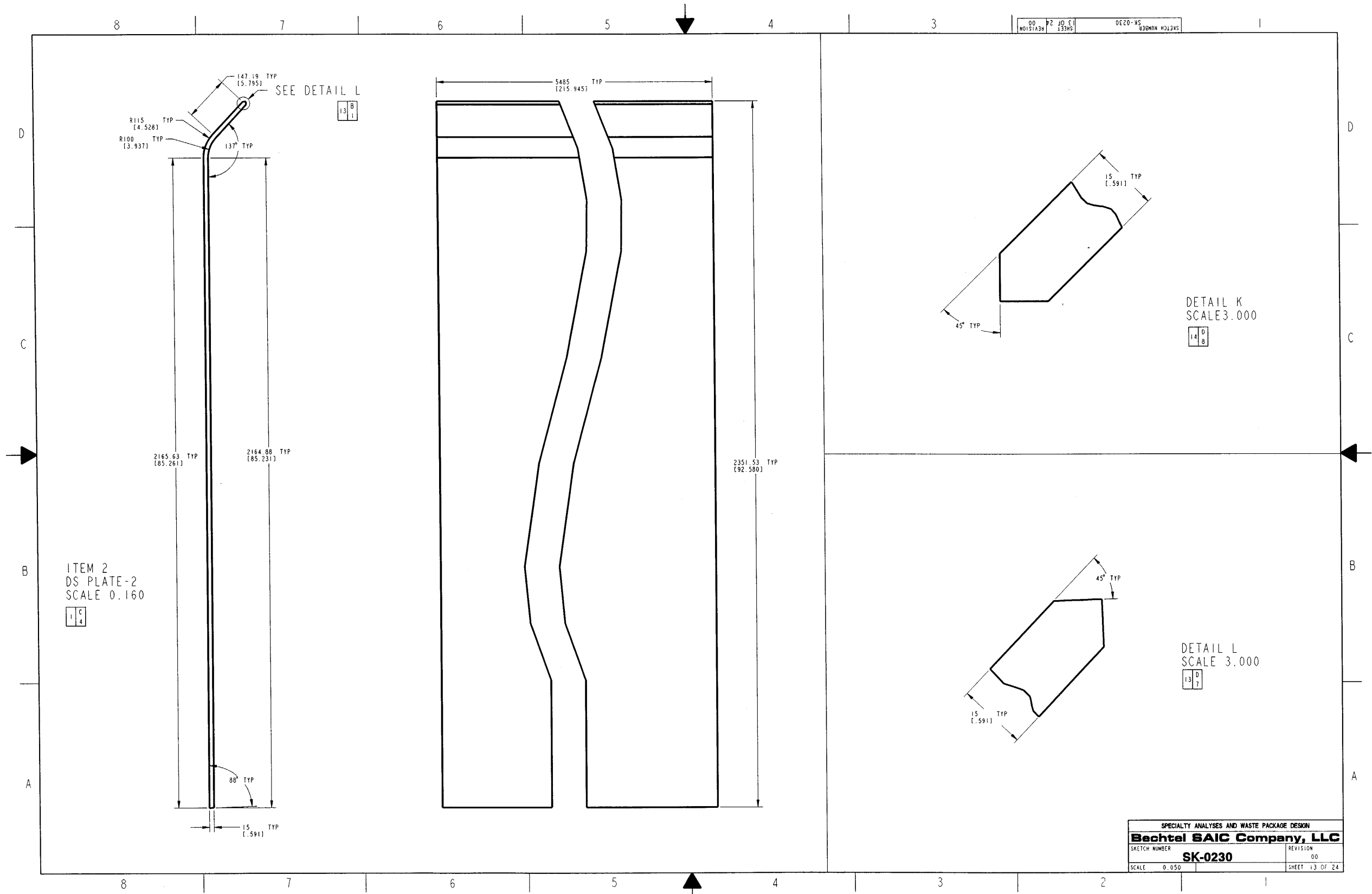
NAME: MCKENZIED2    OBJECT: SK-0230\_REV00\_11    DATE: 06-Nov-02 12:38:49



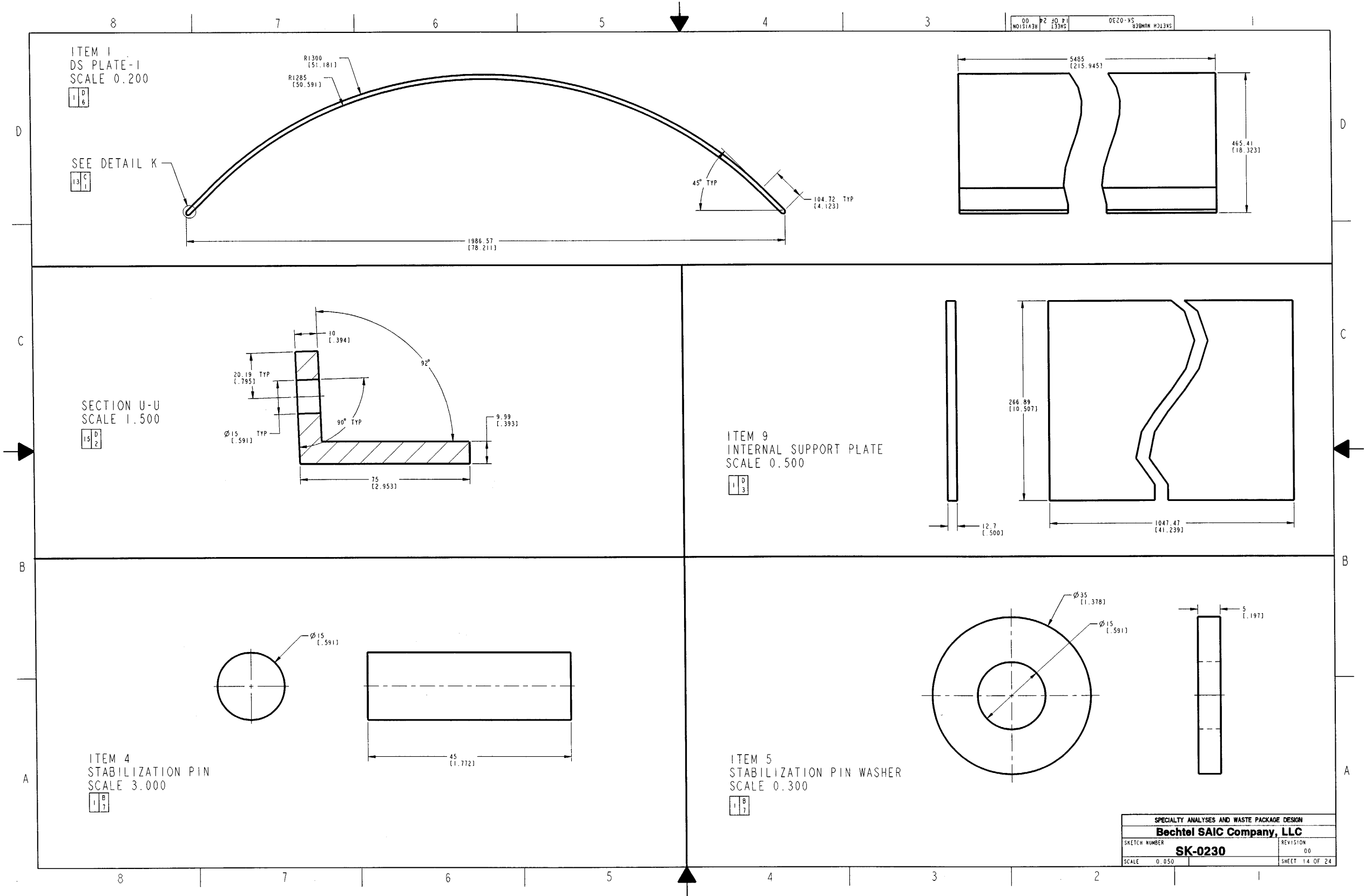
NAME: MCKENZIED2    OBJECT: SK-0230\_REV00\_12    DATE: 06-Nov-02 12:38:50



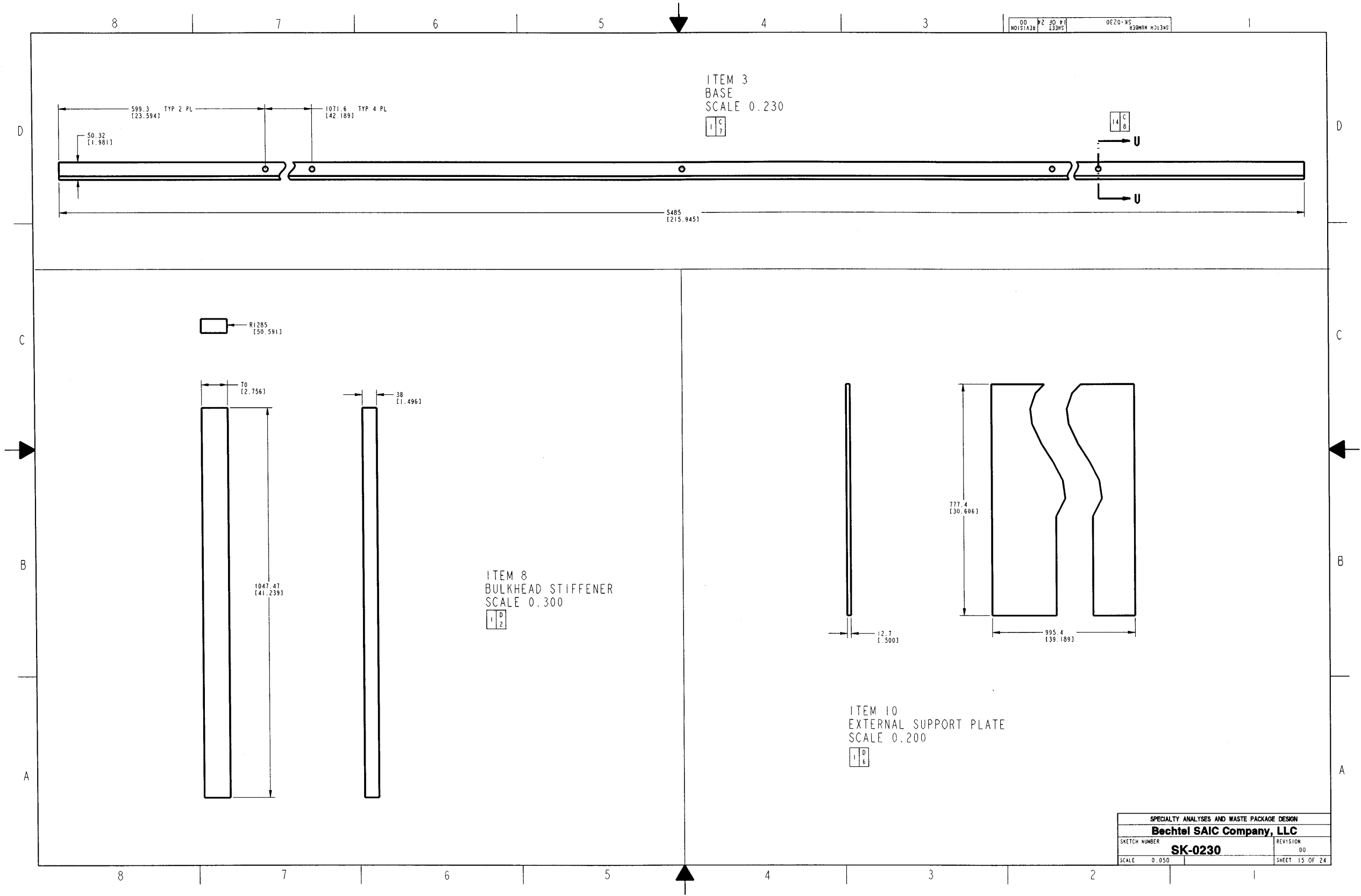
NAME: MCKENZIED2    OBJECT: SK-0230\_REV00\_13    DATE: 06-Nov-02 12:38:52



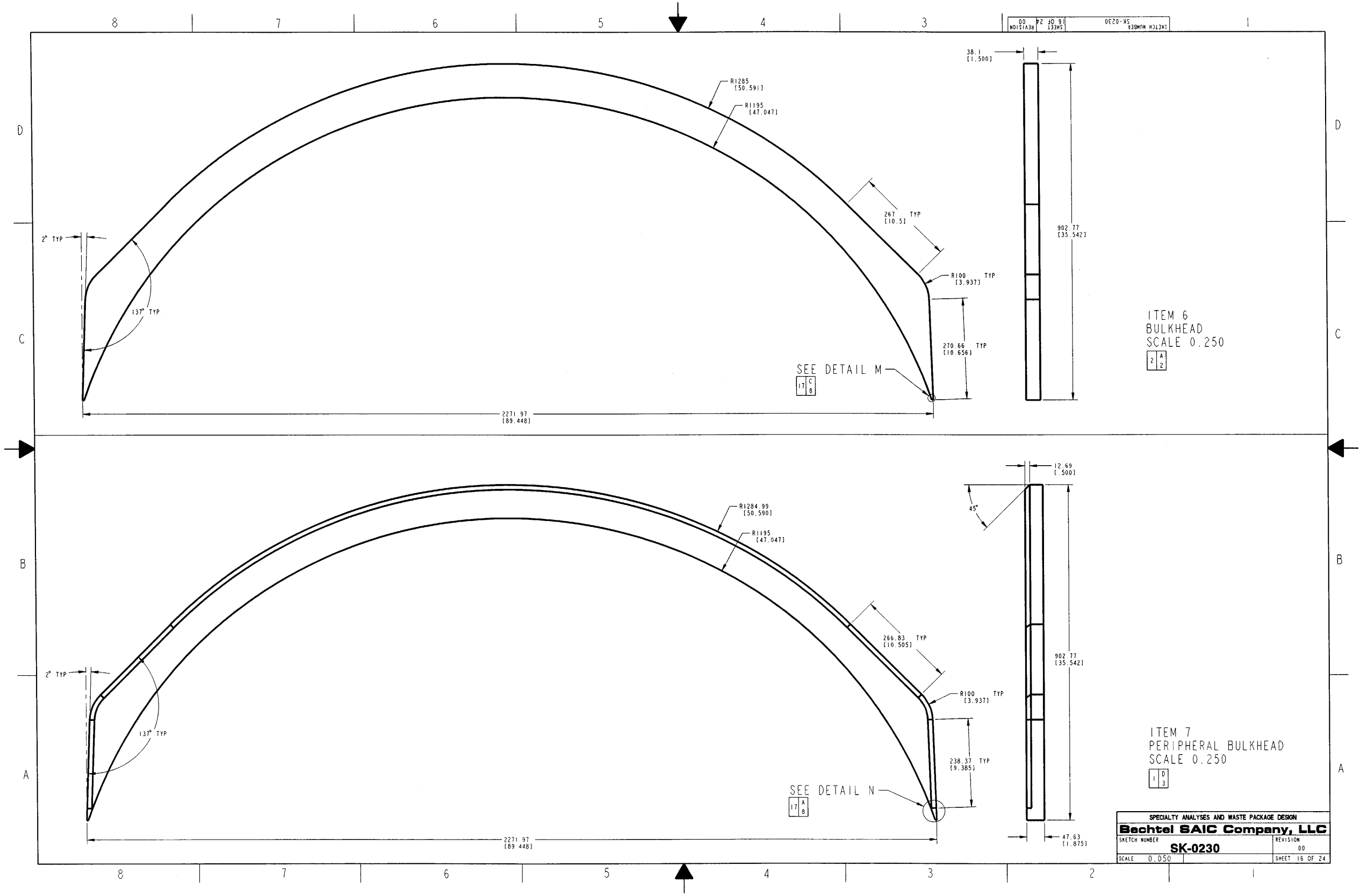
NAME: MCKENZIED2    OBJECT: SK-0230\_REV00\_14    DATE: 06-Nov-02 12:38:53



NAME: MCKENZIE D2    OBJECT: SK-0230\_REV00\_15    DATE: 06-Nov-02 12:38:53

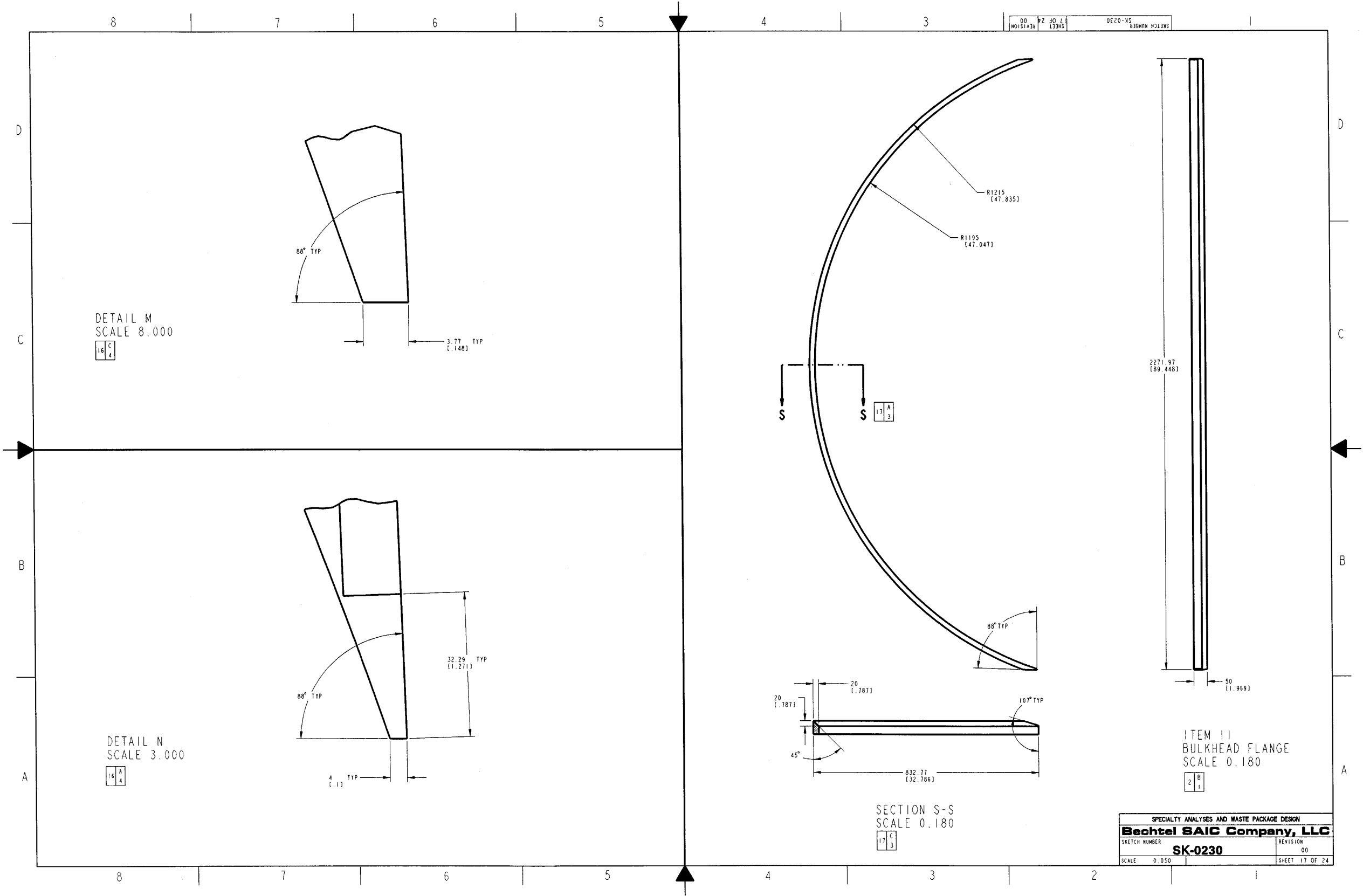


NAME: MCKENZIE D2    OBJECT: SK-0230\_REV00\_16    DATE: 06-Nov-02 12:38:54

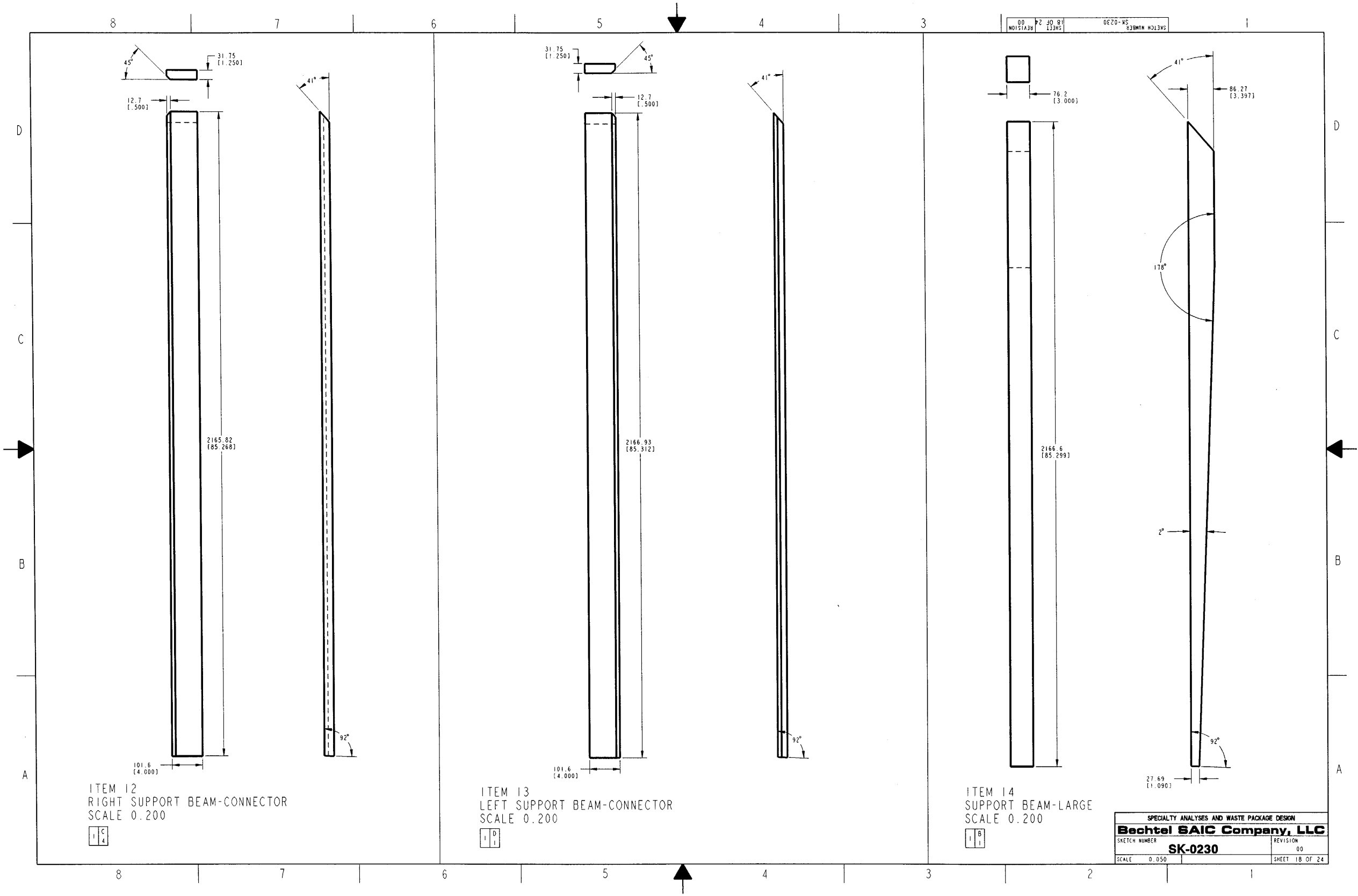




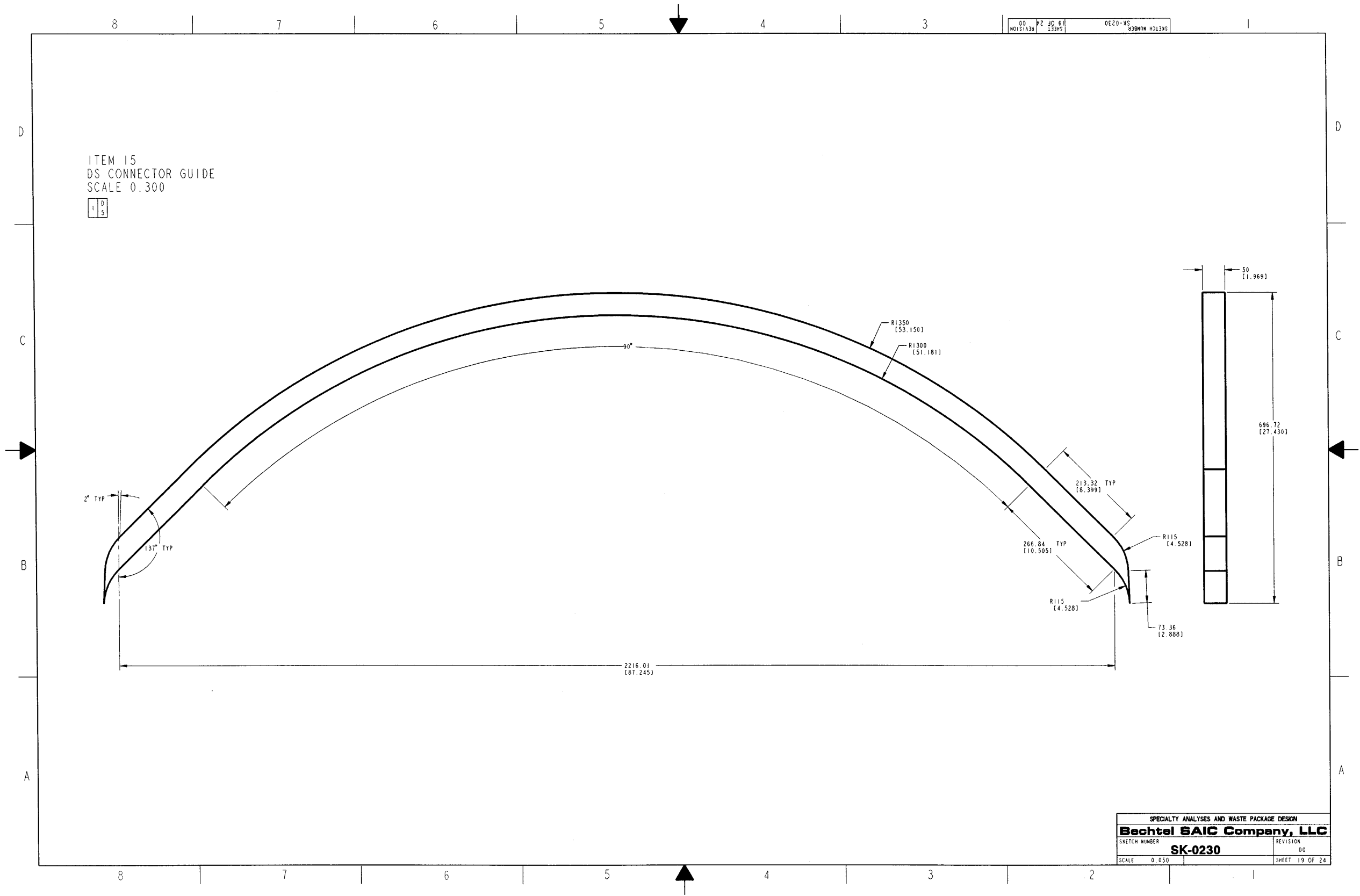
NAME: MCKENZIED2    OBJECT: SK-0230\_REV00.17    DATE: 06-Nov-02 12:38:54



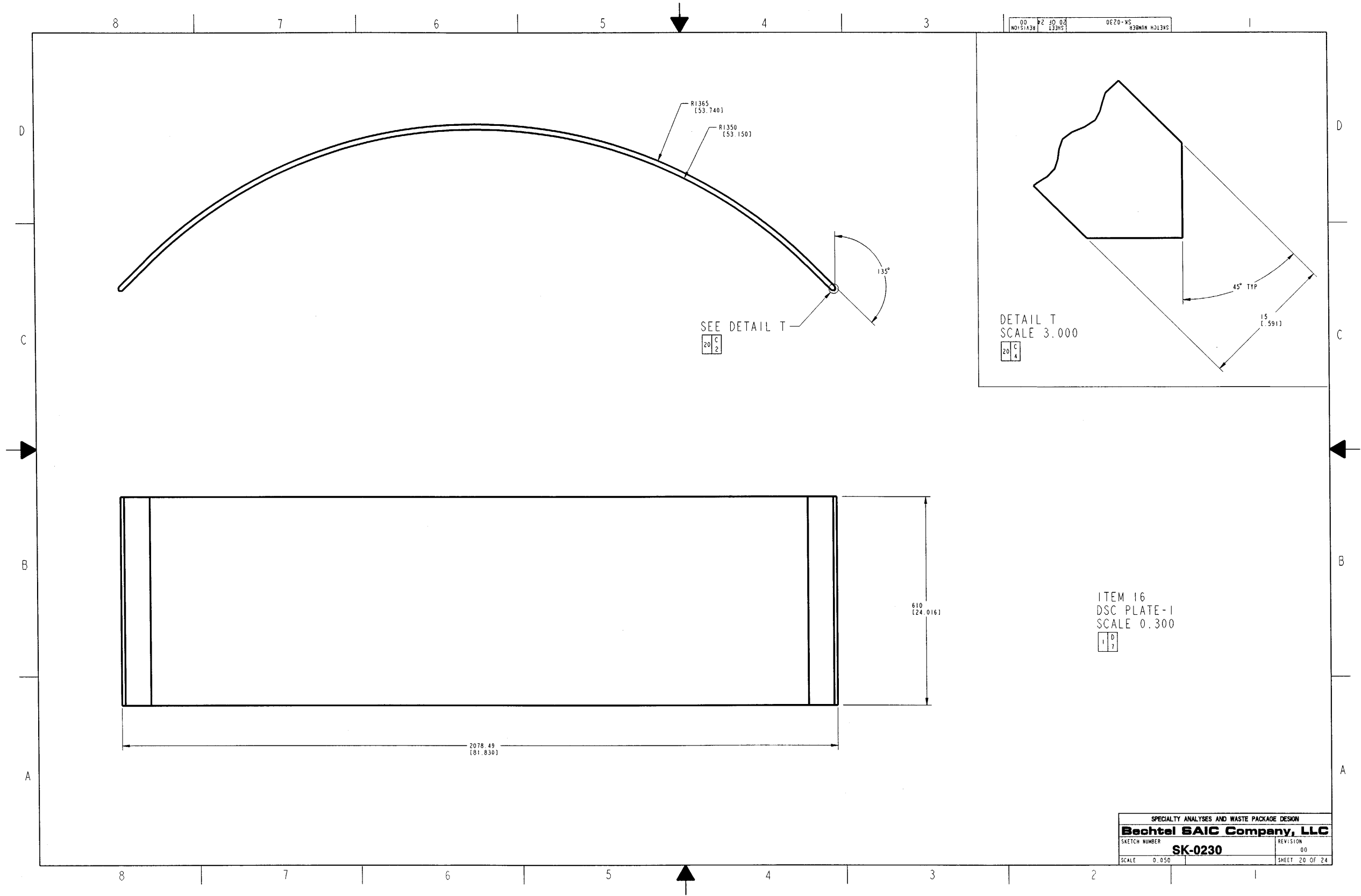
NAME: MCKENZIED2    OBJECT: SK-0230\_REV00\_18    DATE: 06-Nov-02 12:38:55



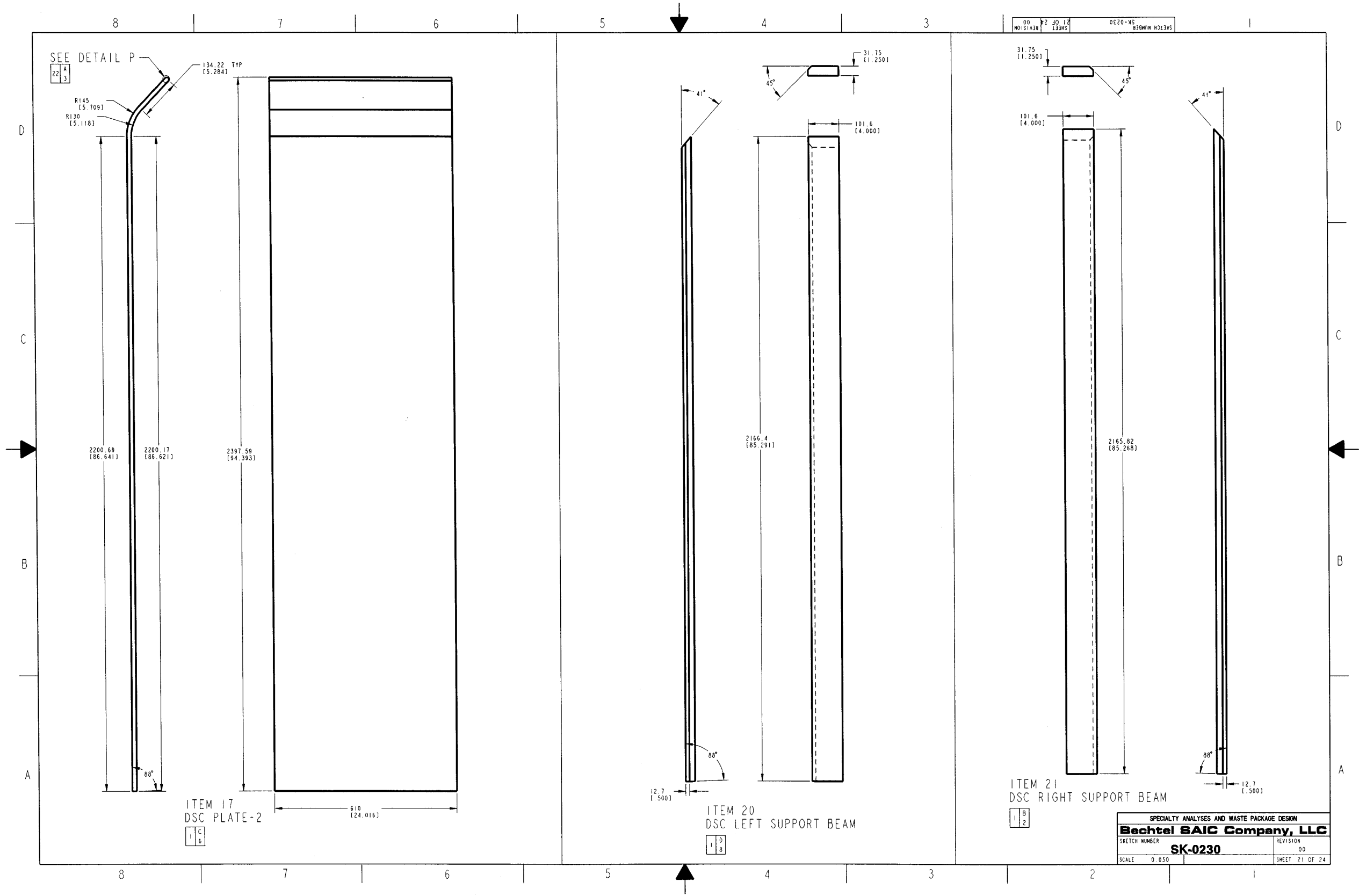
NAME: MCKENZIE D2    OBJECT: SK-0230\_REV00\_19    DATE: 06-Nov-02 12:38:55



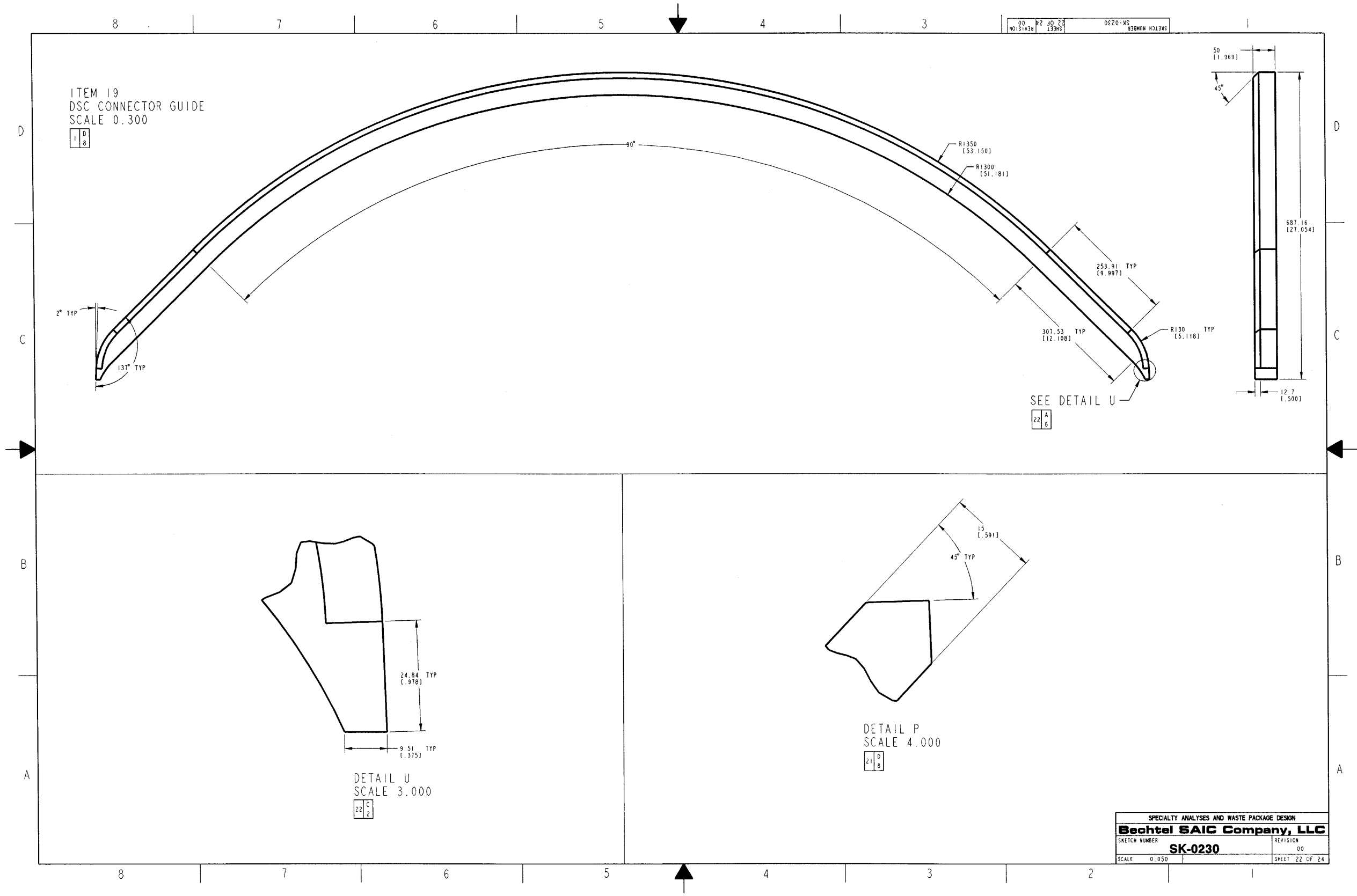
NAME:MCKENZIED2    OBJECT:SK-0230\_REV00\_20    DATE:06-Nov-02 12:38:56



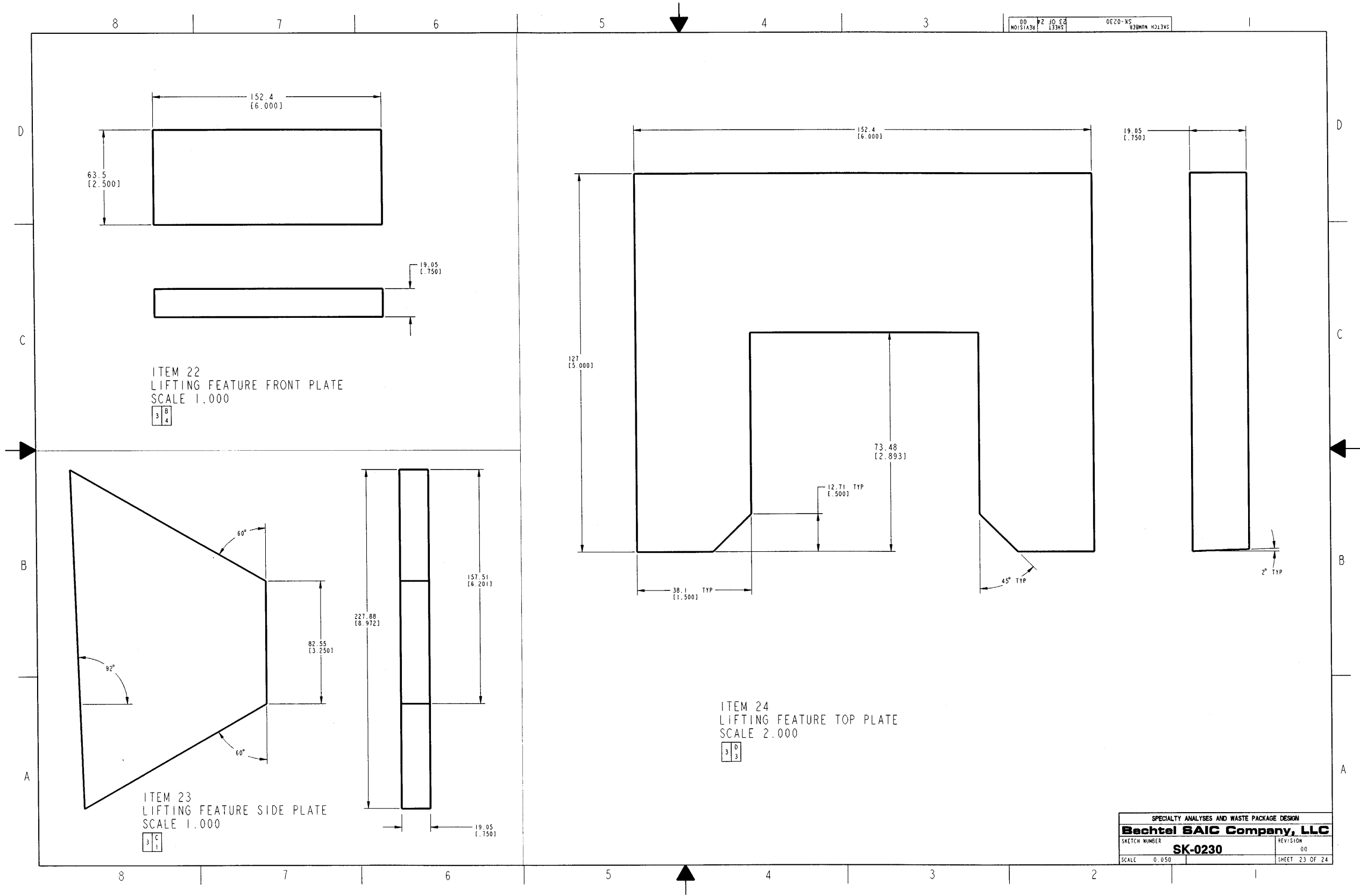
NAME: MCKENZIED2    OBJECT: SK-0230\_REV00\_21    DATE: 06-Nov-02 12:38:56



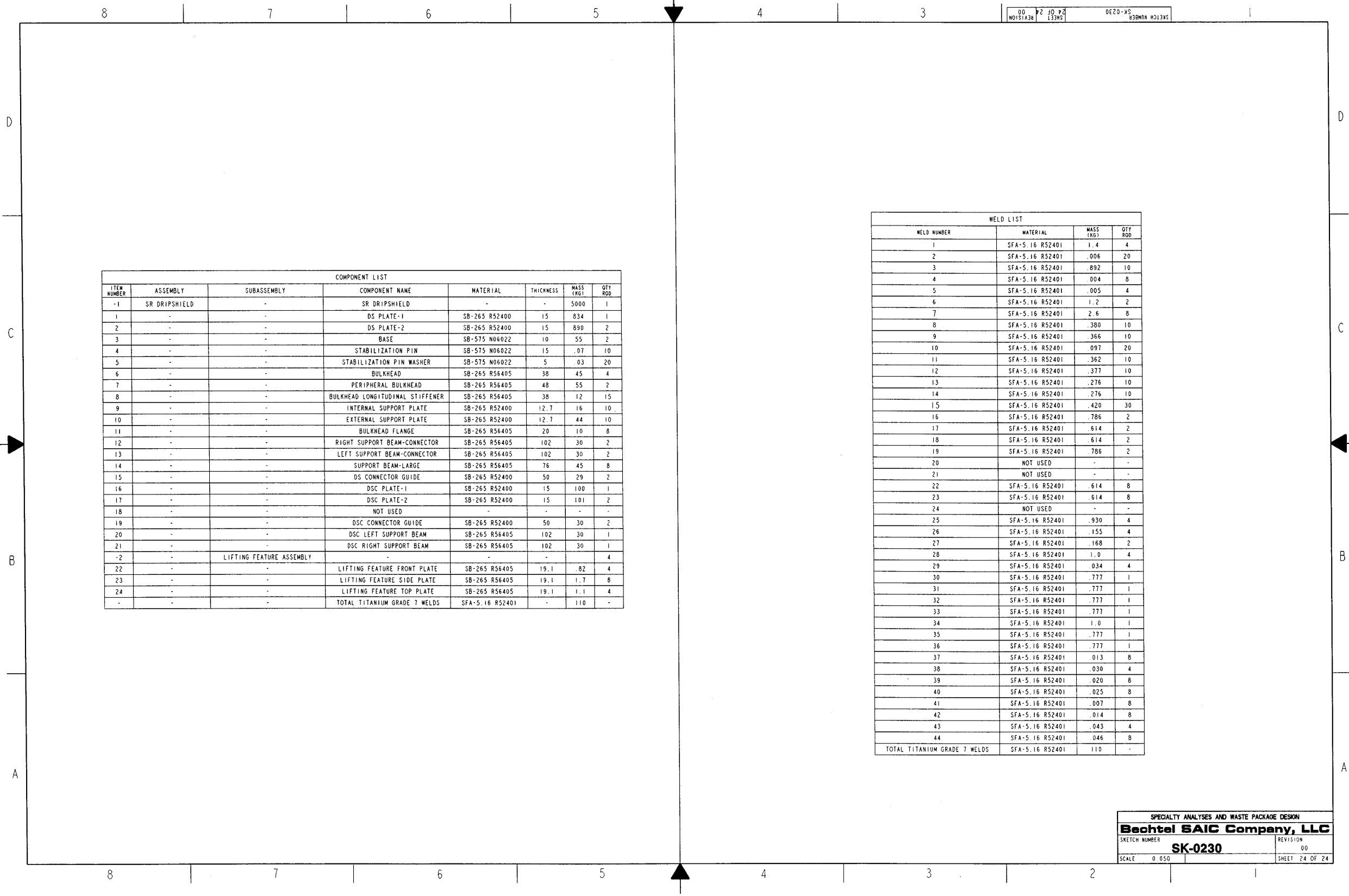
NAME : MCKENZIED2    OBJECT : SK-0230\_REV00\_22    DATE : 06-Nov-02 12:38:56



NAME: MCKENZIED2    OBJECT: SK-0230\_REV00\_23    DATE: 06-Nov-02 12:38:57



NAME: MCKENZIED2    OBJECT: SK-0230\_REV00\_24    DATE: 06-Nov-02 12:38:57





## ATTACHMENT II

### EFFECT OF ACCELERATION TIME HISTORY CUTOFF ON RESULTS

The structural calculations of DS exposed to vibratory ground motion are extremely time-consuming. This is not surprising keeping in mind that:

- the phenomena are highly nonlinear (large-deformation plasticity, friction, impact),
- the meshing requirements are very difficult,
- the number of contacting parts is extremely large and contacts are difficult to predict,
- the unavoidably small time step (approximately  $1\mu s$ ) is necessary for simulation of a long-duration event ( $\approx 30 - 40 s$ ).

Consequently, it is requisite to reduce the duration of the simulation without sacrificing any pertinent feature of the problem. The cutoff of ground-motion time history is elaborated in detail in Section 5.2.1. It will be verified in this section that the cutoff indeed has no effect on the simulation results.

The effect of the time history cutoff on the damaged area is studied for realizations 11 and 15 at annual frequency of occurrence  $1 \cdot 10^{-6} 1/yr$ . For both realizations, the damaged area is first evaluated at 95%-time (the time corresponding to 95 percent energy of ground motion); both realizations are then extended beyond 95%-time. Specifically, for realization number 11, the damaged area is also evaluated following the relaxation starting 9.7 s after 95 percent energy is reached (i.e., at  $t = 20.0 s$ , see Table II-1). For realization number 15, the damaged area is also evaluated following the relaxation starting 2 s after 95 percent energy is reached (i.e., at  $t = 7.0 s$ , see Table II-2). The results are summarized in Tables II-1 and II-2.

Table II-1. Damaged Area Obtained for Realization Number 11 at Two Different Times  
(Annual Frequency of Occurrence  $1 \cdot 10^{-6} 1/yr$ )

Relaxation Starting Time (s)	Damaged Area ( $m^2$ ; % of DS plate area)
10.3	0.446; 1.166
20.0	0.456; 1.192
Difference (%)	2.2

Table II-2. Damaged Area Obtained for Realization Number 15 at Two Different Times

(Annual Frequency of Occurrence  $1 \cdot 10^{-6} 1/yr$ )

Relaxation Starting Time (s)	Damaged Area ( $m^2$ ; % of DS plate area)
5.0	0.0984; 0.257
7.0	0.0989; 0.258
Difference (%)	0.5

Based on the results presented in Tables II-1 and II-2, and the fact that at the moment of the simulation termination the ground motion is already far in the low-intensity region (not more than 5 percent of the total energy is cut off), it can be concluded that overwhelming majority of the damage is accounted for. Thus, it is not necessary to run simulation after the maximum of 95 percent of the ground motion energy is reached.

**ATTACHMENT III****MESH OBJECTIVITY**

The purpose of this inquiry is to verify the objectivity of the mesh (i.e., that the calculation results are not mesh-sensitive). An approach used to achieve this goal is presented in detail in Reference 8 (Section 6.2.3). The damaged area of the DS plates is presented in this section for two different meshes. The results obtained by the first mesh are considered mesh-objective (i.e., mesh-insensitive) if the relative difference of results between the first and the second mesh are much smaller (approximately an order of magnitude smaller) than the relative difference of areas of their representative (average, typical) elements.

The first mesh is obtained by following the guidance in Reference 8 (Section 6.2.3). The second mesh is refined version of the first mesh. The typical DS element area of the first mesh is 300 percent (four times) larger than the area of the corresponding element in the second mesh. (Note that the areas of individual elements can be directly verified by using LS-POST V2.) Numbers of divisions in the axial, tangential, and thickness directions in the standard mesh and the refined mesh directions are available in Attachment V. For the standard mesh, check 1E-6\FER\drip2.inp, and for the refined mesh 1E-6\Refined Mesh\FER\drip2rm2.inp. Element number 6442 of the first mesh and element number 9617 of the second (refined) mesh can be compared as typical elements for the two FE representations.

The mesh sensitivity of the DS damaged area is studied for realization number 10 at annual frequency of occurrence  $1 \cdot 10^{-6} \text{ 1/yr}$ . The results are presented in Table III-1.

Table III-1. Damaged DS Area for Two Different FE Meshes for Realization Number 10  
(Annual Frequency of Occurrence  $1 \cdot 10^{-6} \text{ 1/yr}$ )

<b>Mesh</b>	<b>Damaged Area (<math>m^2</math>; % of DS plate area)</b>
<b>First Mesh</b> $A = 4.0 \cdot A_0$	0.192; 0.502
<b>Second Mesh</b> $A = A_0$	0.169; 0.441

According to results presented in Table III-1 the reduction of typical element size by 300 percent for realization number 10 results in decrease of the damaged area by 12.0 percent. The decrease of the damaged area in the case of the refined mesh can be explained by more localized DS deformation (following the impacts between DS and WPP assembly) for the refined mesh compared to the one for the coarser mesh. Thus, the results obtained by using the first mesh meet the mesh-objectivity criterion from Reference 8 (Section 6.2.3). Hence, all calculations presented in this document are performed by using the first mesh.

## ATTACHMENT IV

## PLOTS

Time = 2.95

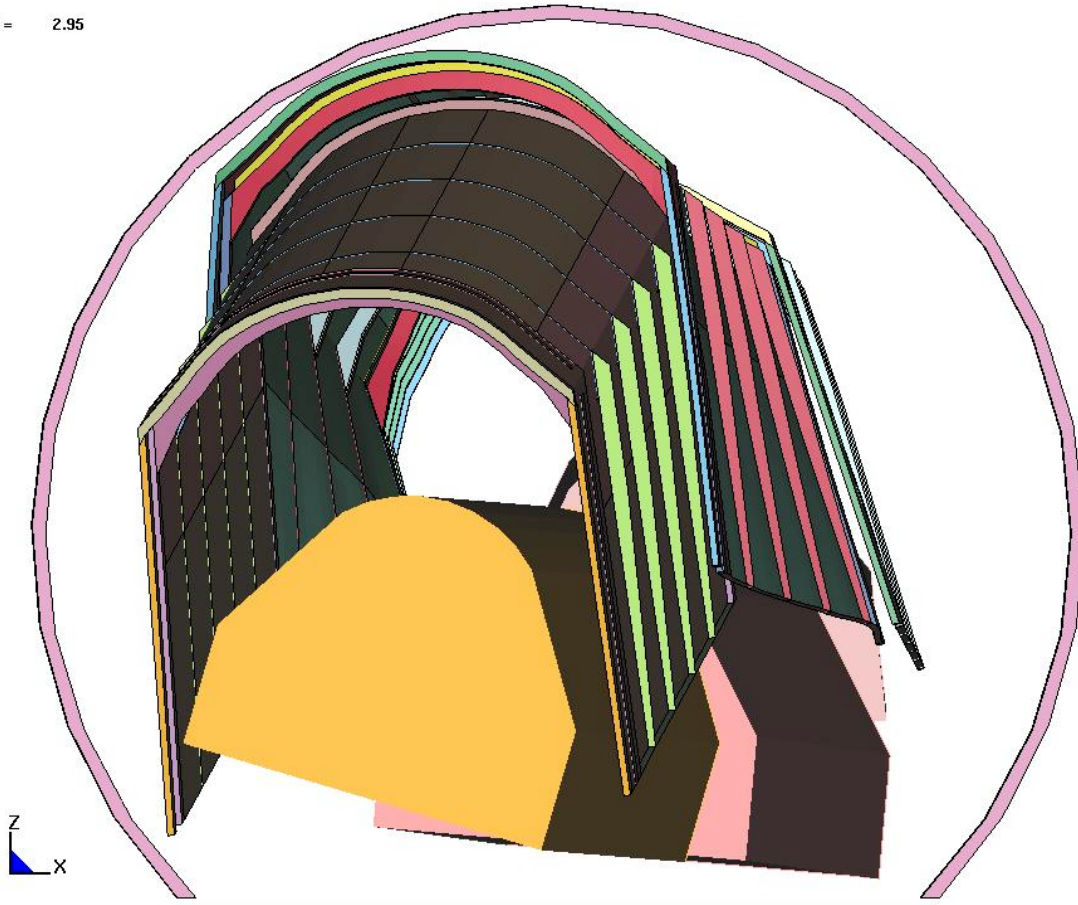


Figure IV-1. Front View at Component Locations in Realization Number 6 at  $1 \cdot 10^{-7}$   $1/yr$  Annual Frequency of Occurrence ( $t = 2.95$  s)

Time = 3

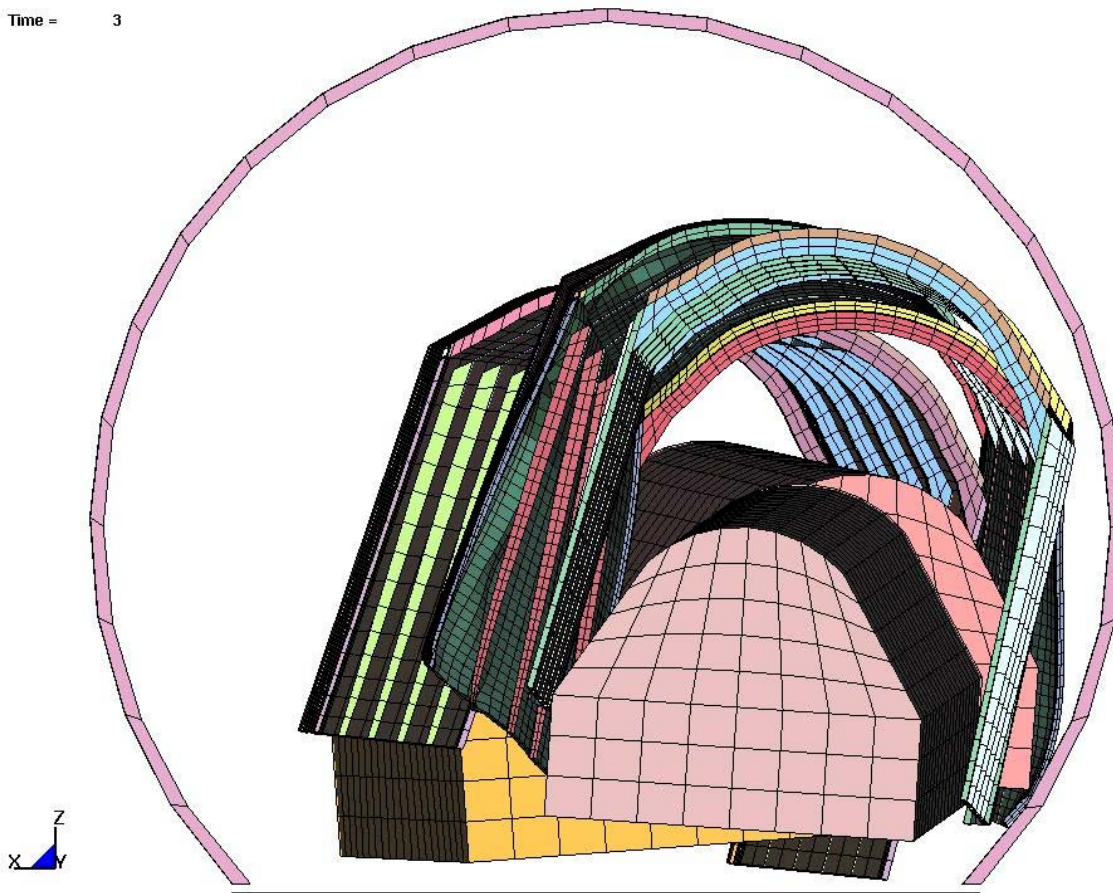


Figure IV-2. Front View at Component Locations in Realization Number 8 at  $1 \cdot 10^{-7}$   $1/yr$  Annual Frequency of Occurrence ( $t = 3.00$  s)

Time = 8.7

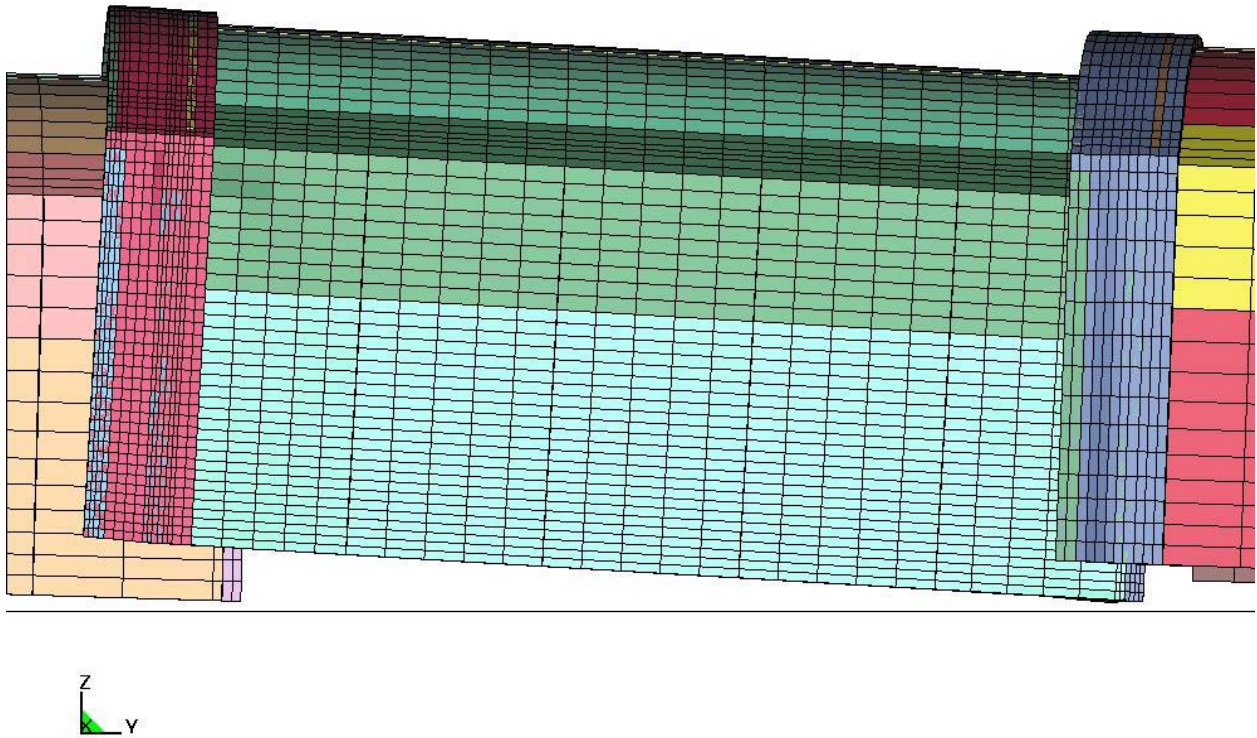


Figure IV-3. Detail of Side View at Component Locations in Realization Number 5 at  $1 \cdot 10^{-7}$  1/yr Annual Frequency of Occurrence ( $t = 8.70$  s)



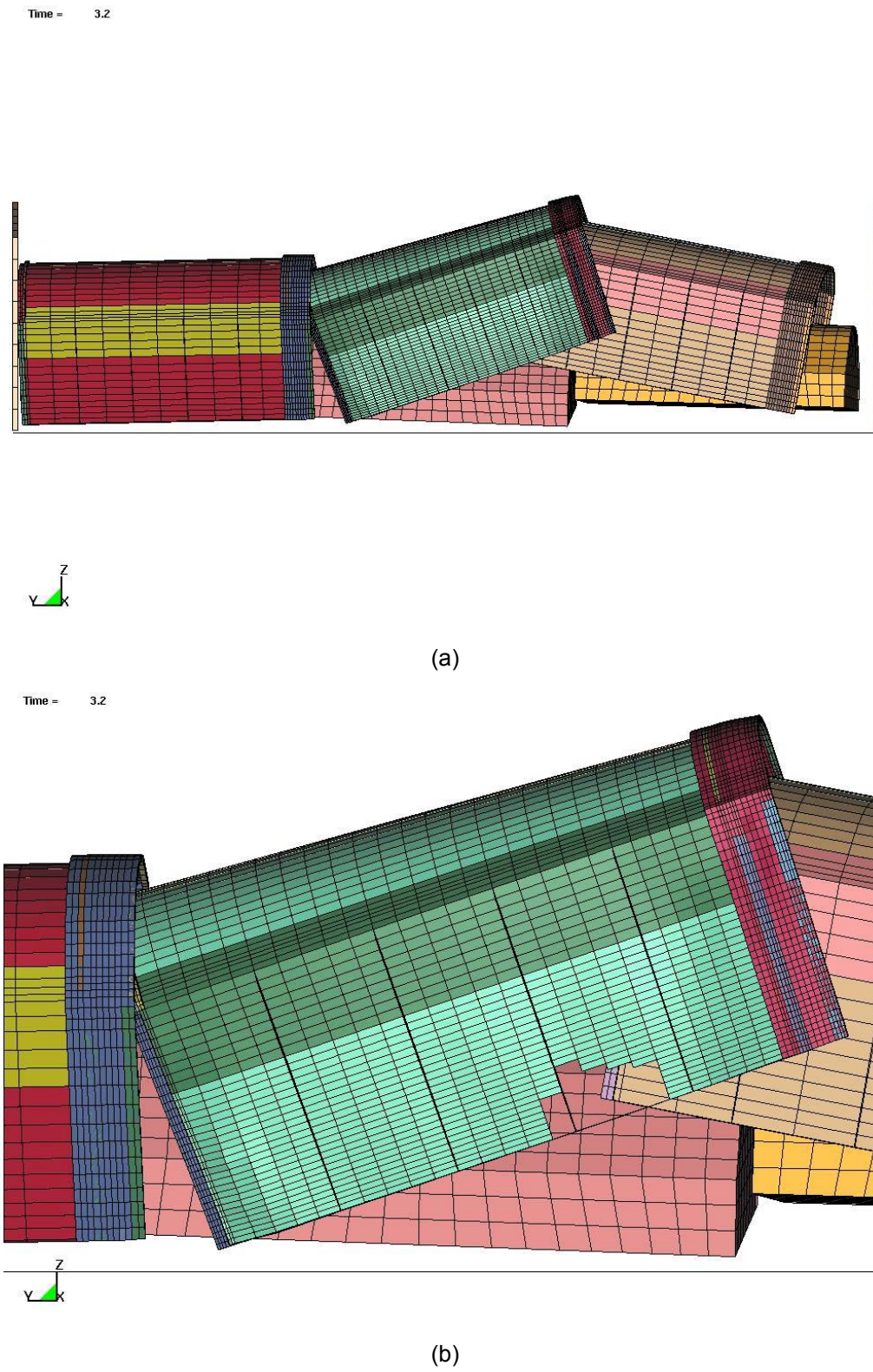


Figure IV-4. Side View at Component Locations in Realization Number 6 at  $1 \cdot 10^{-7}$  1/yr Annual Frequency of Occurrence ( $t = 3.20$  s): (a) Full View, and (b) Detail

Time = 3.2

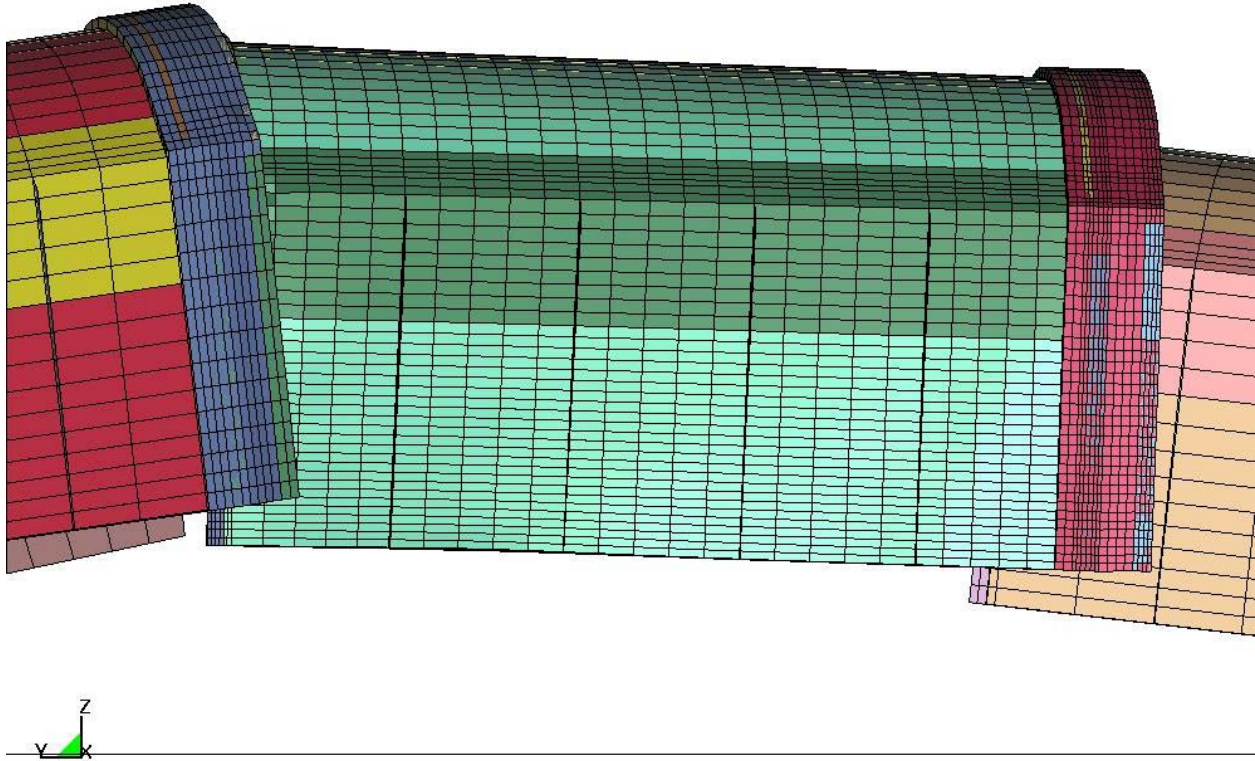


Figure IV-5. Side View at Component Locations in Realization Number 7 at  $1 \cdot 10^{-7}$  1/yr Annual Frequency of Occurrence ( $t = 3.20$  s)



Time = 3.1

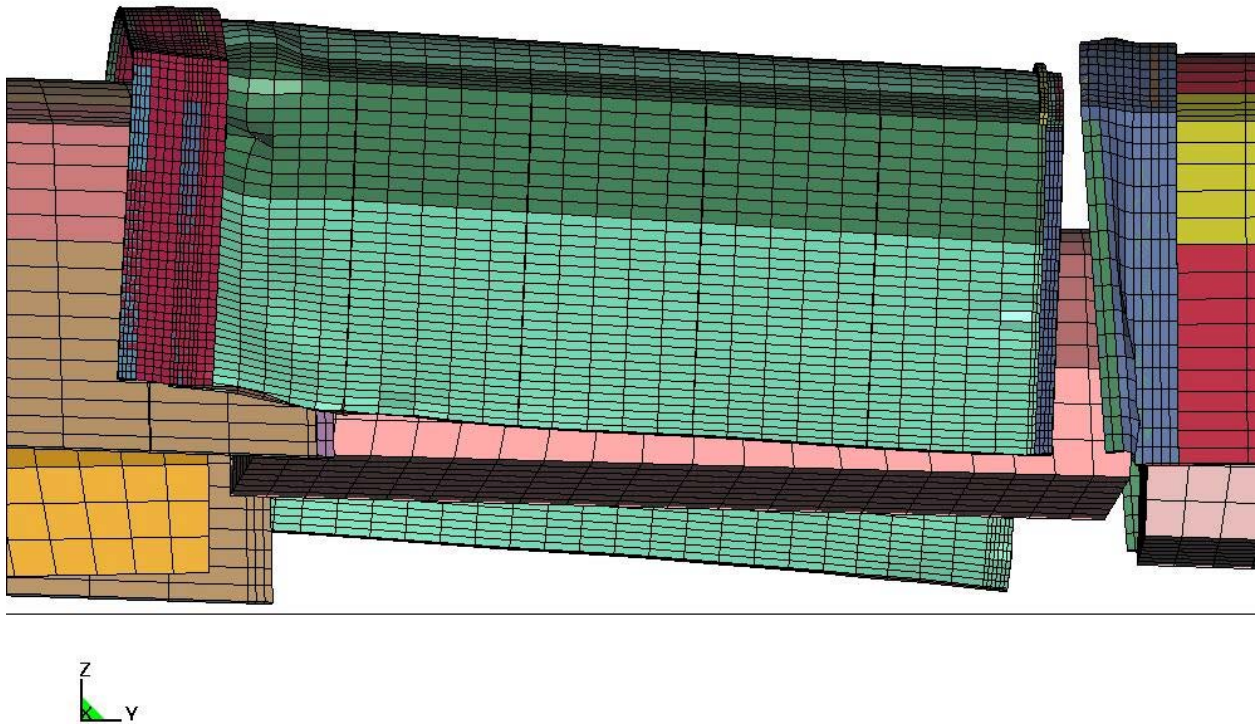


Figure IV-6. Side View at Component Locations in Realization Number 8 at  $1 \cdot 10^{-7}$  1/yr Annual Frequency of Occurrence ( $t = 3.10$  s)

Time = 3.6

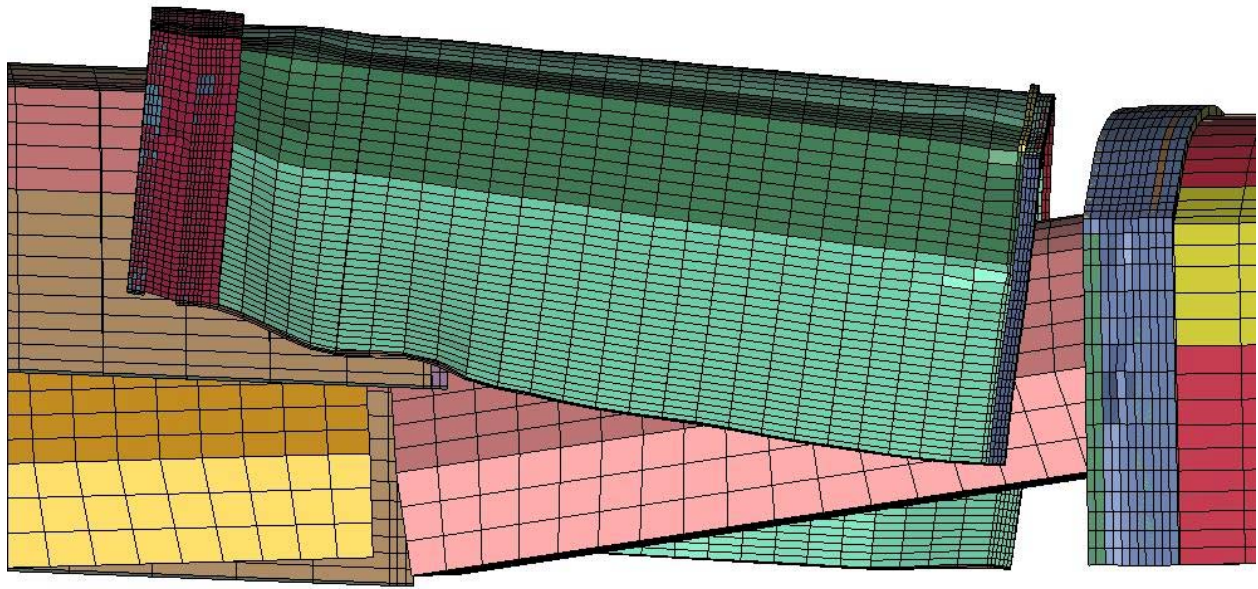


Figure IV-7. Side View at Component Locations in Realization Number 10 at  $1 \cdot 10^{-7}$  1/yr Annual Frequency of Occurrence ( $t = 3.60$  s)

Time = 7.6

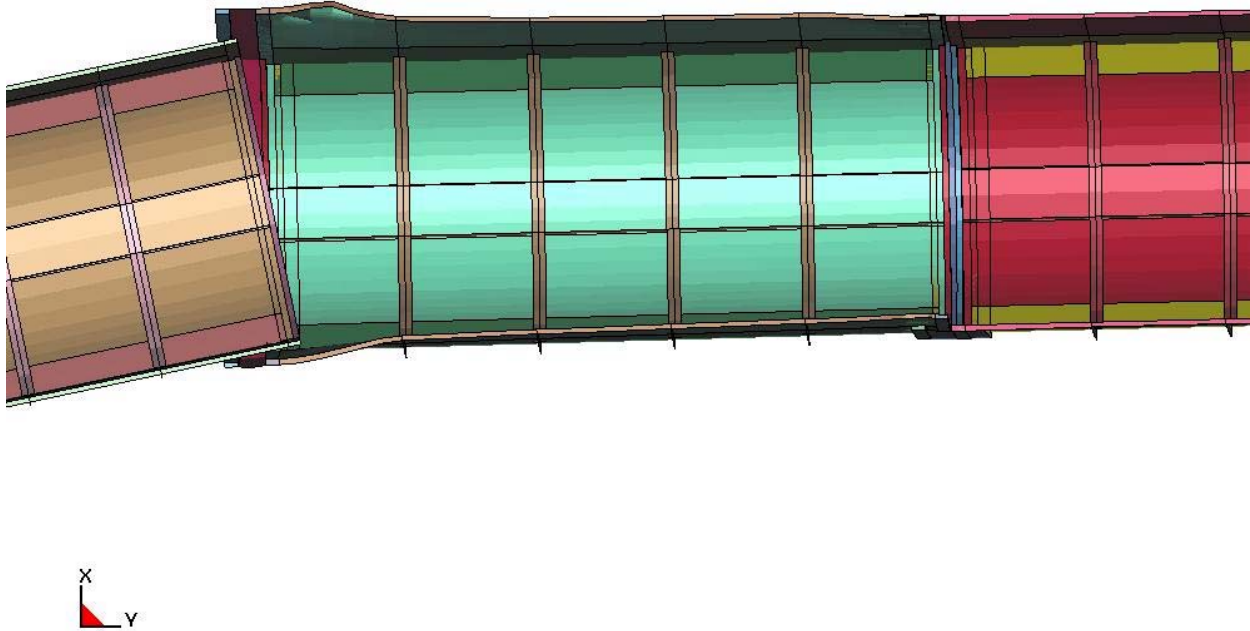


Figure IV-8. Detail of Bottom View at Final Configuration in Realization Number 6 at  $1 \cdot 10^{-6}$   $1/yr$  Annual Frequency of Occurrence ( $t = 7.60$  s)

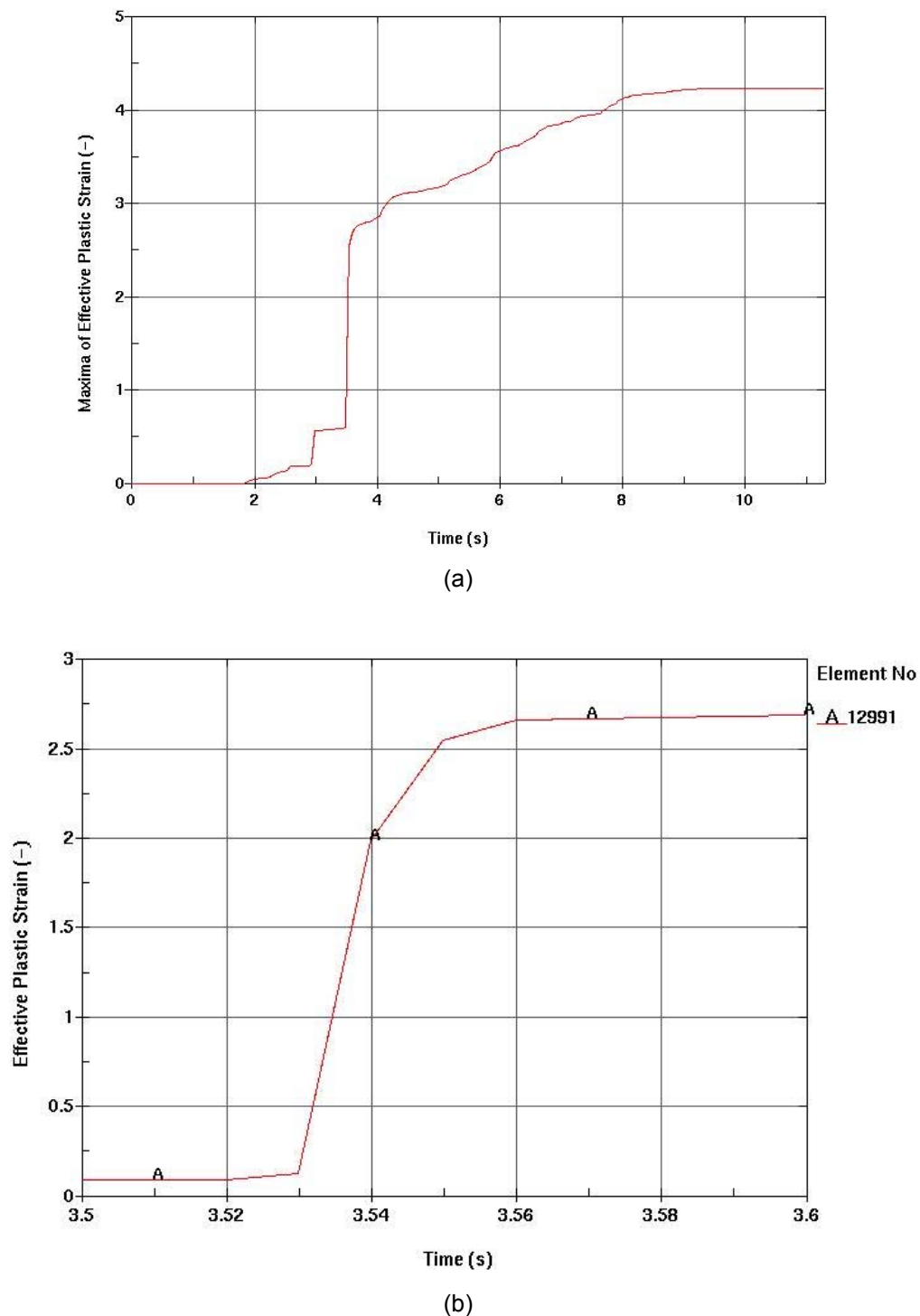
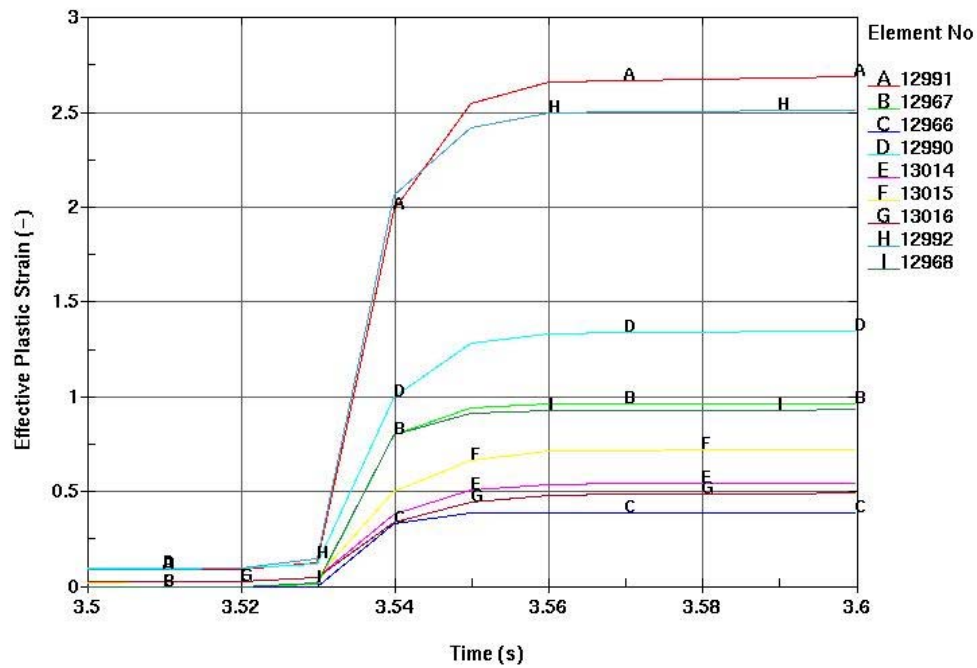
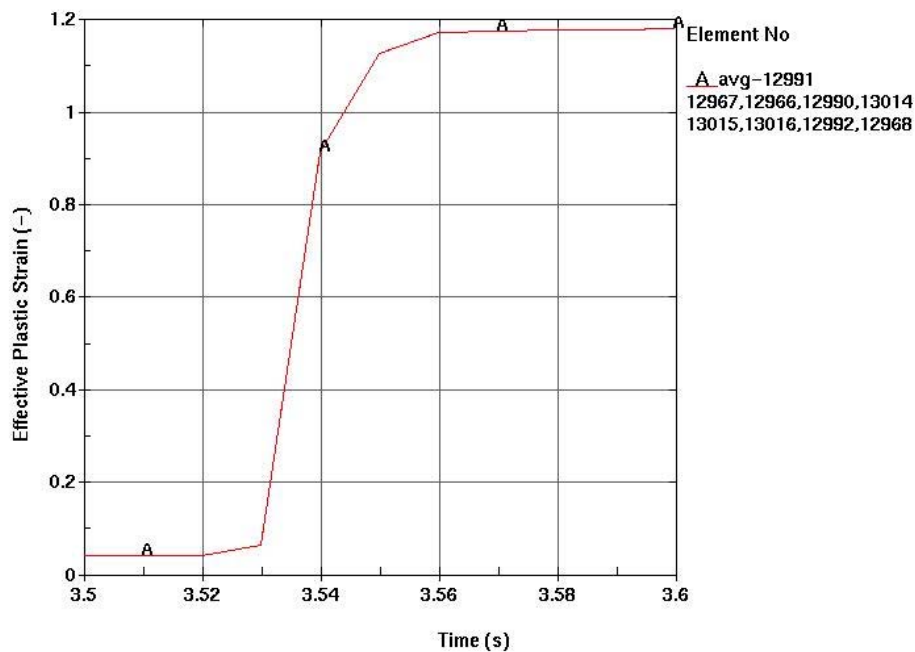


Figure IV-9. Effective Plastic Strain for DS plates for Realization Number 9 at  $1 \cdot 10^{-6}$   $1/yr$  Annual Frequency of Occurrence : (a) Maximum Values, and (b) Detail Corresponding to Maximum Strain Rate



(a)



(b)

Figure IV-10. Effective Plastic Strain for DS plates for Realization Number 9 at  $1 \cdot 10^{-6}$  1/yr Annual Frequency of Occurrence : (a) Element Number 12991 (characterized by the maximum strain rate) and Neighboring Elements, and (b) Averaged Value

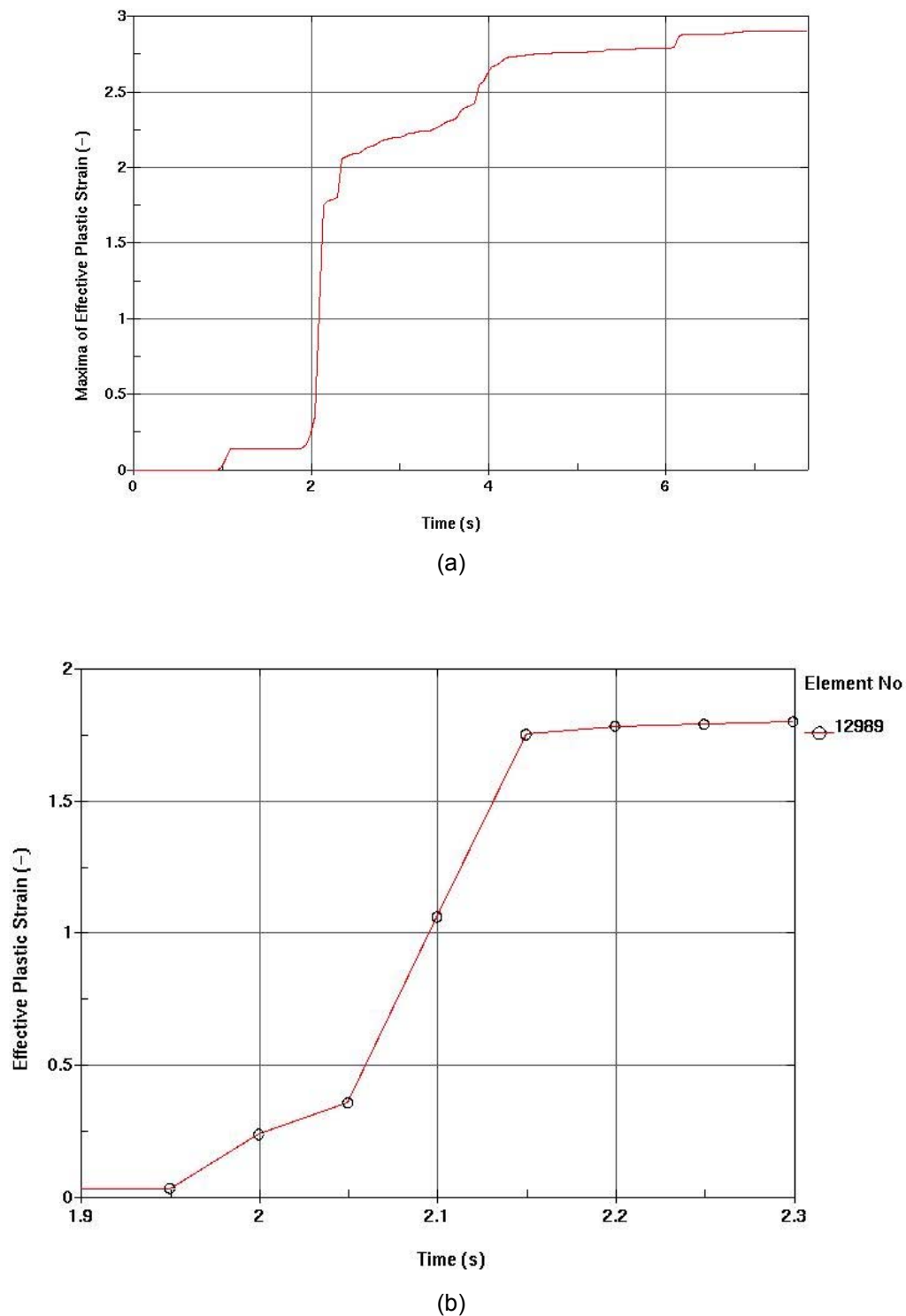


Figure IV-11. Effective Plastic Strain for DS plates for Realization Number 6 at  $1 \cdot 10^{-6}$  1/yr Annual Frequency of Occurrence : (a) Maximum Values, and (b) Detail Corresponding to Maximum Strain Rate (output points are indicated by circles)



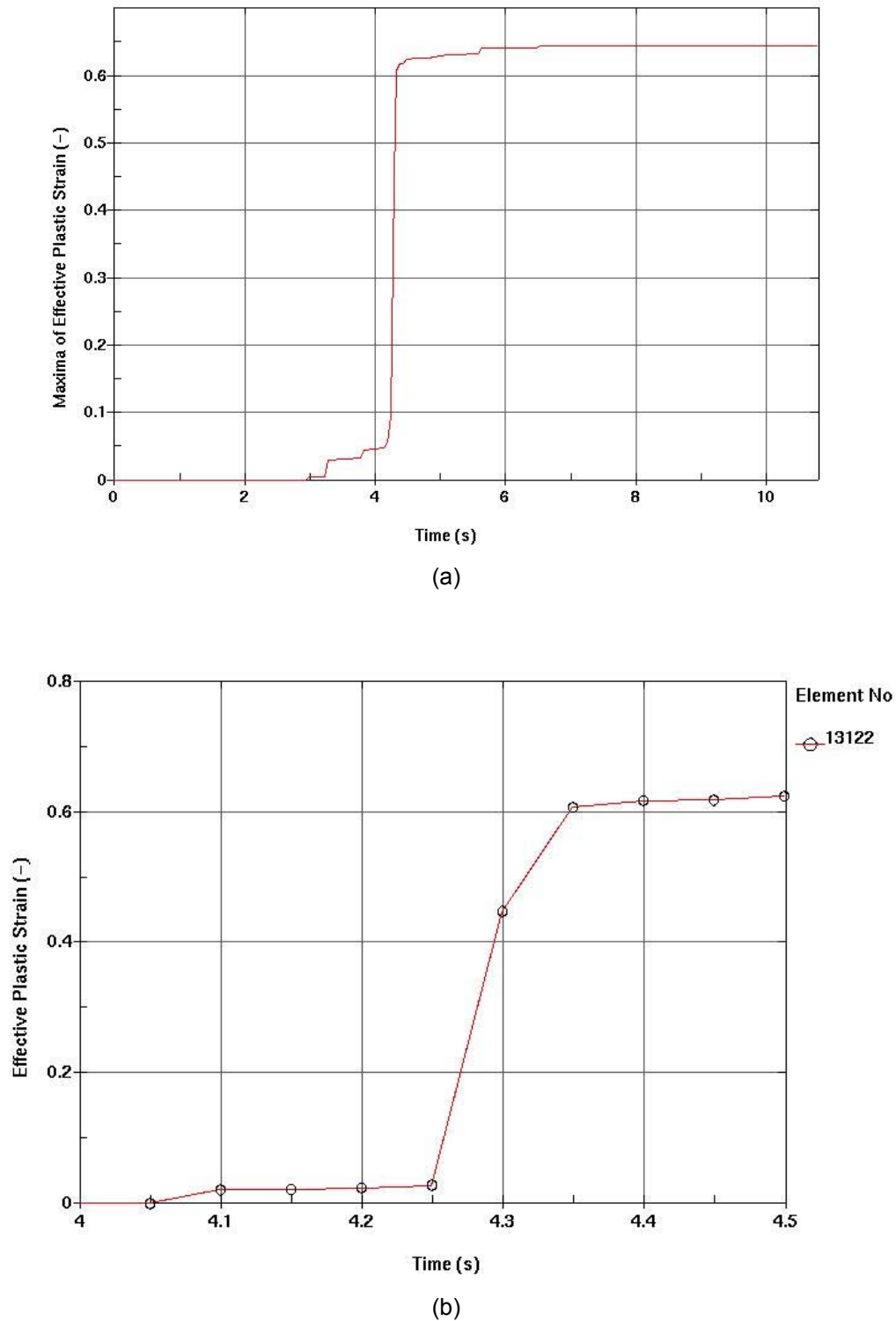


Figure IV-12. Effective Plastic Strain for DS plates for Realization Number 11 at  $1 \cdot 10^{-6}$  1/yr Annual Frequency of Occurrence : (a) Maximum Values, and (b) Detail Corresponding to Maximum Strain Rate (output points are indicated by circles)